

	<p>Research and Development Programme on Seismic Ground Motion</p> <p>CONFIDENTIAL <i>Restricted to SIGMA scientific partners and members of the consortium, please do not pass around</i></p>	<p>Ref : SIGMA-2013-D2-71 Version : 01</p> <p>Date : Page :</p>
--	--	---



STOCHASTIC GMPEs FOR FRANCE

AUTHORS			REVIEW			APPROVAL		
NOM	DATE	VISA	NOM	DATE	VISA	NOM	DATE	VISA
S. DROUET (Drouet Consulting)			F. Scherbaum (Postdam University)	In written review attached		P. Traversa		
			J. Savy (Savy Risk Consulting)	In written review attached		G. Senfaute		

DISSEMINATION: Authors; Steering Committee; Work Package leaders, Scientific Committee, Archiving.

	<p>Research and Development Programme on Seismic Ground Motion</p> <p>CONFIDENTIAL <i>Restricted to SIGMA scientific partners and members of the consortium, please do not pass around</i></p>	<p>Ref : SIGMA-2013-D2-71 Version : 01</p> <p>Date : April 29, 2013 Page :</p>
--	--	--

Executive Summary

The study presented in this document is a follow-up of a previous study which aimed at developing Ground-Motion Prediction Equations (GMPEs) for France, regionally adjusted and valid over a broad magnitude range. The results of this first study have been presented in the deliverable SIGMA-2012-D2-33 (Drouet, 2012), and discussed during the Scientific Committee, held in Roma on 24th and 25th of May 2012.

The first stochastic models presented in the above-mentioned document may be improved in several ways which will be described in this document. Moreover, a sensitivity study regarding the influence of the uncertainty on each input parameter on the total stochastic model uncertainty was required in order to better understand which are the controlling parameters that need to be better determined.

Some other aspects need to be investigated like the stress parameter model used, especially regarding the stress parameter value for large magnitude events, or the influence of the regression method used in the last stage of the GMPE development. Finally, two recent stochastic models have been developed in Europe, one for the United Kingdom (Rietbrock et al., 2013), and the other for Switzerland (Chiou, 2011; Edwards & Fäh, 2013). Some comparisons will be made between these models and the ones developed in the present study.

Three stochastic ground-motion prediction equations have been developed in this study for three regions in France: the Alps, the Pyrenees and the Rhine Graben. The primary input data are the results of the source, path and site terms inversion from Drouet et al. (2010). The models are built in two steps. First, synthetic ground-motion data is computed using the Stochastic Model SIMulation tool, SMSIM (Boore, 2003). Second, the synthetic data are used to build a GMPE by regression analysis assuming a functional form.

SMSIM uses a point-source model but given some adjustments on the single distance used for the simulation, extended fault effects can be included in the simulations. We used two different types of adjustments and showed that the Reff model (Boore, 2009) better takes into account the finite-fault. Consequently, all the simulations are done using this model. As in the previous version of the model, the time domain simulations are used, as opposed to the Random Vibration Theory (RVT) option also available in SMSIM (see Drouet, 2012). Simulations are carried out for $M_w=3$ to 8, epicentral distances from 1 to 250 km, and 20 spectral periods between 0.01 and 3 s, as well as for PGA and PGV. Two site conditions are considered: “standard” rock site with $v_{S30}=800$ m/s and $\kappa=0.03$ s, and hard rock site with $v_{S30}=800$ m/s and $\kappa=0.03$ s.

For each simulated magnitude, 40 simulations are done varying the fault orientation, dimensions, and hypocenter location on the fault (note that this information is only used to compute the different distance metrics, the simulations are done using a point-source model: SMSIM), and the stress parameter. The stress parameter model is built considering observed stress parameters in the three regions from Fourier spectral analysis (Drouet et al., 2010), and extrapolating towards larger magnitude using information available in the literature. Different versions of the models are built regarding different hypotheses on stress parameter for large events. All the parameters used as input in the stochastic simulations are considered as random variables assuming normal or log-normal distributions. Consequently, uncertainty on the input parameters is propagated to the synthetic ground-motions.

GMPEs are built by regression of the synthetic data using two different methods: least-squares and random-effect. Tests have been made to assess the influence of the starting model on the regression and the influence of the functional form. GMPEs coefficients are determined for the 4 distance

	<p style="text-align: center;">Research and Development Programme on Seismic Ground Motion</p> <p style="text-align: center;">CONFIDENTIAL <i>Restricted to SIGMA scientific partners and members of the consortium, please do not pass around</i></p>	<p>Ref : SIGMA-2013-D2-71 Version : 01</p> <hr/> <p>Date : April 29, 2013 Page :</p>
--	--	--

metrics considered: Repi, Rhypo, RJB, and Rrup. A sensitivity analysis is carried out to understand the influence of the uncertainty on each input parameter to the total GMPE uncertainty. The major contributors to the total uncertainty are the stress parameter model, the site model (both site amplification and kappa). The uncertainties on the attenuation parameters have a second order influence, and those linked with duration, fault orientation and hypocenter location are negligible compared to the other. Stress parameter uncertainty directly maps into between-event variability, while the uncertainties on the other parameters mainly influence the within-event term. The total ground-motion variability obtained is comparable to that obtained in empirical GMPEs under the ergodic assumption (variability of ground-motion including various sites and various sources). The within- and between-event terms are also similar to that obtained in empirical GMPEs, especially those that include small magnitudes events. In order to perform site-specific PSHA, the model is flexible enough to refine the variability on v_{S30} and kappa in order to produce a model using single-station variability.

The stochastic GMPEs are compared with data from large earthquakes included in the Resorce database (Akkar et al., 2011, SIGMA WP2) including data from the Euro-Mediterranean region, and data from the NGA project including mainly data from California and Taiwan and some other active regions (Chiou et al., 2008). Statistical analysis of the residuals following the methods of Scherbaum et al. (2004, 2009) allowed us to compare the performance of the different versions of the stochastic models (variations in the stress parameter for large events). It appears that a stress parameter of 5 MPa is a good choice to achieve a good fit between the models and the real data especially for the European data.

The stochastic models are also compared to the small magnitude data recorded in the different regions. The main difficulty in this exercise is the poorly known site characteristics for the French stations. Different rock site classifications are consequently considered. A reasonable fit is obtained for the three regions. However, for the Pyrenees, small magnitude data are overestimated by the models which have a too weak magnitude scaling. This is probably due to the large stress parameter values obtained in this region which are of the same order as the stress parameter used for large events. However, the scaling with magnitude of the observed stress parameters appears to be strong. Moreover, the stochastic models for the three regions are also compared with each other. The main difference is seen between the model for the Alps with the stronger dependence of stress parameter on magnitude and the other two models. The differences between the three regions due to the attenuation parameters are rather low. A more detailed analysis of the Fourier spectra including more data (for example the RSSP data), and trying to use a reference site coherent with the other regions may help to better characterize stress parameters in this region. In this context, results from site characterization of SIGMA WP3 are very important.

Even if improvements are still possible for the stochastic models presented in this study, we feel that they can be used in PSHA analysis. Indeed, comparisons with data show a good fit throughout the magnitude range, and the analysis of the total variability obtained shows a good coherency with results from other studies. Moreover, these models can be used in site-specific analysis if a detailed knowledge of the site response is available.

To:

EDF - DPI - DIN – CEIDRE
TEGG - Service Géologie Géotechnique
905, av. du Camp de Menthe
13090 AIX EN PROVENCE

Stochastic GMPEs for France

Contents

1.Introduction.....	1
2.Improvement of the stochastic model.....	2
2.1.Near-source saturation effect.....	2
2.2.Input parameters.....	4
a)Simulation settings.....	4
b)Stress drop model.....	5
c)Site model.....	9
d)Attenuation model.....	11
3.Regression method.....	11
3.1.Test on the input parameters.....	12
3.2.Test on the regression form.....	13
3.3.Test using different distance metric.....	14
4.Sensitivity study.....	15
5.Stress parameter for large events.....	19
5.1.Testing using the European data.....	19
5.2.Testing using the NGA data.....	21
6.Stress parameter for small events.....	23
6.1.Alps.....	24
6.2.Pyrenees.....	26
6.3.Rhine Graben.....	28
7.Comparison of stochastic models for France, United Kingdom and Switzerland.....	29
8.Rock and Hard Rock site conditions.....	34
9.Conclusion.....	35
10.References.....	36
11.Annex.....	39
11.1.Comparison plots of the different model versions for the Alps.....	39
11.2.Comparison plots of the different model versions for the Pyrenees.....	41
11.3.Comparison plots of the different model versions for the Rhine Graben.....	43
11.4.Divers.....	45

1. Introduction

The study presented in this document is a follow-up of a previous study which aimed at developing Ground-Motion Prediction Equations (GMPEs) for France, regionally adjusted and valid over a broad magnitude range. The results of this first study have been presented in the deliverable SIGMA-2012-D2-33 (Drouet, 2012), and discussed during the Scientific Committee, held in Roma on 24th and 25th of May 2012.

The first stochastic models presented in the above-mentioned document may be improved in several ways which will be described below. Moreover, a sensitivity study regarding the influence of the uncertainty on each input parameter on the

total stochastic model uncertainty was required in order to better understand which are the controlling parameters that need to be better determined.

Some other aspects need to be investigated like the stress parameter model used, especially regarding the stress parameter value for large magnitude events, or the influence of the regression method used in the last stage of the GMPE development.

Finally, two recent stochastic models have been developed in Europe, one for the United Kingdom (Rietbrock et al., 2013), and the other for Switzerland (Chiou, 2011; Edwards & Fäh, 2013). Some comparisons will be made between these models and the ones developed in the present study.

2. Improvement of the stochastic model

2.1. Near-source saturation effect

The method used to develop the stochastic models for France is the stochastic point-source simulations as implemented in the SMSIM code (Boore, 2003). The point-source simulations work well for small earthquakes and at large distances, and are comparable to finite-fault simulations (i.e. that take into account the extension of the fault plane) (Boore, 2009). For large earthquakes and close to the fault, some adjustments to the single distance used in the point-source simulation can be used to mimic near-source effects such as the saturation at close distance. In the previous version of the stochastic models for France, the approach proposed by Atkinson & Silva (2000) was used. These authors computed an effective depth h as a function of magnitude:

$$\log_{10}(h) = -0.05 + 0.15 \times M_w$$

and proposed to modify the distance used in point-source simulation such that:

$$R_{mod} = \sqrt{d^2 + h^2}$$

where d is the closest distance to the fault plane, and R the distance to use in the simulations. More recently, Boore (2009) proposed another modification of the distance. Considering the fault plane as a superposition of N sub-faults, and assuming that the contributions from the sub-faults add incoherently, the author compute an effective distance (R_{eff}) such that:

$$G(R_{eff}) \exp(-\pi f_Q R_{eff} / Q(f_Q) v_s) = \left[\frac{1}{N} \sum_1^N (G(R_i) \exp(-\pi f_Q R_i / Q(f_Q) v_s))^2 \right]^{1/2}$$

where f_Q is a reference frequency (10 Hz is used here; Boore, 2009 showed that the choice of f_Q as a small impact), Q is the anelastic attenuation factor, v_s the S-wave velocity, and R_i is the distance from the observation site to the center of the subfault i .

In order to assess the influence of the two options to account for near-source saturation, ground-motions have been computed for $M_w=4$ and 6. Fault plane dimensions have been estimated using the Wells & Coppersmith (1994) equations, and are used to compute the different distance metrics for a given station. Although the Wells & Coppersmith (1994) relationships may not be the most recent ones, for instance Pavlides & Caputo (2004) and Caputo et al. (2008) developed new relationships for Europe. However, since, in the present study, these relationships are only used to compute the distance metrics we feel that it is not necessary to update them for the time being.

In this test, vertical fault planes are used, and the hypocenter is placed in the middle of the fault along the strike direction and at 0.7 times the fault width in the downdip direction. Ground-motions for stations located along the strike, at 45° and 90° from the strike, and at epicentral distances from 1 to 250 km are computed (Figure 1). SMSIM is used to compute the ground-motion using the two different options to mimic near-source saturation, i.e. R_{mod} and R_{eff} .

Figure 2 shows the ratios R_{mod}/R_{rup} and R_{eff}/R_{rup} for $M_w=6$, and for R_{rup} between about 4 and 250 km, obtained for the three different orientations for the lines of stations (along strike and at 45 and 90° from the strike). Note that along the strike, the first 5 stations are located directly above the rupture plane and hence are at the same distance from the rupture plane. In the present case, the minimum distance from the rupture plane is the depth-to-top of rupture which is equal here to 4.6 km. There are some interesting remarks about Figure 1. First, the R_{mod} model do not show any dependence on the orientation relative to the fault strike while the R_{eff} model does. Second, at 90° from the fault strike, the two models are equivalent. Finally, in the R_{eff} model the ratio of the modified distance over R_{rup} decreases less rapidly with distance when the angle from the strike decreases. This means that the distance used for the simulations will be greater and lower amplitudes will be computed. Physically, this can be understood as the distance from the fault plane as a whole, since in the R_{eff} model each part of the fault is considered and, for distance along the strike, the distance from the sub-faults located at the opposite end of the fault will be large. Figure 3 Shows the response spectra

computed at similar rupture distance for the two model in the 90° from strike and along strike directions. The two simulations are equivalent for direction perpendicular to the fault and the R_{eff} model produces lower amplitudes in the along strike direction.

The effects of the R_{eff} model depends on magnitude since it uses the fault extension to compute an equivalent distance which reflects the attenuation of the waves coming from different part of the fault. For small magnitudes, its effect is negligible. Indeed, Figure 4 shows that the ratios $R_{\text{mod}}/R_{\text{rup}}$ and $R_{\text{eff}}/R_{\text{rup}}$ are the same for $M_w=4$ whatever the orientation of the stations profile. In the following we will use the R_{eff} model since it better takes into account the effect of extended-fault.

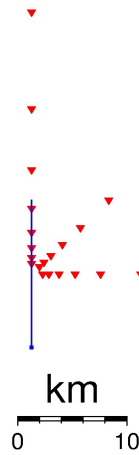


Figure 1: Vertical fault corresponding to $M_w=6$ and projected on surface (blue line) and recording stations (red triangles).

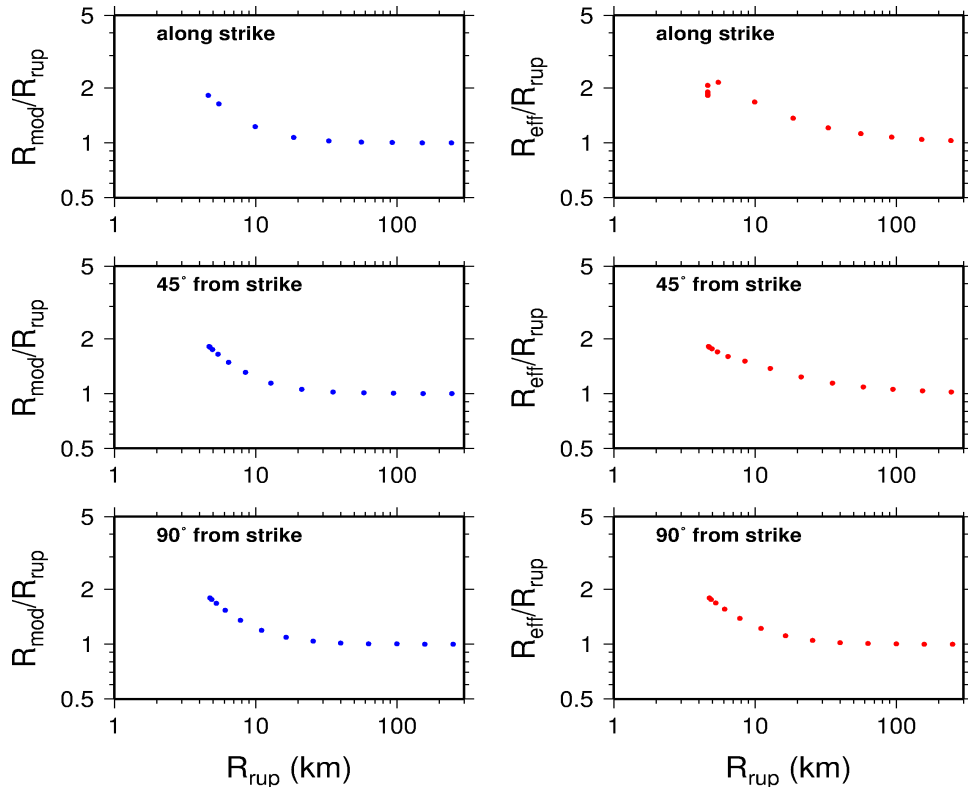


Figure 2: Ratios $R_{\text{mod}}/R_{\text{rup}}$ (left) and $R_{\text{eff}}/R_{\text{rup}}$ (right) as a function of R_{rup} for stations located along strike, and at 45 and 90 ° from strike, for $M_w=6$.

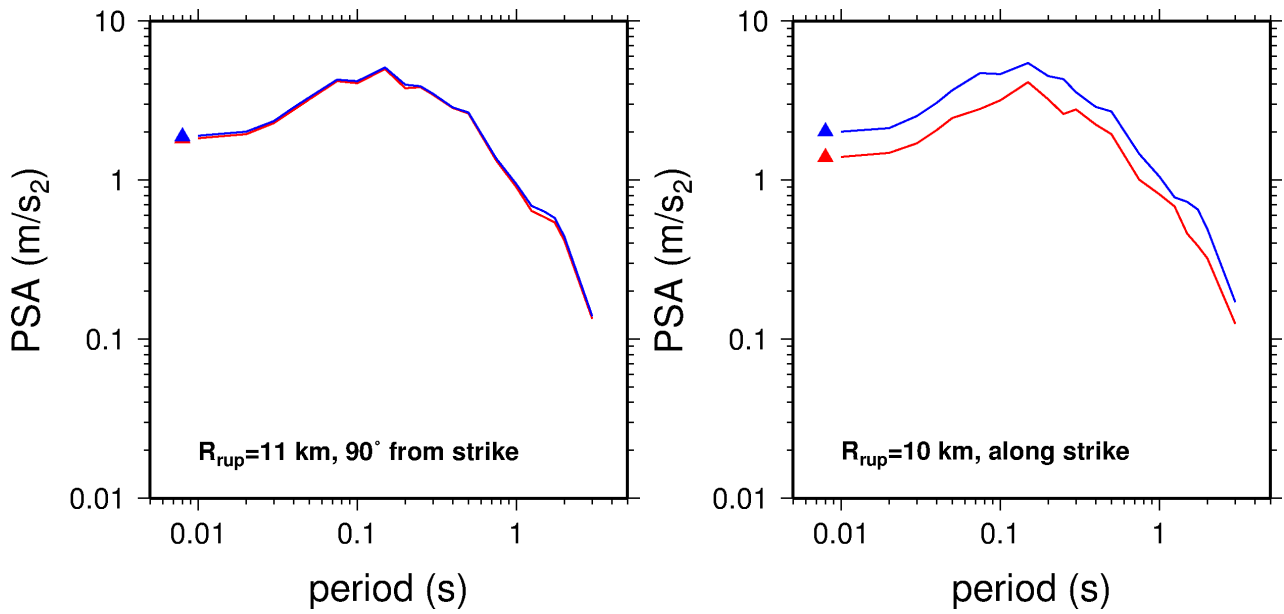


Figure 3: Comparison of the response spectra for $M_w=6$, obtained at similar R_{rup} 90° from the strike (left) and along strike (right) for the R_{mod} model (blue) and R_{eff} model (red).

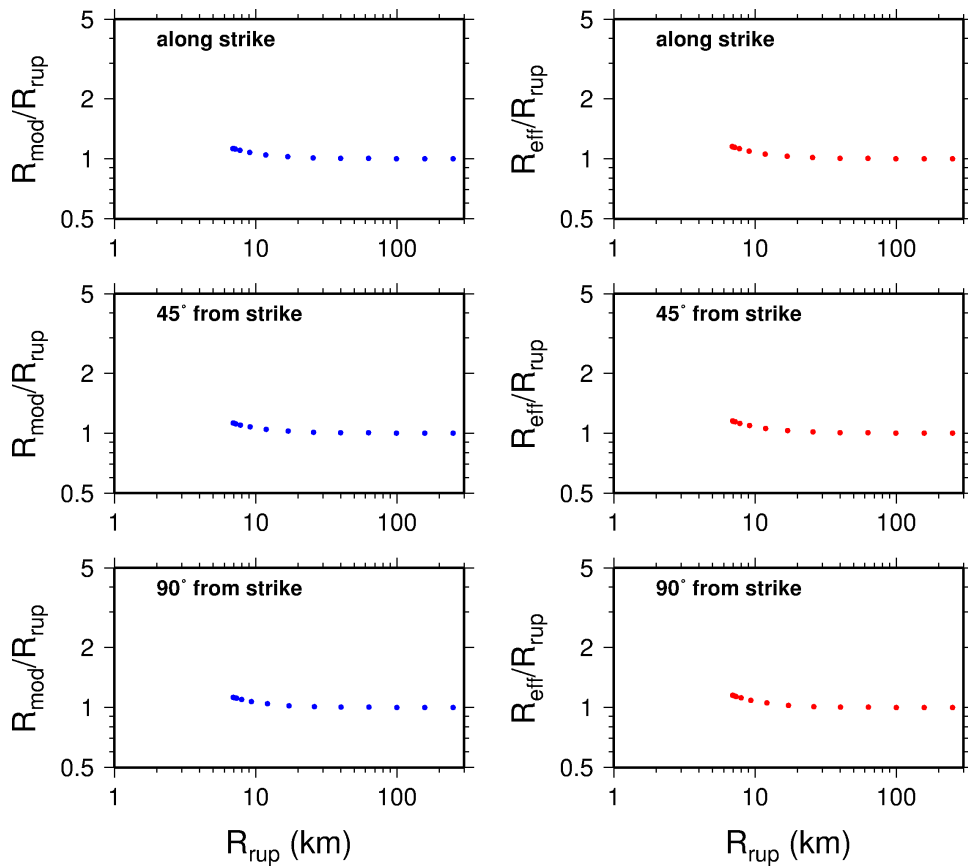


Figure 4: Ratios R_{mod}/R_{rup} (left) and R_{eff}/R_{rup} (right) as a function of R_{rup} for stations located along strike, and at 45 and 90° from strike, for $M_w=4$.

2.2. Input parameters

a) Simulation settings

In the initial version of the model, presented in the deliverable SIGMA-2012-D2-33 (Drouet, 2012), stochastic

simulations were performed for $M_w=3$ to 8. For each magnitude, 10 different scenarios were built varying fault orientation and stress parameter. Computations were then ran for 13 epicentral distances between 1 and 250 km, for each of which hypocenter-station azimuths varied between 0 and 360°. Finally, for each scenario (magnitude, mechanism/stress parameter, distance, azimuth), 10 different simulations were used varying the attenuation parameters (γ, Q_0, α). These additional simulations are not necessary and time consuming. Indeed, using only 1 simulation per scenario leads to similar results in terms of median and standard deviation of the simulations. These simulations only increased the sampling of the attenuation parameters which are found to have a relatively small influence on the simulations with respect to other parameters such as stress parameter or site effect as will be shown in the sensitivity study. Moreover, the only 10 different stress parameter values used for each magnitude lead to output stress drop distributions which are not densely sampled and with mean values that may be far away from the mean of the input distributions as illustrated in Figure 5 (left-hand side). As shown in this figure, in the initial study histograms of stress parameter have a relatively flat shape while the input model is a gaussian distribution. In order to overcome this problem, we decided to use 40 different mechanism/stress parameter values for each magnitude. In this case (Figure 5 right-hand side) the distributions are closer to gaussian distributions and mean values match with input mean values of the model.

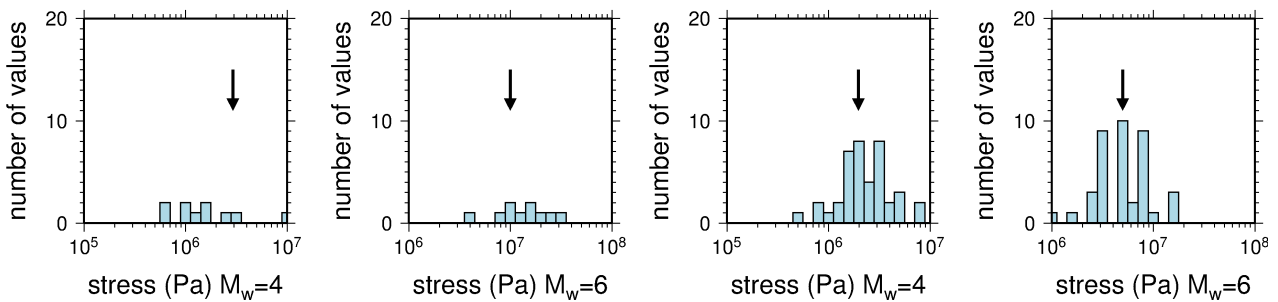


Figure 5: Histograms of stress drop values used for the simulations for $M_w=4$ and 6, as used in the initial study (left), and updated in this report (right). Black arrows indicate mean stress drop value from the input stress drop model (note that the median of the input stress parameter model has changed as will be explained later).

b) Stress drop model

Stress drops have been estimated through inversion of source, path and site effects for the three regions under study (Drouet et al., 2010), as well as for an aftershock sequence in the French West Indies using the same inversion scheme (Drouet et al., 2011). There is a considerable scatter in the inverted stress drops but there seems to exist a general trend of increasing stress drop with increasing magnitude in the range $M_w=3$ to 4.5. The data from the French West Indies mainly help to define a kink point at $M_w=4.6$ above which stress drop stops to increase with magnitude. For the larger magnitudes, stress drop values were taken from the NGA flatfile (<http://peer.berkeley.edu/nga/> last accessed March 2012). It is not clear however how these values were estimated and they may not be directly comparable to the other ones. Depending on the source model used, estimated stress drops may be different (Atkinson & Beresnev, 1997).

Based on these observations, the stress parameter model used in the previous study consisted of a linear increase between an anchoring point (which is region dependent), and a reference point at $M_w=4.6$ and stress parameter 10 MPa. The anchoring point is defined as the mean M_w and mean stress parameter determined by Drouet et al. (2010) for each region. Moreover, a decay of the stress parameter from 10 MPa to 5 MPa between $M_w=7.0$ and 7.5 was included. The initial stress parameter model is shown in Figure 6.

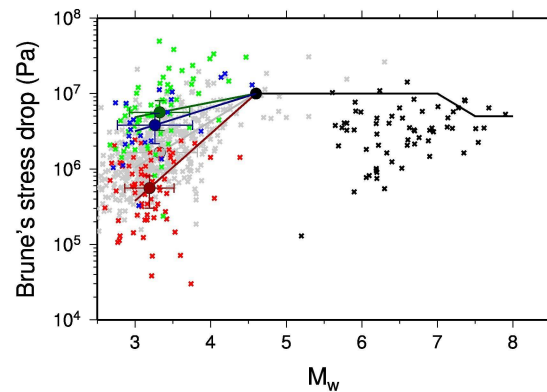


Figure 6: Stress parameter model used in the initial version of the stochastic GMPEs for France. Crosses are measured stress parameter values for the Alps (red), The Rhine Graben (blue), the Pyrenees (green), the French West Indies (grey), and California (black). Large colored dots reflect median M_w and stress drops from regional data sets, and the large black dot is located at the kink point $M_w=4.6$ and stress parameter=10 MPa.

Two recent stochastic models have been developed in Europe, one for the United Kingdom (Rietbrock et al. (2013)), and the other for Switzerland (Edwards & Fäh 2013; Chiou, 2011). They are both based on Fourier spectral analysis of weak-motion data followed by a stochastic simulation step using SMSIM (Boore, 2003). The analysis of the weak-motion data revealed a scaling of stress parameter which is modeled in the two stochastic models (Figure 7).

Rietbrock et al. (2013) built a stress parameter model based on observations for stable continental regions. The median stress parameter increases linearly from 0.7 MPa at $M_w=3$ to 10 MPa at $M_w=4.5$. Below and above these two magnitudes, the stress parameter remains constant. The stress parameter at each magnitude follows a log-normal distribution around the median with a magnitude-dependent standard deviation which decreases linearly from 0.6 at $M_w=1.5$ to 0.45 at $M_w=3.0$, and again to 0.4 at $M_w=4.5$, and then remains constant. Rietbrock et al. (2013) also used a constant stress parameter model with a median value of 1.8 MPa, and a standard deviation of 0.6. The two models are shown in Figure 7.

For the Swiss stochastic model based on Edwards & Fäh (2013) and Chiou (2011), the stress parameter model is anchored on a median value of 0.2 MPa at $M_w=2.5$, and then increases linearly up to a given point above which it remains constant. In Chiou et al. (2011) the kink point coordinates (M_{cut} , magnitude cutoff, and $\Delta\sigma$, the constant stress parameter value) are input parameters to the GMPE. M_{cut} can take values of 4.5, 5.0, 5.5, and 6.0, and $\Delta\sigma$ can take values of 3, 6, 12, 24 and 48 MPa (Figure 7). Note that Edwards & Fäh (2013) calibrated their model on intensity observations and found a best fit for a cut-off magnitude of 4.5 and stress parameter of 6.3 MPa. Note that no uncertainty is considered in this model.

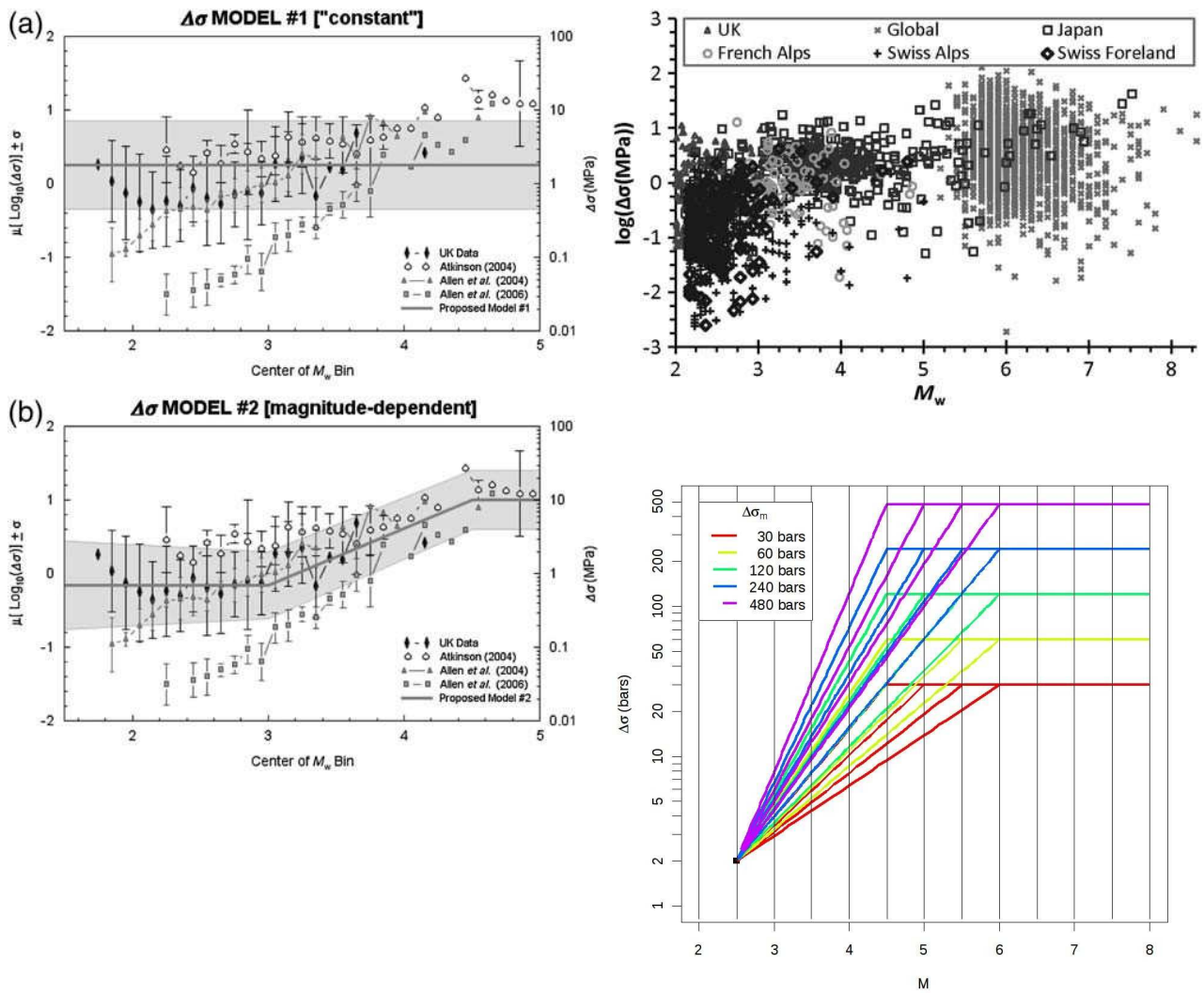


Figure 7: Stress parameter models used in the development of stochastic GMPEs for the UK (left, from Rietbrock et al., 2013), and for Switzerland (right, from Edwards & Fäh, 2013, and Chiou, 2011).

It is interesting to note that all the models do share similarities. In particular, the magnitude at which the transition between the increasing stress-parameter and the constant level occurs seem to converge at about magnitude 4.5. The level of the stress parameter at large magnitude is the most subjective parameter in these models. The choice of 10 MPa adopted in Rietbrock et al. (2013) and in the initial version of the model for France is more based on usual practice rather than on observations. The global study from Allmann & Shearer (2009) investigate global variations of stress drop for large events ($m_b > 5.5$) and found an average stress drop of 4 MPa without magnitude-dependence. They also found differences in average stress drop for active and stable regions, 3.31 and 5.95 MPa, respectively.

In order to take into account different stress drop level for large events, we build two alternative stress parameter models using stress drops of 5 and 2.5 MPa for large events (Figure 8). The models obviously differ for large magnitude because different stress drop values are used, but they also differ for small magnitude events since the rate of increase of the stress parameter with magnitude depends also on the stress drop used for large magnitude events. Note also that using a stress drop of 2.5 MPa would lead to decreasing stress parameter with magnitude for $M_w < 4.6$ in the Pyrenees and Rhine Graben regions, which we will not consider. Alternatively, we will use stress parameter models with a constant value of 2.5, 5.0 or 10 MPa over the whole magnitude range in order to test if the variable stress-parameter model is required to explain observed data. All these models will be used in a testing procedure with observed data. The formulation of the different models is given below:

- Stress parameter for large magnitude 10 MPa
 - Alps:

$$\ln(\Delta\sigma) = \begin{cases} 6.703216 + 2.046715 \times M_w \text{ MPa} & \text{for } M_w < 4.6 \\ 10 \text{ MPa} & \text{for } M_w \geq 4.6 \end{cases}$$

- Pyrenees

$$\ln(\Delta\sigma) = \begin{cases} 14.062932 + 0.446776 \times M_w \text{ MPa} & \text{for } M_w < 4.6 \\ 10 \text{ MPa} & \text{for } M_w \geq 4.6 \end{cases}$$

- Rhine Graben

$$\ln(\Delta\sigma) = \begin{cases} 12.806811 + 0.719846 \times M_w \text{ MPa} & \text{for } M_w < 4.6 \\ 10 \text{ MPa} & \text{for } M_w \geq 4.6 \end{cases}$$

- Stress parameter for large magnitude 5 MPa

- Alps:

$$\ln(\Delta\sigma) = \begin{cases} 8.272197 + 1.554936 \times M_w \text{ MPa} & \text{for } M_w < 4.6 \\ 5 \text{ MPa} & \text{for } M_w \geq 4.6 \end{cases}$$

- Pyrenees

$$\ln(\Delta\sigma) = \begin{cases} 15.872194 - 0.097238 \times M_w \text{ MPa} & \text{for } M_w < 4.6 \\ 5 \text{ MPa} & \text{for } M_w \geq 4.6 \end{cases}$$

- Rhine Graben

$$\ln(\Delta\sigma) = \begin{cases} 14.498678 + 0.201353 \times M_w \text{ MPa} & \text{for } M_w < 4.6 \\ 5 \text{ MPa} & \text{for } M_w \geq 4.6 \end{cases}$$

- Stress parameter for large magnitude 2.5 MPa

- Alps:

$$\ln(\Delta\sigma) = \begin{cases} 9.840951 + 1.063229 \times M_w \text{ MPa} & \text{for } M_w < 4.6 \\ 2.5 \text{ MPa} & \text{for } M_w \geq 4.6 \end{cases}$$

Regarding the standard deviation of the stress parameter, Cotton et al. (2013) used the Brune's source model (Brune, 1970, 1971) and the random vibration theory (Mc Guire & Hanks, 1980) to estimate a relationship between the standard deviation of stress drop and of PGA:

$$\sigma_{\ln(\text{stress drop})} = \frac{6}{5} \sigma_{\ln(\text{PGA})}$$

Considering various empirical GMPEs, they estimated standard deviations of stress parameter between 0.26 and 0.59 in natural log units (between 0.11 and 0.26 in base 10 log). They also showed that stress parameter variability indicated in studies using spectral analysis of Fourier spectra is 3 to 4 times larger, linked to the fact that uncertainties in corner frequency measurement lead to large uncertainties in stress parameter. Some GMPEs (e.g Abrahamson & Silva, 2008; Chiou & Youngs, 2008) include a variable total uncertainty with magnitude, smaller event showing larger uncertainty. This issue is still not resolved and could be simply an effect of poor quantification of predictive variables (magnitude, distance) for the small events (Bommer et al., 2007) rather than reflecting a real difference in the physical process. Regarding stress parameter we will assume a constant uncertainty of 0.3 in base 10 logarithm unit. Note that Rietbrock et al. (2013) used a magnitude-dependent uncertainty for the stress parameter.

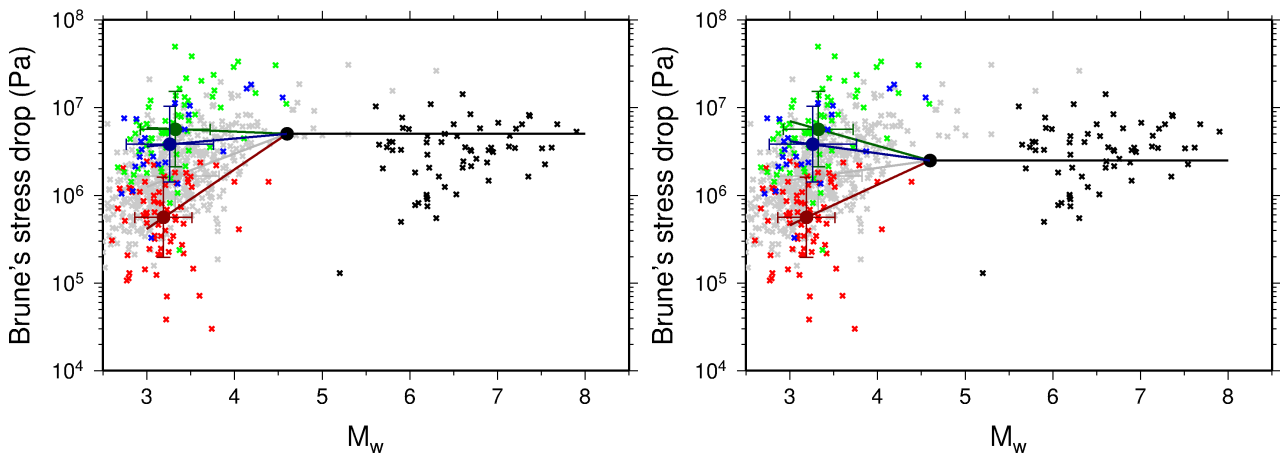


Figure 8: Two alternative stress parameter models regarding stress drop level for large events ($M_w > 4.6$): 5 MPa (left), and 2.5 MPa (right). Crosses are measured stress parameter values for the Alps (red), the Rhine Graben (blue), the Pyrenees (green), the French West Indies (grey), and California (black). Large colored dots reflect median M_w and stress drops from regional data sets, and the large black dots are located at the kink point $M_w = 4.6$ and stress parameter = 5.0 (left) and 2.5 (right) MPa.

c) Site model

The site model uses the generic site amplification functions of Boore & Joyner (1997) which are parametrized in terms of v_{S30} (average shear-wave velocity over the top 30 meters) as in Cotton et al. (2006). However, since site with the same v_{S30} may present different amplifications at different frequencies we used different site amplification functions, built from the generic functions and assuming a log-normal distribution. The value of sigma to use in this process is arbitrarily fixed to 0.2 in \log_{10} unit. The high-frequency attenuation parameters K is determined from the Van Houtte et al. (2011) correlation between K and v_{S30} . A log-normal distribution is also used to propagate uncertainties with a standard deviation of 0.2 which covers the observations from Van Houtte et al; (2011). The resulting site amplifications and kappa values used in the simulations are shown in Figure 9. As a comparison, observed site amplifications for the RAP stations as determined in Drouet et al. (2010) are shown in Figure 10. There is a very large variability in the observed amplifications, and the variability in amplification between EC8 class A site is almost as large as the variability between all the stations. It should be noted that EC8 class for the French RAP station are estimated using data from various different approaches and are not very homogeneous and accurate (Régner et al., 2010).

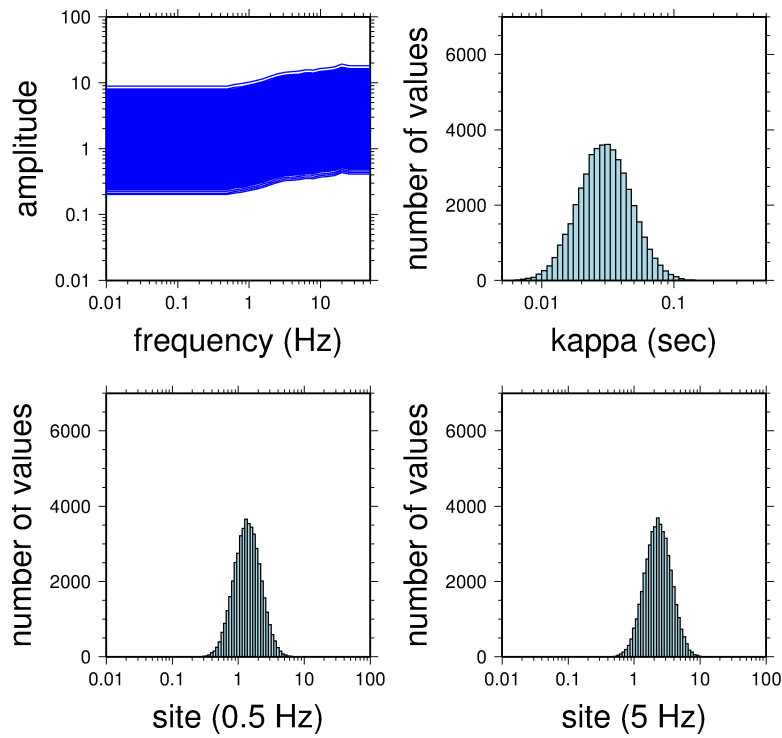


Figure 9: Site amplification functions (top left), histogram of kappa values (top right), and distribution of site amplification at 0.5 Hz (bottom left), and 5 Hz (bottom right), using $\sigma=0.2$ in \log_{10} units.

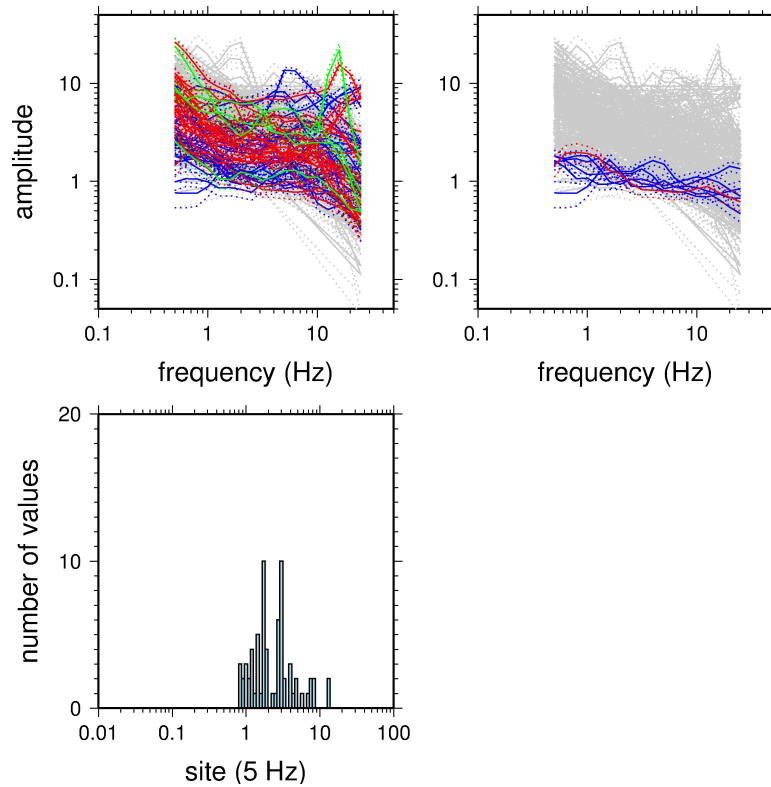


Figure 10: Site amplifications from Drouet et al. (2011) for all the stations in the Alps, Pyrenees and Rhine Graben. Mean amplification is shown as solid line and mean \pm -sigma as dotted line. All stations (grey); Right: EC8 class A stations (blue: Alps; red: Pyrenees; green: Rhine Graben); Left: stations with amplification lower than 2 (blue: Alps; red: Pyrenees; green: Rhine Graben). Histogram of the observed amplification at 5 Hz for the stations with EC8 class A (bottom).

d) Attenuation model

In the previous development of the stochastic models for France, the results of Drouet et al. (2010) were further analysed using a bootstrap analysis in order to better define the uncertainties on attenuation parameters. The results are summarized in Table 1. In order to increase the variability, the uncertainties on the attenuation parameters were arbitrarily increased to 0.1, 0.2 and 0.05 for γ , Q_0 , and α , respectively.

However, there is already a risk of double counting uncertainties since correlations between attenuation parameters are not taken into account. Moreover, the influence of the attenuation parameters is of second order compared to stress parameter, site amplification and kappa, at least for PGA, as will be shown in the sensitivity analysis later on. Consequently, in the current version of the stochastic models, the uncertainties on attenuation parameters used are those from Table 1.

The different attenuation models used in the simulations, after random sampling of the attenuation parameters are compared in Figure 11, using the distributions as defined in the previous deliverable SIGMA-2012-D2-33 (Drouet, 2012), and in the present study.

Table 1: Attenuation parameters for the three regions under study

	γ	$\log_{10}(Q_0)$	α
Alps	1.04 ± 0.07	2.52 ± 0.12	0.28 ± 0.08
Pyrenees	1.17 ± 0.05	2.90 ± 0.08	0.15 ± 0.06
Rhine Graben	1.04 ± 0.12	2.92 ± 0.22	0.11 ± 0.14

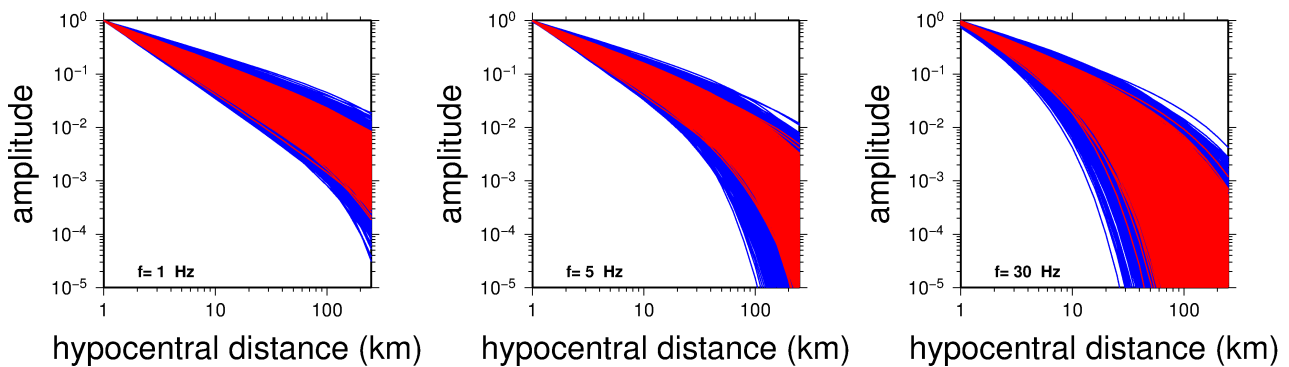


Figure 11: Comparison of the attenuation models used in the simulations using standard deviations on attenuation parameters as determined in the bootstrap analysis presented in SIGMA-2012-D2-33 (Drouet, 2012) (red), and using the same standard deviations slightly increased as also presented in SIGMA-2012-D3-33 (blue).

3. Regression method

Synthetic data produced by the stochastic simulations is subsequently regressed assuming a functional form in order to produce a GMPE. There exists various types of functional forms in the literature from very simple ones including only a linear magnitude term, and a single distance term (Berge-Thierry et al., 2003), to very complex ones like the recent NGA equations. In this study we want to keep the functional form as simple as possible.

There are some physical constraints one can use to define the functional form. First, Fukushima (1996) showed that a simple linear magnitude term is not consistent with the theory, and recent GMPEs include a quadratic magnitude term. Second, the distance term can be split into two contributions from the geometric attenuation which leads to a term in $\log(R)$, and the anelastic attenuation which gives a term in R . When the number of data is small it may be difficult to resolve both terms simultaneously (Akkar & Bommer, 2007). In our case, since simulated data are abundant, we will use both terms. The geometrical spreading is also magnitude-dependent as observed by Cotton et al. (2008), and may be explained as a finite-fault effect (Anderson, 2000). An analysis of the physical phenomena that cause a magnitude-dependent decay is under way within the SIGMA project (Dujardin, SIGMA-2013-D2-73). Each set of stochastic data corresponds to a single site condition and consequently no site term is included. It is also usual to have a term in GMPEs to reflect differences due to the different style-of-faulting types, but this is also not included in the present study since the simulations do not include such term. Two regression techniques are also compared, the standard least-squares

and the random-effect method (Joyner & Boore, 1993).

3.1. Test on the input parameters

The following equation gives the functional form that is adopted considering the above-mentioned constraints:

$$\ln(y) = b_1 + b_2 \times (M_w - 8) + b_3 \times (M_w - 8)^2 + (b_4 + b_5 \times M_w) \times \ln(\sqrt{(R_{rup}^2 + b_6^2)}) + b_7 \times R_{rup}$$

Both regression methods used require an initial guess of the parameters. In order to analyse the influence of these input coefficients we defined three very different sets of coefficients (Table 2). The first one follows some physical considerations on the different terms. For example, the scaling with magnitude has been observed to decrease with increasing magnitude (Douglas & Jousset, 2011). Consequently, we assumed that the b_3 term is negative. Also, the term b_7 which reflects anelastic attenuation is chosen small and negative. For the two other sets, all the input parameters have the same values, 0.1 or -2.0, respectively. Figure 12 shows the coefficients and sigma (standard deviation) determined using least-squares regression from the three input models. The GMPE coefficients are absolutely insensitive to the starting model.

Table 2: Starting models used for the least-squares regression.

Coefficient	b1	b2	b3	b4	b5	b6	b7
Starting model 1	0.0	-1.0	-0.1	-1.0	0.5	8.0	-0.002
Starting model 2	0.1	0.1	0.1	0.1	0.1	0.1	0.1
Starting model 3	-2.0	-2.0	-2.0	-2.0	-2.0	-2.0	-2.0

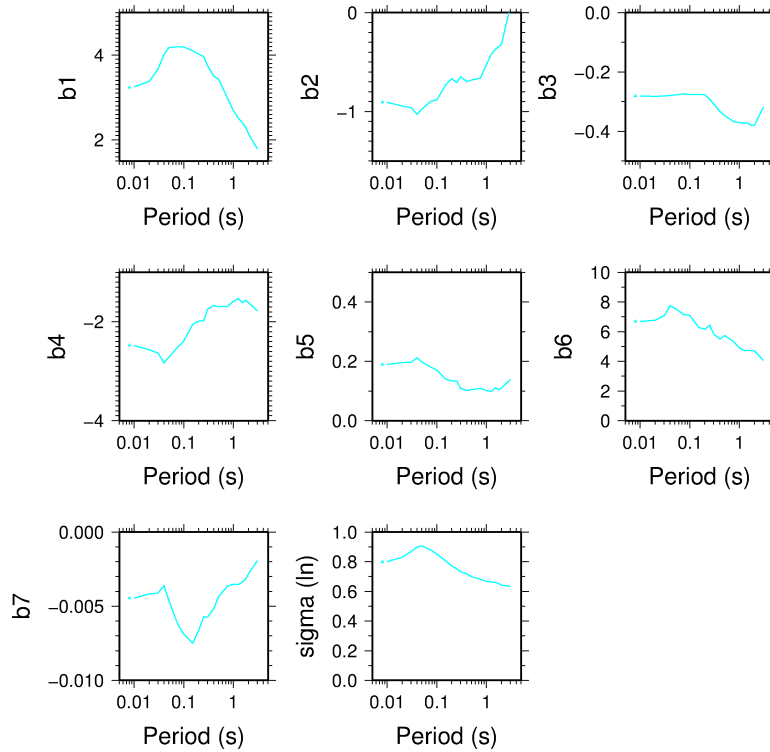


Figure 12: Comparison of the coefficients determined using least-squares regression and the three different starting models presented in Table 2 (starting model 1: blue; starting model 2: black; starting model 3: cyan).

Apparently the random regression method is more sensitive to the input model. Figure 13 shows the coefficients determined using both least-squares and random effect methods from the input model 1 of Table 2. The results from the random effect method present rapid variations with period for some coefficients. To overcome this problem, a two-step scheme is used, first the coefficients are determined using the least-squares method, and then these are used as input for the random effect method. The results of this approach are also shown in Figure 13. In this case the output coefficients do present smooth variations with period. One may not that the terms b_1 and b_6 are slightly different between the two

methods.

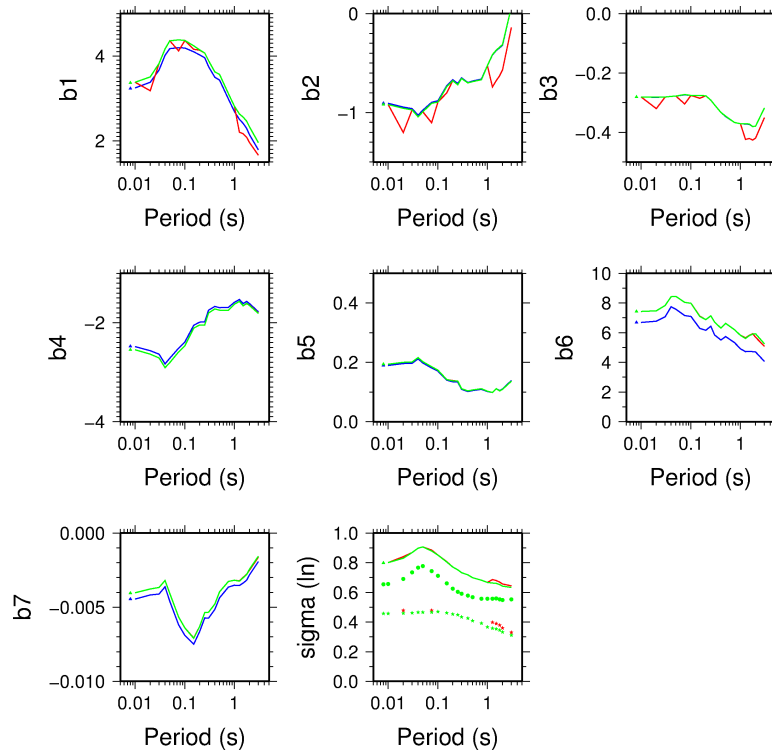


Figure 13: Comparison of the coefficients determined using least-squares regression with starting model 1 from Table 1 (blue), and using random-effect regression with starting model 1 from Table 1 (red), and with the results from the least-squares regression as starting model (green).

3.2. Test on the regression form

There are two factors in the regression form that may be discussed. First, we used in the magnitude terms ($M_w - 8$). This is a completely arbitrary choice. We performed test without the -8 , and the models are strictly the same, although the absolute values of the coefficients change. The other term to be discussed is the b_6 term, the pseudo-depth. Figure 14 Shows synthetic PGAs and regressed model for $M_w = 4$ and 7 , using two different distance metric (Joyner-Boore and rupture distance). Clearly, the b_6 term is necessary to reproduce the near-source saturation, especially when the rupture distance is used due to the limited amount of close distances in this case.

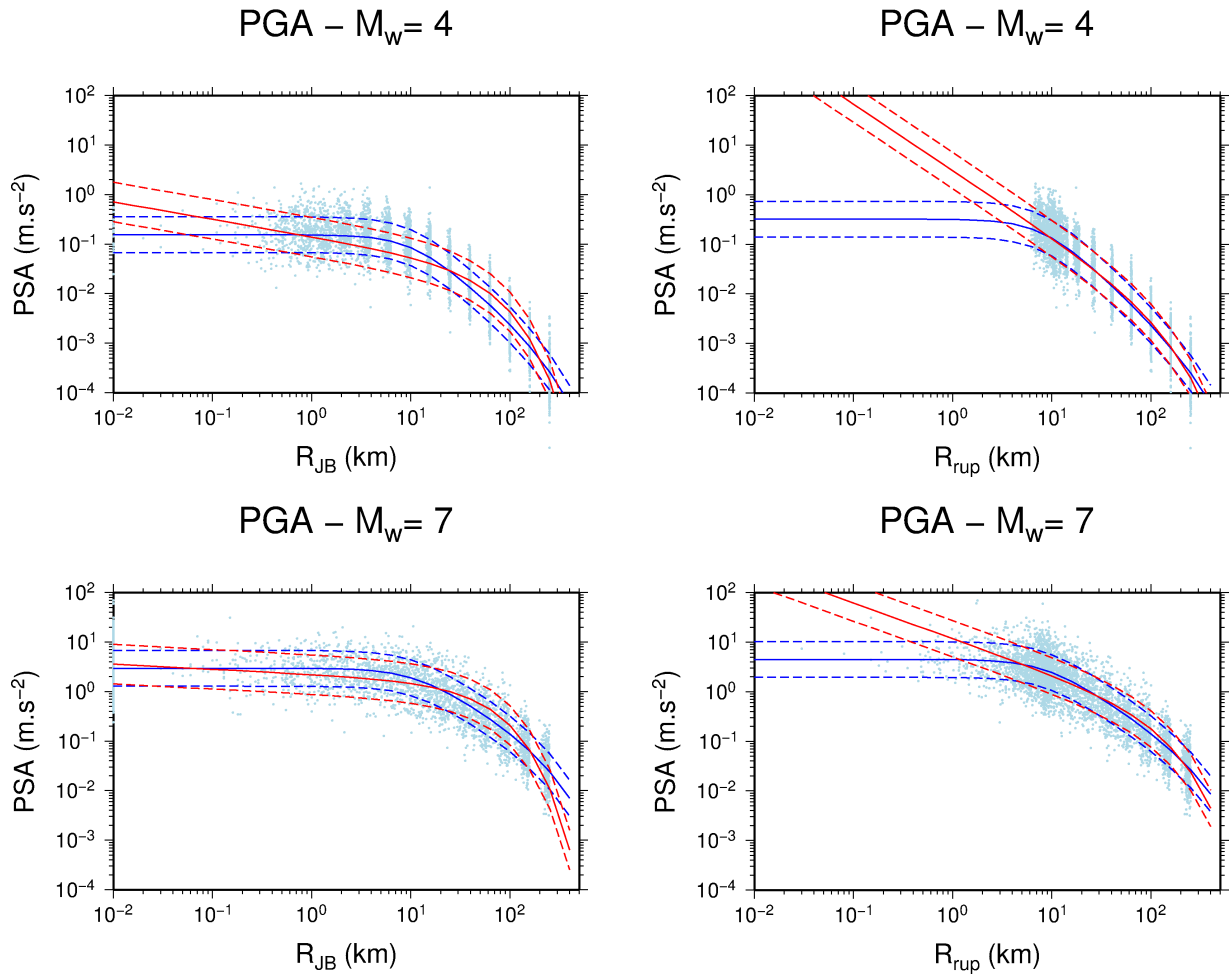


Figure 14: Stochastic simulated PGA (light blue dots) for $M_w=4$ (top) and $M_w=7$ (bottom) plotted versus Joyner-Boore distance (left) and rupture distance (right). Regressed models including the b_6 term (blue) and without the b_6 term (red) are also plotted.

3.3. Test using different distance metric

Figure 15 shows the coefficients determined using the least-squares method and the first starting model in Table 2, for different distance metrics. The shapes of the coefficients versus period are similar in any case. The model using the Joyner-Boore distance gives a low b_1 coefficient and a high b_4 coefficient compared to the other models. The model using rupture distance gives a slightly higher b_7 term (anelastic attenuation). The term b_6 is the most variable, it is the highest for epicentral distance, followed by Joyner-Boore distance, rupture distance, and hypocentral distance. It makes sense since rupture and hypocentral distances already take into account some depth of the hypocenter while the other two distance metrics do not. Note also slightly lower sigmas for rupture and Joyner-Boore distances as compared to the other ones. This may be explained by a better representation of finite-fault using these two distance metrics.

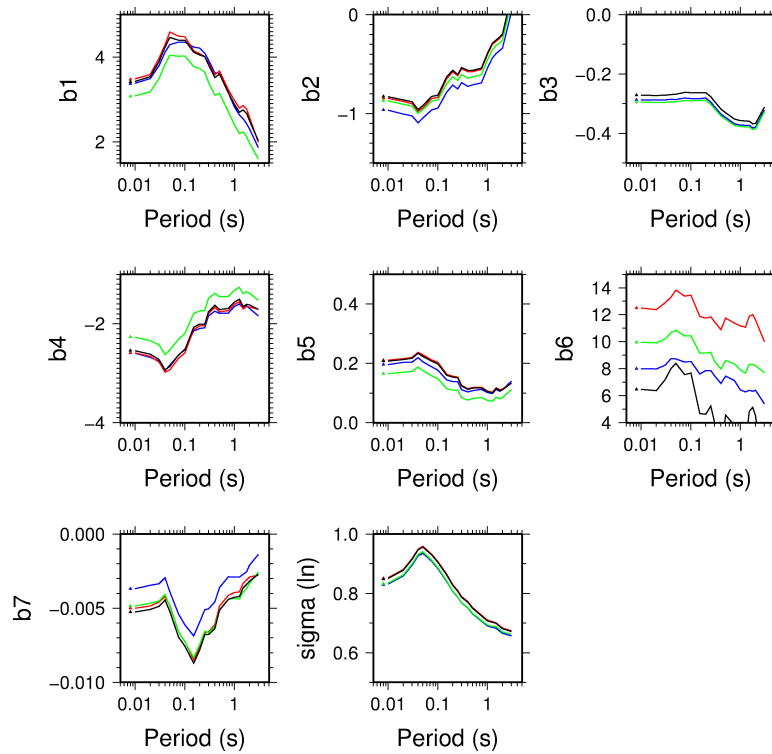


Figure 15: Comparison of the coefficients determined using least-squares regression with starting model 1 from Table 2 (blue), and using different distance metrics (rupture distance: blue; epicentral distance: red; Joyner-Boore distance: green; hypocentral distance: black).

4. Sensitivity study

One of the main remarks about the previous version of the stochastic GMPEs for France made by the SIGMA Scientific Committee concerned the uncertainties. Several input parameters are needed for the simulations. These parameters are determined with some uncertainty which is propagated into the simulations. In order to assess the influence of each single parameter uncertainty on the total GMPE uncertainty, a sensitivity study is performed. Simulations are made fixing all the parameters except one at a time for which uncertainty is considered and propagated. The different cases analysed are:

- 1: “No uncertainty”: Faults are all vertical, with fixed azimuth (to the North), and the hypocenter is always in the middle of the fault along strike and at a depth of 70% of fault width along width. Fault dimensions are estimated using Wells & Coppersmith (1994) relationships.
- 2: “Uncertainty on duration”: Uniform distributions are considered at the nodes of the duration model (see Drouet, 2012).
- 3: “Uncertainty on the fault plane”: Azimuth and dip of the fault, as well as the hypocenter position is randomly determined for each scenario. Moreover, in order to compute fault dimensions, the moment magnitude used in the Wells & Coppersmith (1994) relationships is randomly selected from a normal distribution with mean the actual M_w simulated and sigma 0.3.
- 4: “Uncertainty on Q_0 and α ”: The two parameters are considered simultaneously using a log-normal and a normal distribution, respectively, with means and sigmas as determined from the bootstrap analysis (see Table 1).
- 5: “Uncertainty on γ ”: A normal distribution is used with mean and sigma as determined from the bootstrap analysis (see Table 1).
- 6: “Uncertainty on κ ”: A log-normal distribution is considered with mean $\log_{10}(0.03)$ and sigma 0.2 (in \log_{10} unit).
- 7: “Uncertainty on site amplification”: A log-normal distribution is considered with mean equals to the generic amplification curve corresponding to $v_{S30}=800$ m/s, and sigma equals 0.2 (in \log_{10} unit).
- 8: “Uncertainty on stress parameter”: A log-normal distribution for the stress parameter is used with mean as

given in section 2.2.b and standard deviation equals to 0.3 (in \log_{10} unit).

- 9: “All uncertainties”: All the parameters are considered with their uncertainties.

The coefficients determined with each of these models are not significantly different as shown in Figure 16. However, the total GMPE uncertainty varies very much depending on the model. The major contributions to the total uncertainty are coming from the uncertainty on stress parameter, site amplification and κ for periods lower than 0.1-0.2 s (Figure 16). The influence of the uncertainty on κ decreases rapidly for longer periods and its influence becomes smaller than that of the uncertainty on γ . Such a decrease is also observed for the influence of the uncertainty on the stress parameter but it remains a large contributor to the total uncertainty. At small periods, the influence of the uncertainty on the anelastic attenuation parameters are of the same order as that of the geometrical decay exponent, but it also decreases at longer periods. Comparatively, the uncertainties linked with duration and fault plane orientation or hypocenter location on the faults are almost negligible.

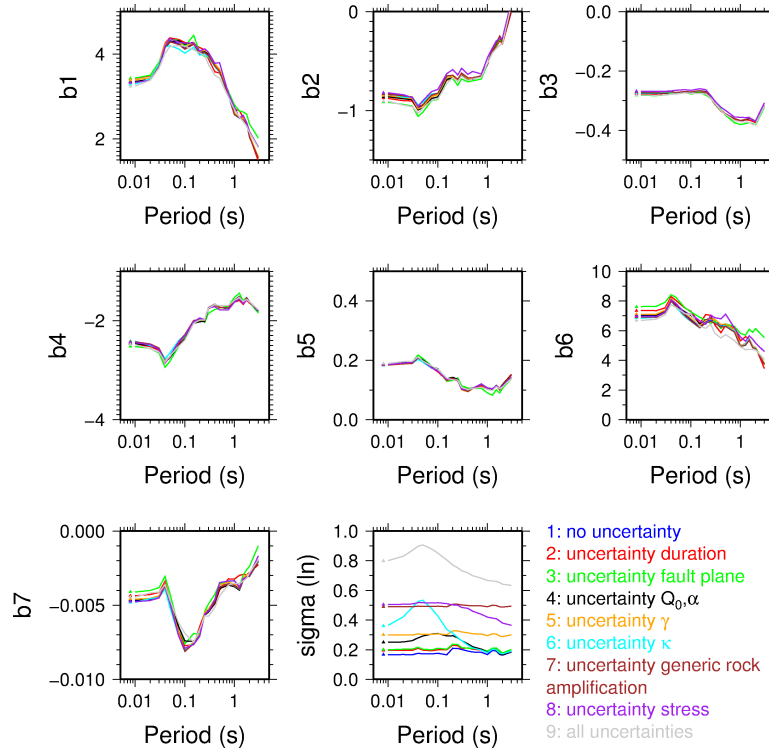


Figure 16: Comparison of the coefficients determined using least-squares regression with starting model 1 from Table 1 (blue), and for the sensitivity analysis cases (standard deviations on single parameters are considered at a time, see legend).

In order to further analyse the influence of each parameter uncertainty on the total uncertainty, we split the total uncertainty into within-event and between-event uncertainties (Al-Atik et al., 2010). Figure 17 shows the total uncertainty as well as the within-event and between-event terms for PGA, depending on the model of propagation of uncertainty. It shows that the between-event term is almost entirely driven by the uncertainty on the stress parameter which has a negligible impact on the within-event term. On the other hand, the uncertainties on attenuation parameters and site parameters (both kappa and site amplification) affect the within-event uncertainty and their impact on the between-event term is almost negligible. Table 3 gives the actual total, within-event and between-event uncertainties depending on the uncertainty propagation model.

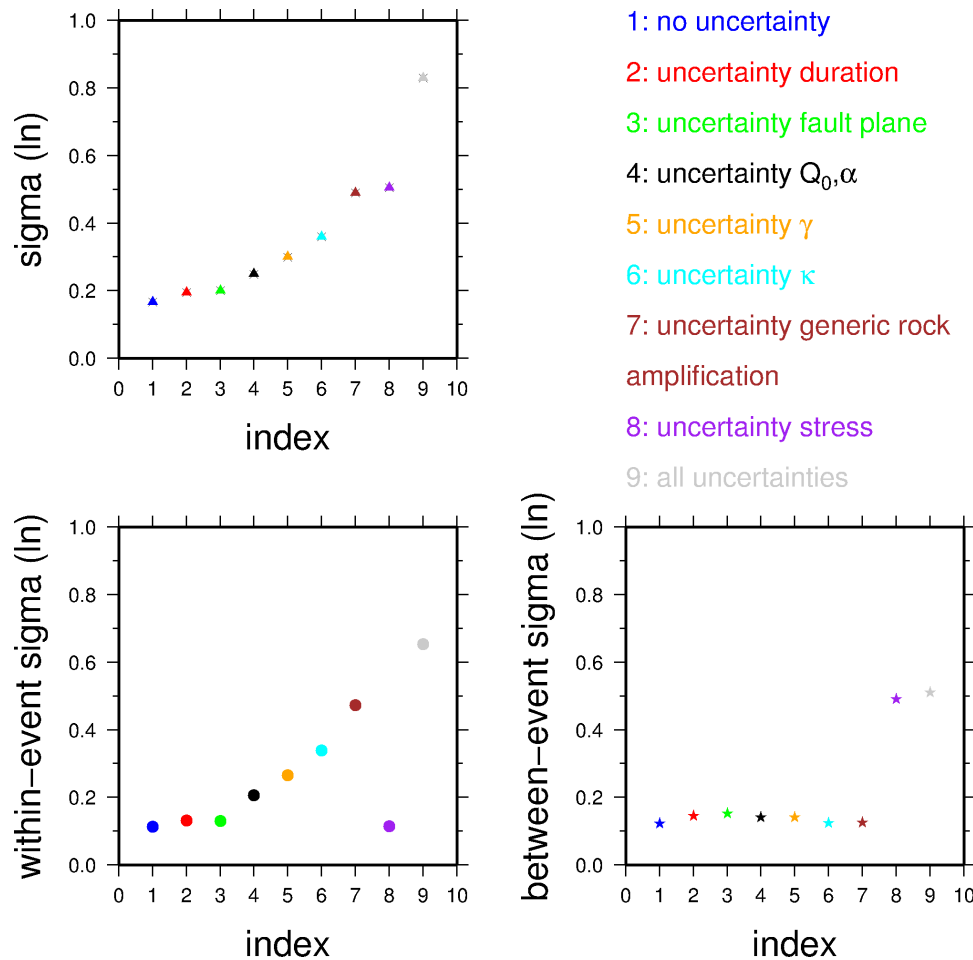


Figure 17: Comparison of total sigma (top), within-event sigma (bottom left), and between-event sigma (bottom right) for PGA using the models of the sensitivity study.

Table 3: Total, within-event and between-event sigma for PGA determined in the sensitivity study.

	Model 1 "No uncertainty"	Model 2 "Duration"	Model 3 "Fault plane"	Model 4 "Anelastic attenuation"	Model 5 "Geometric attenuation"	Model 6 "Kappa"	Model 7 "Site amplification"	Model 8 "Stress parameter"	Model 9 "All"
Total sigma (ln)	0.17	0.19	0.20	0.25	0.30	0.36	0.48	0.50	0.83
(% variation wrt Model 1)	(0)	(12)	(17)	(47)	(76)	(112)	(182)	(194)	(388)
Within-event sigma (ln)	0.11	0.13	0.13	0.21	0.26	0.34	0.47	0.11	0.65
(% variation wrt Model 1)	(0)	(18)	(18)	(91)	(136)	(209)	(327)	(0)	(500)
Between-event sigma (ln)	0.12	0.14	0.15	0.14	0.14	0.12	0.13	0.49	0.51
(% variation wrt Model 1)	(0)	(17)	(25)	(17)	(17)	(0)	(8)	(308)	(325)

The total sigma of 0.83 for PGA is compatible to results obtained from both stochastic GMPEs or empirical GMPEs. Figure 18 compares the total sigma for various GMPEs as a function of period and shows that the spread is considerable from 0.6 to 1.0 in natural logarithm. Figure 19 shows the within-event and between-event sigma's for the same models. Excluding Rietbrock et al. (2013) model, the within-event sigma seems less variable than the total sigma. Rietbrock et al. (2013) model does not consider variability in the site conditions which explains the low within-event sigma. Regarding the between-event sigma, models that include small magnitude events (Edwards & Fäh, 2013; Rietbrock et al., 2013; Rodriguez-Marek et al., 2011) present a higher between-event sigma around 0.5, than models including mostly events with M_w greater than 5 (Boore & Atkinson, 2008; Akkar & Bommer, 2010) leading to a between-event sigma of about 0.3. This difference decreases for periods greater than about 2 seconds.

The variability included in the present model regarding site conditions leads to an ergodic standard deviation, which is the variability of ground-motion including various sites and various sources. In the context of site-specific PSHA analysis, additional information on the site response may be used to remove the ergodic assumption. Al-Atik et al. (2010) showed that the single-station sigma (standard deviation of ground-motion at a single site) can be used as a lower bound value to the standard deviation that would be used in site-specific PSHA. Rodriguez-Marek et al. (2011) and Edwards & Fäh (2013) computed single-station sigmas. It is interesting to note that the within- and between-event terms from these two models are very close to the ones from the model presented in this analysis. Consequently, the single-station standard deviations of the two mentioned models could be used as a first approximation for site-specific analysis using the model presented in this study. However, for site-specific analysis, v_{s30} and/or κ may be known with a smaller variability than those used for the model presented. Due to the flexibility of the model, it is very easy to build a new model adjusted to specified site-conditions.

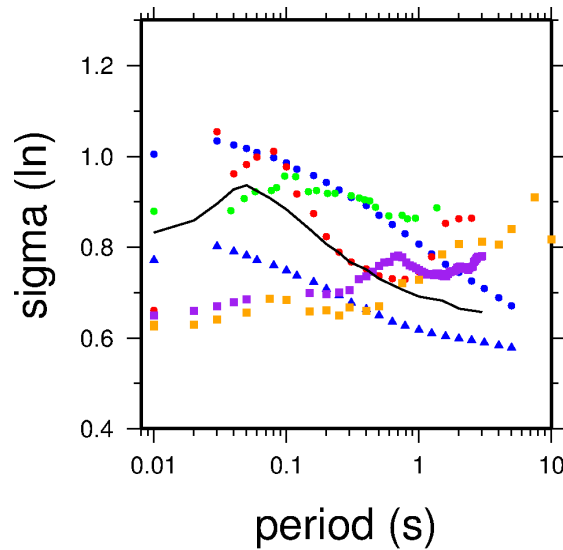


Figure 18: Comparison of total sigma from this study (solid black line), Edwards & Fäh (2013) (red dots), Rietbrock et al. (2013) (blue dots: variable stress model; blue triangles: constant stress model), Boore & Atkinson (2008) (orange dots), Akkar & Bommer (2010) (purple squares), and Rodriguez-Marek et al. (2011) (green dots).

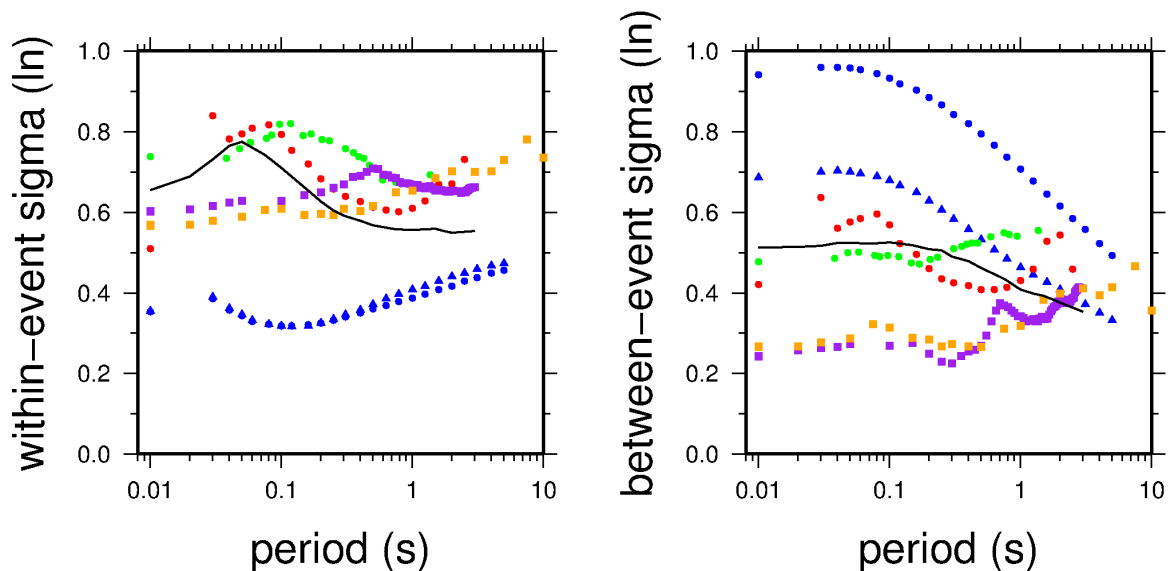


Figure 19: Comparison of within- and between-event sigma from this study (solid black line), Edwards & Fäh (2013) (red dots), Rietbrock et al. (2013) (blue dots: variable stress model; blue triangles: constant stress model), Boore & Atkinson (2008) (orange dots), Akkar & Bommer (2010) (purple squares), and Rodriguez-Marek et al. (2011) (green dots).

5. Stress parameter for large events

One of the question is how to choose the large magnitude stress parameter. Three models for each region (Alps, Pyrenees and Rhine Graben) are built using different stress parameter for the large events (2.5 Mpa, 5.0 Mpa, and 10 Mpa). Note that in our models, the stress parameter for large events ($M_w > 4.6$) remains constant. In order to quantify the fit between these models and data, we use two recent databases of strong ground-motion: the Resorce database (Akkar et al., 2011) built in the context of the SIGMA Project, and the NGA database which includes recordings from many active regions (Chiou et al., 2008).

The residuals between observations and predictions are analysed using the methods described in Scherbaum et al. (2004 and 2009). Normalised residuals with respect to a given GMPE are computed as:

$$\text{Norm. Residuals} = \frac{\log_{10}(\text{obs}) - \mu}{\sigma}$$

where μ and σ are the median ground-motion and the standard deviation, respectively, predicted by the GMPE (in base 10 logarithm). The mean, median, and standard deviation of the distribution of the normalised residuals are computed as well as the median of the LH distribution (see Scherbaum et al., 2004). The combination of this information may be used to rank (in a subjective way) the ability of the GMPE to fit the data distribution. Also the LLH criterion (see Scherbaum et al., 2009) is estimated which is a also measure of the quality of the fit. In this way, we can quantify which of the stress parameter model best describes recorded strong-motion data.

5.1. Testing using the European data

The stochastic models are compared to the data included in the Resorce database (Akkar et al., 2011). Only data corresponding to $M_w > 5$ are considered (which is the magnitude above which the stress parameter is constant in our stochastic models), and also data with $v_{s30} > 750$ m/s are used to be consistent with the definition of our models for rock sites. After the selection, data from $M_w = 5$ to 7.6, and $R_{JB} = 0$ to 547 km ($R_{rup} = 1$ to 548 km) are kept. 22 periods between 0.01 and 3 sec are used, including PGA and PGV which results in a total of 551 data points. Figure 20 shows the magnitude distance scatter of the selected data.

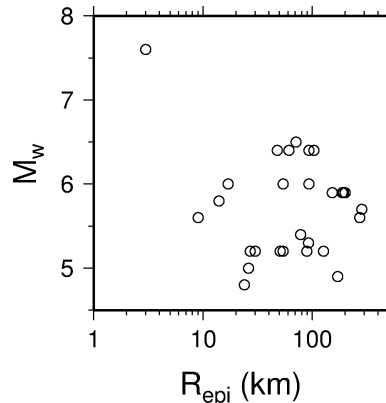


Figure 20: Magnitude-distance scatter for the rock data ($v_{s30} \geq 750$ m/s) included in the Resorce database.

The results of the residuals analysis are shown in Table 4. There is a general good agreement between the models and the data since good ranking scores are achieved (A or B), and LLH values are relatively small. Beauval et al. (2012) quantified the interval of variation of the LLH values using synthetic tests. They showed that LLH around 1.5-1.6 are indicating a very good fit, while for values above 3-4 the normalised residual distribution (which for a perfect fit would be Gaussian with zero mean and unit standard deviation: standard Gaussian distribution) moves away from the standard Gaussian distribution.

In the case of the models for the Alps, it seems clear that a stress parameter for large events of 5.0 Mpa leads to a better fit than the other two options (larger and smaller stress parameters). The mean, median, and standard deviation of the residuals improve, as well as the LH and LLH criterion. The same seems also true for the Rhine Graben models although the quality of the fit is not as good. For the Pyrenees, the results show the same quality of fit for the models using a stress parameter of 5 or 10 Mpa.

One can also note that the quality of the fit increases when the Joyner-Boore distance is used instead of the rupture distance, linked with a small decrease of the normalised residuals standard deviation. The difference is very small but it is observed with each model.

It is interesting to note that that standard deviations of the normalised residual distributions are close to 1, indicating that the GMPE standard deviation is coherent with data dispersion. In turn, it shows that the uncertainties on the input parameters are well defined.

Table 4: Analysis of the normalised residuals using Scherbaum et al. (2004, 2009) methods for the Resorce data.

Model	Distance metric	Mean normalised residuals	Median normalised residuals	Standard deviation normalised residuals	Median LH	Rank	LLH
Model for the Alps							
Stress par. 10 MPa	R_{rup}	-0.489 (B)	-0.558 (C)	1.030 (A)	0.425 (A)	C	2.263
Stress par. 5 MPa	R_{rup}	0.121 (A)	0.060 (A)	1.002 (A)	0.528 (A)	A	2.060
	R_{JB}	0.119 (A)	0.085 (A)	0.950 (A)	0.568 (A)	A	1.985
Stress par. 2.5 MPa	R_{rup}	0.656 (C)	0.611 (C)	1.031 (A)	0.476 (A)	C	2.401
Model for the Pyrenees							
Stress par. 10 MPa	R_{rup}	-0.085 (A)	-0.188 (A)	1.171 (B)	0.411 (A)	B	2.318
Stress par. 5 MPa	R_{rup}	0.447 (B)	0.373 (B)	1.123 (A)	0.467 (A)	B	2.378
	R_{JB}	0.449 (B)	0.393 (B)	1.038 (A)	0.486 (A)	B	2.247
Stress par. 2.5 MPa	R_{rup}	---	---	---	---	---	---
Model for the Rhine Graben							
Stress par. 10 MPa	R_{rup}	-0.686 (C)	-0.729 (C)	0.994 (A)	0.389 (B)	C	2.377
Stress par. 5 MPa	R_{rup}	-0.254 (B)	-0.289 (B)	0.975 (A)	0.518 (A)	B	2.057
	R_{JB}	-0.262 (B)	-0.283 (B)	0.950 (A)	0.528 (A)	B	2.024
Stress par. 2.5 MPa	R_{rup}	---	---	---	---	---	---

Figure 21 compares the Resorce data and the best fitting models in Table 4 using R_{rup} (i.e. models for the Alps and Rhine Graben with a stress parameter of 5 MPa, and model for the Pyrenees with a stress parameter of 10 MPa). The scaling with magnitude or distance of the three models are very similar and fit well the observed data. The scaling with magnitude was expected to be the same since in this magnitude range, the stress parameter is constant. The main difference between the models is the large distance attenuation observed in the model for the Alps and not in the other two. However, due to the limited amount of data for rock sites, such small differences are probably hidden by the uncertainties.

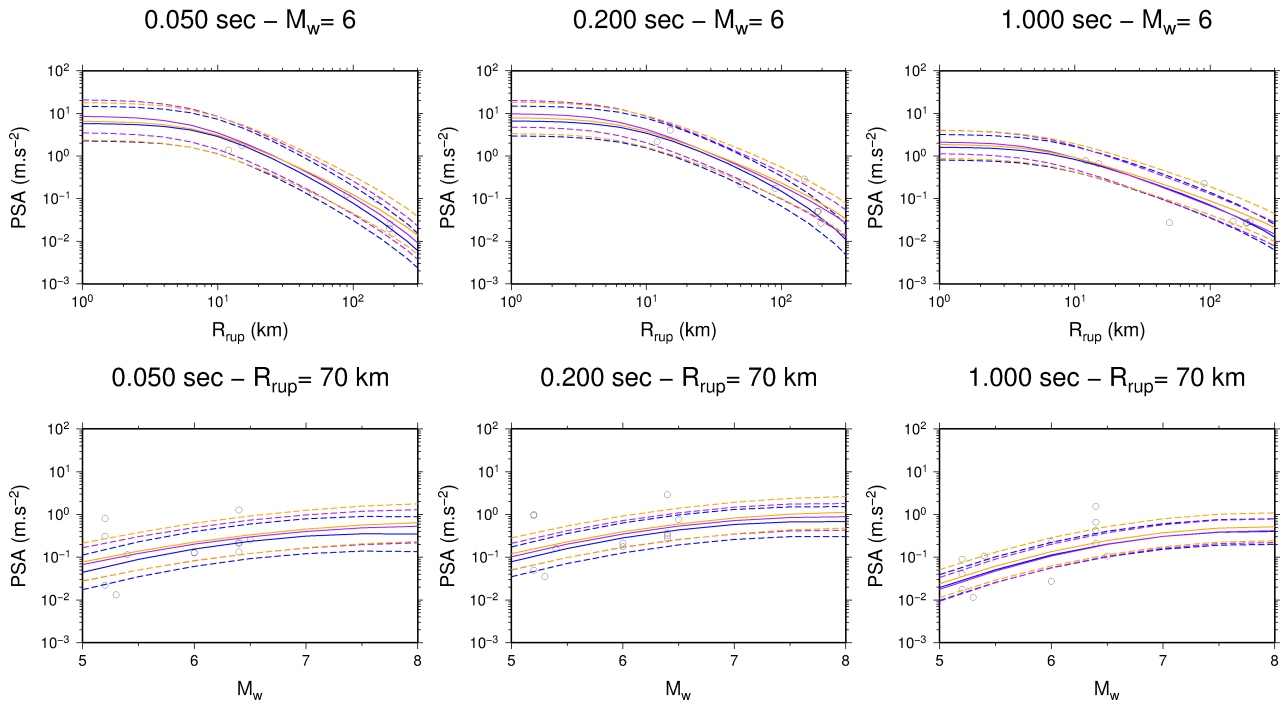


Figure 21: Spectral acceleration versus distance for $M_w=6$ (top) and magnitude for $R_{rup}=70$ km (bottom), for three periods 0.05 sec (left), 0.200 sec (middle), and 1.000 sec (right). Resorce data (circles) are compared to the three best fitting stochastic models in Table 5 using R_{rup} (i.e. models for the Alps and Rhine Graben with a stress parameter of 5 MPa plotted in blue and orange, respectively, and model for Pyrenees with a stress parameter of 10 MPa plotted in orange).

5.2. Testing using the NGA data

The stochastic models are compared to the data included in the NGA database (Chiou et al., 2008). Only data corresponding to $M_w \geq 5$ are used (which is the magnitude above which the stress parameter is constant in our stochastic models), and also data with $v_{S30} > 750$ m/s are used to be consistent with the definition of our models for rock sites. After the selection, data from $M_w=5.2$ to 7.9, and $R_{JB}=0$ to 365 km ($R_{rup}=0$ to 366 km) are used. 20 periods between 0.01 and 3 sec are used, including PGA and PGV which results in a total of 1420 data points. Figure 22 shows the magnitude distance scatter of the selected data.

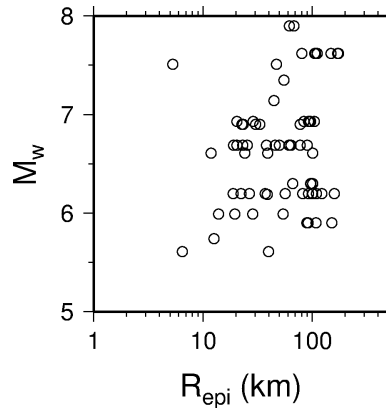


Figure 22: Magnitude-distance scatter for the rock data ($v_{s30} > 750$ m/s) included in the NGA database.

The results of the residuals analysis are shown in Table 5. The general ranking and LLH values are of the same order as for the Resorce data. However, in this case, the better agreement is achieved with the models for the Rhine Graben. The quality of the fit is equivalent for both stress parameter options (5 or 10 Mpa). For the two other sets of models, for the Alps and the Pyrenees, the models with a stress parameter of 10 MPa better fits the data, although for the Alps, the difference is very small.

Table 5: Analysis of the normalised residuals using Scherbaum et al. (2004, 2009) methods for the NGA data.

Model	Distance metric	Mean normalised residuals	Median normalised residuals	Standard deviation normalised residuals	Median LH	Rank	LLH
Model for the Alps							
Stress par. 10 MPa	R_{rup}	-0.436 (B)	-0.453 (B)	0.774 (A)	0.547 (A)	B	1.894
Stress par. 5 MPa	R_{rup}	0.361 (B)	0.395 (B)	0.877 (A)	0.504 (A)	B	1.975
	R_{JB}	0.397 (B)	0.432 (B)	0.877 (A)	0.500 (A)	B	1.993
Stress par. 2.5 MPa	R_{rup}	0.979 (D)	1.015 (D)	0.903 (A)	0.290 (C)	D	2.605
Model for the Pyrenees							
Stress par. 10 MPa	R_{rup}	0.222 (A)	0.220 (A)	0.936 (A)	0.536 (A)	A	1.993
Stress par. 5 MPa	R_{rup}	0.770 (D)	0.758 (D)	0.890 (A)	0.397 (B)	D	2.325
	R_{JB}	0.786 (D)	0.763 (D)	0.889 (A)	0.401 (A)	D	2.341
Stress par. 2.5 MPa	R_{rup}	---	---	---	---	---	---
Model for the Rhine Graben							
Stress par. 10 MPa	R_{rup}	-0.436 (B)	-0.453 (B)	0.774 (A)	0.547 (A)	B	1.894
Stress par. 5 MPa	R_{rup}	0.080 (A)	0.075 (A)	0.776 (A)	0.606 (A)	A	1.765
	R_{JB}	0.116 (A)	0.090 (A)	0.787 (A)	0.596 (A)	A	1.782
Stress par. 2.5 MPa	R_{rup}	---	---	---	---	---	---

Figure 23 compares the NGA data and the best fitting models in Table 5 using R_{rup} (i.e. models for the Alps and Pyrenees with a stress parameter of 10 MPa, and model for Rhine Graben with a stress parameter of 5 MPa). Again, the scaling with magnitude or distance are very similar and fit well with the observed data. One difference between the models is the slightly higher ground-motions predicted by the model for the Alps in the distance range 2 and 40 km. However, due to the limited amount of data for rock sites, such small differences are probably hidden by the uncertainties.

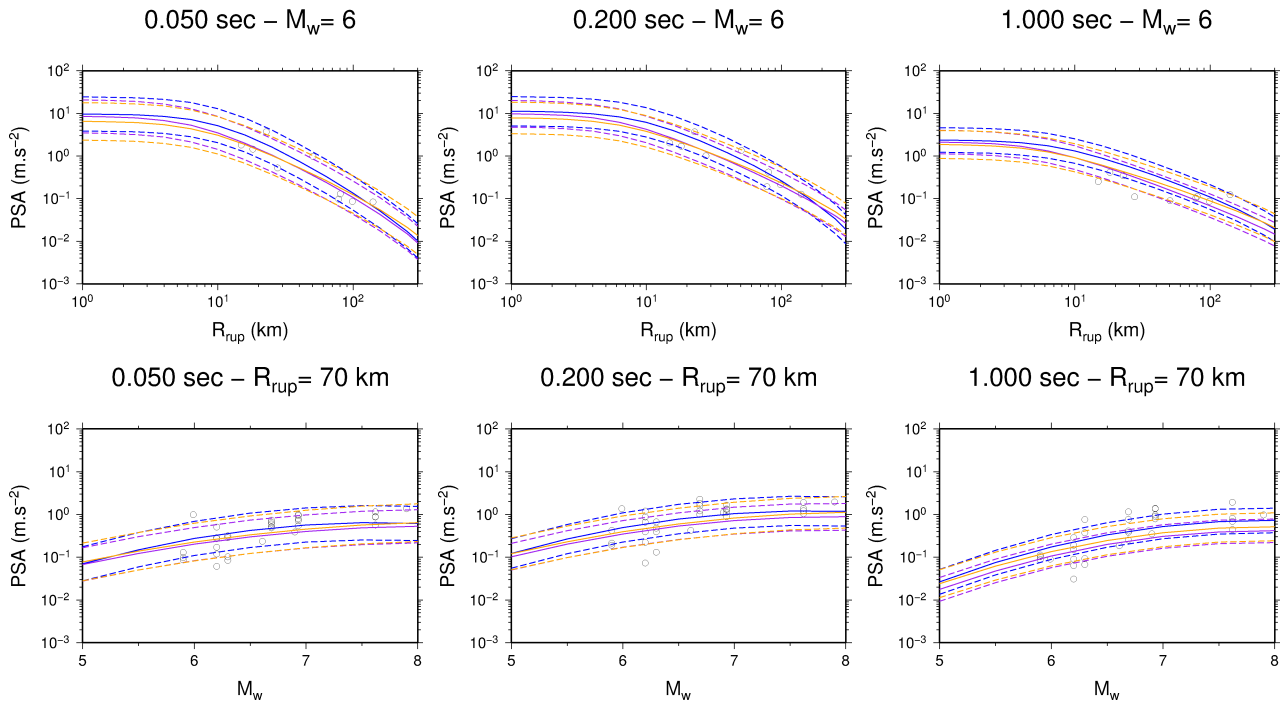


Figure 23: Spectral acceleration versus distance for $M_w=6$ (top) and magnitude for $R_{rup}=70$ km (bottom), for three periods 0.05 sec (left), 0.200 sec (middle), and 1.000 sec (right). NGA data (circles) are compared to the three best fitting stochastic models in Table 5 using R_{rup} (i.e. models for the Alps and Pyrenees with a stress parameter of 10 MPa plotted in blue and purple, respectively, and model for Rhine Graben with a stress parameter of 5 MPa plotted in orange).

6. Stress parameter for small events

Based on observations from weak-motion data there may be a need of a magnitude-dependent stress parameter in order to produce stochastic models (Edwards & Fäh, 2013; Rietbrock et al. 2013). In the deliverable SIGMA-2012-D2-33 (Drouet, 2012), a magnitude-dependent stress parameter was used (Figure 6). This initial model included a reduction of the stress parameter above magnitude 7. We believe that there is not enough justification for such a model, and will not be considered further. Instead, as shown in the previous paragraphs, we consider now several values for the large magnitude stress parameter: 2.5, 5 and 10 MPa. Using one or the other of these values also modifies the stress parameter model for the smaller magnitudes, since the slope of the model for the small magnitudes changes (Figure 24). Figure 24 clearly shows that a magnitude-dependent stress parameter model is needed for the Alps since the tests performed in the previous section indicate that stress parameter for large events has to be larger than 2.5 MPa in order to achieve a good fit with strong-motion data. However, for the Pyrenees and the Rhine Graben, the average stress parameters are close to 5 MPa, consequently, models with constant stress parameter may also be considered, and models with a large magnitude stress parameter of 2.5 MPa would lead to a decreasing stress parameter with increasing magnitude which we do not consider appropriate. Consequently, we decided to build models with both magnitude-dependent and constant stress parameter.

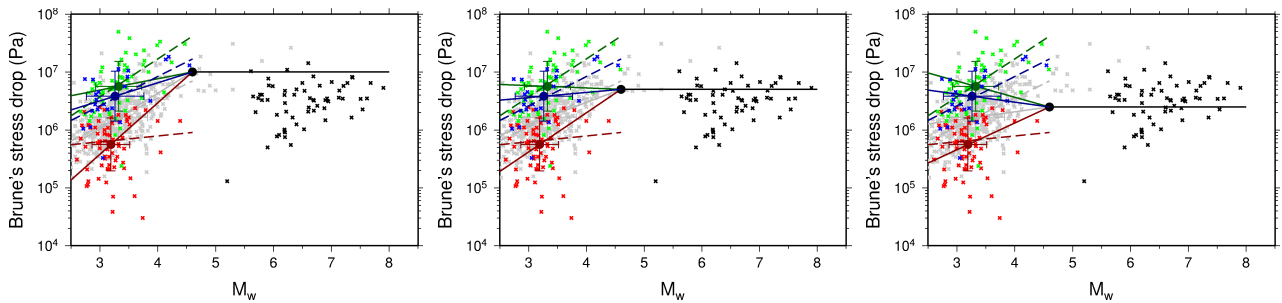


Figure 24: Stress parameter models for 3 different large magnitude stress parameter values: 10 (left), 5 (middle), and 2.5 (right) MPa. Stress parameter versus moment magnitudes for three regions of the French metropolitan area (Alps: red crosses; Pyrenees: blue crosses; Rhine Graben: green crosses) and for the French West Indies (grey crosses) are shown, as well as the average moment magnitudes and stress parameters for each

data set (circles). Stress parameter for the NGA data (<http://peer.berkeley.edu/nga/> last accessed March 2012) are also plotted (black crosses). The solid lines represent the regional stress drops models used in the simulations. The dashed lines are indicating the linear regressions between moment magnitude and stress parameter for the three regions.

In order to try to quantify which model best fits the data, we again used the testing methods of Scherbaum et al. (2004, 2009) using the data recorded by the French Accelerometric Network (Réseau Accélérométrique Permanent, RAP) used in Drouet et al. (2011), and data from the Pyrenean network (Réseau de Surveillance Sismique des Pyrénées, RSSP). Data from the RAP and RSSP have been already used jointly in Drouet et al. (2005). For the RAP and RSSP data, the v_{S30} are not known with precision, but there has been a great effort to compile available data and classify the data according to the EC8 (Régner et al., 2010). For the RSSP data, we assume that they all correspond to rock site EC8 class A because these stations have been installed on rock sites due to the nature of the network (dedicating to seismicity monitoring), and Drouet (2006) showed that they are less affected by site effect than the RAP stations. Finally, for the RAP stations, two other classifications are used. The first is based on the inverted site transfer functions of Drouet et al. (2010), stations showing amplifications less than 2 over the whole frequency band as classified as rocks (see Drouet, 2012). The second uses as rock sites, the reference sites chosen in the inversions presented in Drouet et al. (2010). Figure 25 shows the magnitude distance scatter for each of these data sets.

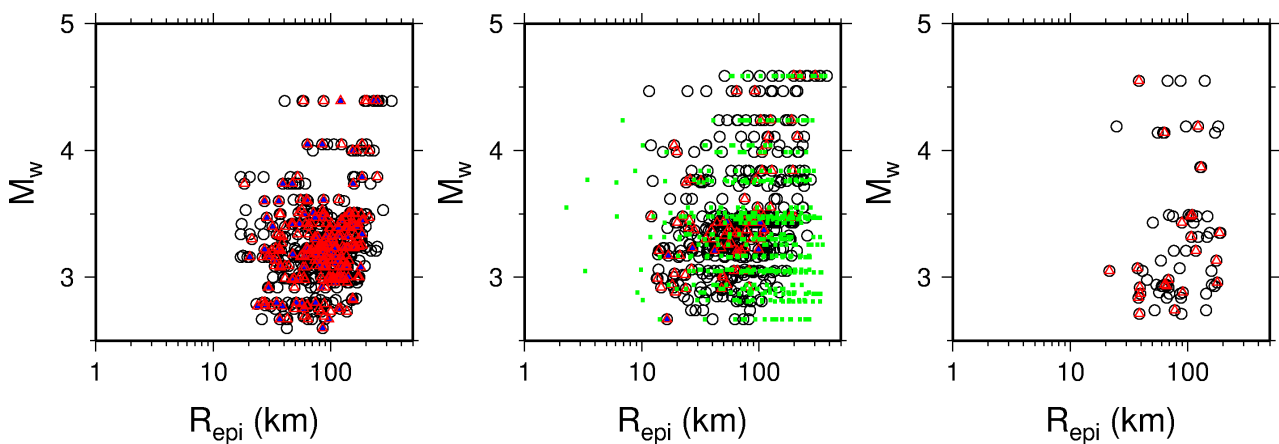


Figure 25: Magnitude versus epicentral distance scatters for the rock data recorded in the Alps (left), Pyrenees (middle), and Rhine Graben (right). Rock sites according to EC8 classes (empty circles), as well as rock sites according to the amplitude of the transfer functions (blue dots), and reference sites used in Drouet et al. (2010) are shown. Data from the RSSP are plotted as green squares.

Table 6 shows that the magnitude and distance ranges do not vary much depending on which rock site classification is used. On the other hand, the number of data varies much and this should be taken into account in the interpretation of the residuals analysis.

Table 6: Magnitude range, distance range and number of data for each region (Alps, Pyrenees, Rhine Graben) for different rock site classifications.

Region	Site classification	M_{\min}	M_{\max}	$R_{rup_{\min}}$	$R_{rup_{\max}}$	Ndata (20 periods between 0.01 and 3 sec)
Alps	EC8	17	329	2.6	4.4	7625
	Flat response	21	251	2.6	4.4	1932
	Reference stations	19	251	2.6	4.4	4514
Pyrenees	EC8	15	379	2.7	4.6	7574
	Flat response	17	302	2.7	4.6	194
	Reference stations	15	302	2.7	4.6	1589
	RSSP	8	368	2.7	4.6	7488
Rhine Graben	EC8	22	189	2.7	4.6	1212
	Flat response	---	---	---	---	0
	Reference stations	22	186	2.7	4.6	391

6.1. Alps

Table 7 shows the results of the residuals analysis for the Alps. Both types of models are tested with either a constant or a magnitude-dependent stress parameter for small events. For each type, 3 values of stress parameter for large events

are used 2.5, 5, and 10 MPa. The testing is also performed for the different site classifications. Clearly, the models with the magnitude-dependent stress parameter are leading to better results than the models with constant stress parameter. This was expected as mentioned previously because inverted stress parameters for the small events in the Alps are low. The results using the EC8 classification, indicate that a better fit is obtained with a stress parameter for large events of 5 MPa. For the other site classifications smaller LLH values are obtained also for the model with a stress parameter for large events of 5 MPa, but the difference in the results is very slight. Another observation is that again, using the Joyner-Boore distance leads to a smaller standard deviations of the normalised residuals as already observed in the testing with strong-motion data. Finally, we compare the fit for the standard rock model used (i.e. $v_{S30}=800$ m/s and $\kappa=0.03$ sec), with the fit using a hard rock site model (i.e. $v_{S30}=2000$ m/s and $\kappa=0.01$ sec) using the reference stations used in the inversions by Drouet et al. (2010) which we believe to be closer to hard rock conditions. The quality of the fit does not improve much but the mean and median of the normalised residuals distribution gets closer to 0, while for the standard rock model they were slightly negative indicating a slight over-prediction of the model. This is coherent with the fact that the reference sites used in Drouet et al. (2010) were chosen so that to keep the best rock sites closer to hard rock conditions.

Table 7: Analysis of the normalised residuals using Scherbaum et al. (2004, 2009) methods for the data recorded in the Alps.

Model	Distance metric	Site classification	Mean normalised residuals	Median normalised residuals	Standard deviation normalised residuals	Median LH	Rank	LLH
Model for the Alps with variable stress parameter								
Stress par. 10 MPa	R_{rup}	EC8	0.148 (A)	0.041 (A)	1.373 (C)	0.404 (A)	C	2.702
		Flat response	-0.423 (B)	-0.418 (B)	1.186 (B)	0.444 (A)	B	2.469
		Reference stations	-0.233 (A)	-0.318 (B)	1.172 (B)	0.443 (A)	B	2.356
Stress par. 5 MPa	R_{rup}	EC8	0.214 (A)	0.094 (A)	1.323 (C)	0.419 (A)	C	2.622
		Flat response	-0.345 (B)	-0.383 (B)	1.139 (B)	0.466 (A)	B	2.347
		Reference stations	-0.159 (A)	-0.247 (A)	1.130 (B)	0.471 (A)	B	2.265
	R_{JB}	Reference stations	-0.128 (A)	-0.232 (A)	1.111 (A)	0.474 (A)	A	2.227
Stress par. 5 Mpa, Hard Rock	R_{rup}	Reference stations	0.018 (A)	-0.046 (A)	1.139 (B)	0.494 (A)	B	2.262
	R_{JB}		0.059 (A)	-0.027 (A)	1.111 (A)	0.503 (A)	A	2.218
Stress par. 2.5 MPa	R_{rup}	EC8	0.257 (B)	0.143 (A)	1.343 (C)	0.412 (A)	C	2.675
		Flat response	-0.321 (B)	-0.373 (B)	1.156 (B)	0.458 (A)	B	2.363
		Reference stations	-0.129 (A)	-0.224 (A)	1.145 (B)	0.469 (A)	B	2.284
Model for the Alps with constant stress parameter								
Stress par. 10 MPa	R_{rup}	EC8	-0.735 (C)	-0.818 (D)	1.354 (C)	0.281 (C)	D	3.037
		Flat response	-1.332 (D)	-1.337 (D)	1.231 (B)	0.162 (D)	D	3.699
		Reference stations	-1.135 (D)	-1.164 (D)	1.138 (B)	0.218 (C)	D	3.189
Stress par. 5 MPa	R_{rup}	EC8	-0.577 (C)	-0.651 (C)	1.313 (C)	0.324 (B)	C	2.809
		Flat response	-1.163 (D)	-1.207 (D)	1.190 (B)	0.202 (C)	D	3.321
		Reference stations	-0.969 (D)	-1.008 (D)	1.109 (A)	0.271 (C)	D	2.889
	R_{JB}	Reference stations	-0.923 (D)	-0.972 (D)	1.079 (A)	0.282 (C)	D	2.781
Stress par. 2.5 MPa	R_{rup}	EC8	-0.316 (B)	-0.402 (B)	1.320 (C)	0.361 (B)	C	2.654
		Flat response	-0.906 (D)	-0.965 (D)	1.176 (B)	0.281 (C)	D	2.915
		Reference stations	-0.711 (C)	-0.767 (D)	1.117 (A)	0.340 (B)	D	2.590

Figure 26 compares the data recorded in the Alps with the best fitting model of Table 7 using R_{rup} . Both scaling with distance and magnitude of the data are well reproduced by the model. One can also note that the scatter in the observed data is larger for the EC8 classification than for the reference sites classification.

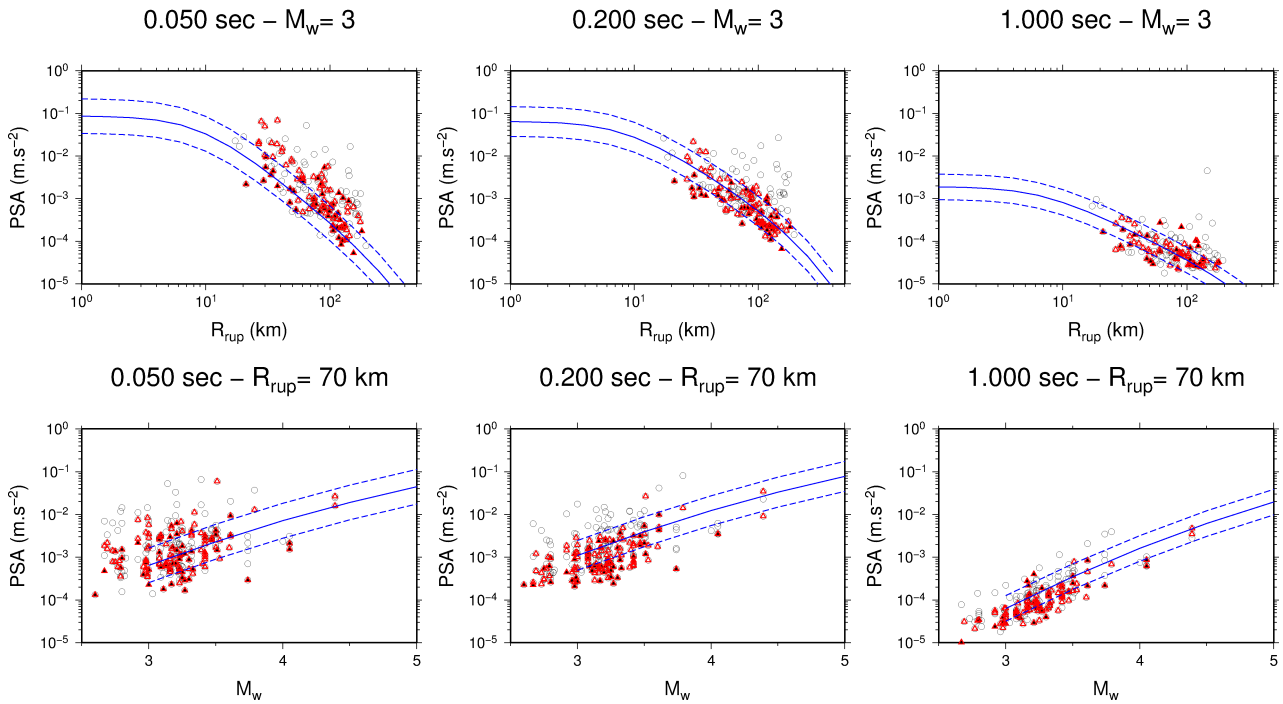


Figure 26: Spectral acceleration versus distance for $M_w=3$ (top) and magnitude for $R_{rup}=70$ km (bottom), for three periods 0.05 sec (left), 0.200 sec (middle), and 1.000 sec (right). RAP data recorded in the Alps (EC8 classification: empty circles; Flat response classification: black dot; Reference site classification: red triangles) are compared to the best fitting stochastic model in Table 7 using R_{rup} (i.e. model for the Alps with a stress parameter of 5 MPa plotted in blue).

6.2. Pyrenees

Table 8 shows the results of the testing for the data recorded in the Pyrenees. In that particular case, the two models using a constant stress parameter of 5 MPa, or a magnitude-dependent stress parameter with a large magnitude stress parameter of 5 MPa are almost identical (see Figure 24), consequently, only one of the 2 is used. In this case, all the models lead to a bad fit of the data.

Table 8: Analysis of the normalised residuals using Scherbaum et al. (2004, 2009) methods for the data recorded in the Pyrenees.

Model	Distance metric	Site classification	Mean normalised residuals	Median normalised residuals	Standard deviation normalised residuals	Median LH	Rank	LLH
Model for the Pyrenees with variable stress parameter								
Stress par. 10 MPa	R_{rup}	EC8	-0.685 (C)	-0.706 (C)	1.258 (C)	0.311 (B)	C	2.806
		Flat response	-1.929 (D)	-1.926 (D)	0.980 (A)	0.054 (D)	D	4.700
		Reference stations	-1.662 (D)	-1.745 (D)	0.981 (A)	0.081 (D)	D	4.013
		RSSP	-1.063 (D)	-0.998 (D)	1.137 (B)	0.284 (C)	D	3.074
Stress par. 5 MPa	R_{rup}	EC8	-0.621 (C)	-0.638 (C)	1.255 (C)	0.316 (B)	C	2.740
		Flat response	-1.842 (D)	-1.910 (D)	1.015 (A)	0.056 (D)	D	4.512
		Reference stations	-1.554 (D)	-1.644 (D)	1.006 (A)	0.100 (D)	D	3.797
		RSSP	-1.009 (D)	-0.972 (D)	1.140 (B)	0.292 (C)	D	2.996
	R_{B}	Reference stations	-1.448 (D)	-1.530 (D)	0.958 (A)	0.126 (D)	D	3.500
Stress par. 5 Mpa, Hard Rock	R_{rup}	Reference stations	-1.754 (D)	-1.734 (D)	0.981 (A)	0.083 (D)	D	4.239
Stress par. 2.5 MPa	R_{rup}	---	---	---	---	---	---	---
Model for the Pyrenees with constant stress parameter								

Model	Distance metric	Site classification	Mean normalised residuals	Median normalised residuals	Standard deviation normalised residuals	Median LH	Rank	LLH
Stress par. 10 MPa	R_{rup}	EC8	-0.832 (D)	-0.848 (D)	1.254 (C)	0.278 (C)	D	2.959
		Flat response	-2.094 (D)	-2.148 (D)	0.993 (A)	0.032 (D)	D	5.195
		Reference stations	-1.812 (D)	-1.870 (D)	0.977 (A)	0.061 (D)	D	4.382
		RSSP	-1.212 (D)	-1.150 (D)	1.148 (B)	0.230 (C)	D	3.336

Figure 27 compares the model using a large magnitude stress parameter of 5 MPa with recorded data in the Pyrenees for $M_w=3$ as a function of distance, and for $R_{rup}=70$ km as a function of magnitude. Obviously, the model over-predicts the data as also indicated by the testing results, for all periods. The rate of distance decay predicted by the model seems to follow the rate of distance decay observed in the data. On the other hand, the magnitude scaling is too weak, and the distance between the model prediction and observations increases with decreasing magnitude. As shown in Figure 24, the scaling of stress parameter with magnitude used in the model (solid green line), and the scaling observed in the data (dashed green line) are very different, the first one is almost 0 while the second is strong. This may be the cause of the discrepancy. Indeed, Figure 28 shows the comparison between recorded data with $M_w=4$ and the same model as in Figure 27, and the fit is much better. Consequently, for the Pyrenees, the stress drop model for magnitude below 4 needs to be refined. Since observed stress drops in the Pyrenees from Drouet et al. (2010) are relatively high, new inversions, including the RSSP and updated information about site conditions (SIGMA WP3) data may help to better characterize stress drops in this region.

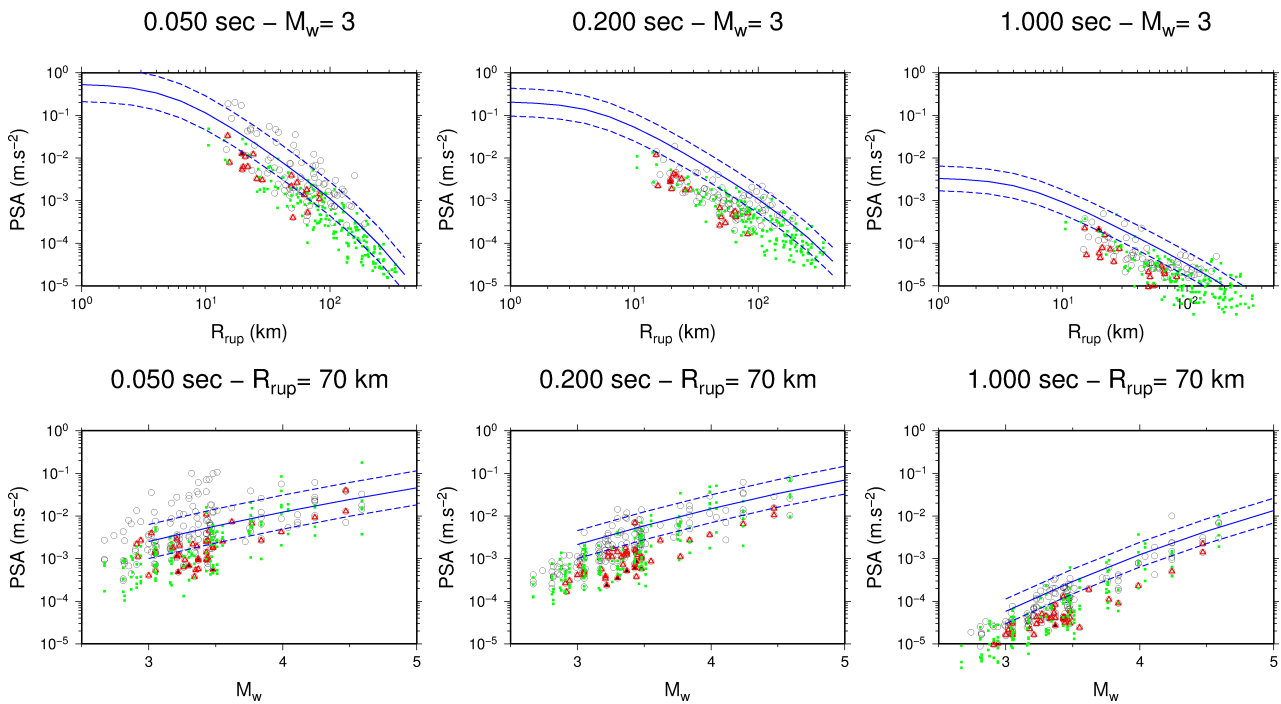


Figure 27: Spectral acceleration versus distance for $M_w=3$ (top) and magnitude for $R_{rup}=70$ km (bottom), for three periods 0.05 sec (left), 0.200 sec (middle), and 1.000 sec (right). RAP data recorded in the Pyrenees (EC8 classification: empty circles; Flat response classification: black dot; Reference site classification: red triangles; RSSP data: green squares) are compared to the model for the Pyrenees with a stress parameter of 5 MPa (blue curves).

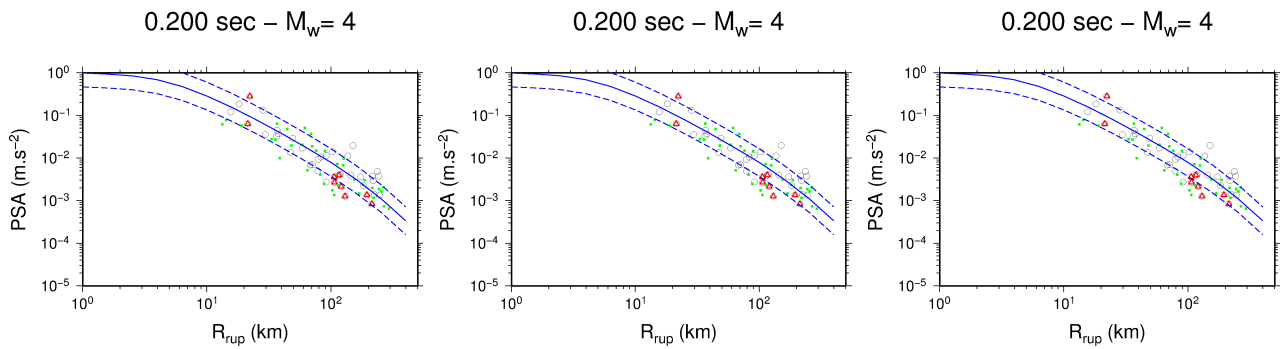


Figure 28: Spectral acceleration versus distance for $M_w=4$ and for three periods 0.05 sec (left), 0.200 sec (middle), and 1.000 sec (right). RAP data recorded in the Pyrenees (EC8 classification: empty circles; Flat response classification: black dot; Reference site classification: red triangles; RSSP data: green squares) are compared to the model for the Pyrenees with a stress parameter of 5 MPa (blue curves).

6.3. Rhine Graben

As in the case of the models for the Pyrenees, the constant or magnitude-dependent stress parameter model using a large magnitude stress parameter of 5 MPa are almost identical (see Figure 24), consequently, only one of the 2 is used. Moreover, for the Rhine Graben all the RAP station present site amplifications which exceed 2, consequently, there are no rock sites according to that classification. One may also note that for the Rhine Graben only one reference station is used in Drouet et al. (2010). Table 9 shows the results of the analysis of the normalised residuals for the Rhine Graben. The results indicate that all the models are leading to the same level of fit to the data. The better fit using R_{rup} is obtained with the magnitude-dependent stress parameter model with a large magnitude stress parameter of 10 MPa, but the ranking and LLH values are very close to those obtained with the magnitude-dependent stress parameter model with a large magnitude stress parameter of 5 MPa. One has to keep in mind that the data set with the rock reference sites includes data from only one station in this region and the number of data is very limited. Consequently, the results of the ranking must be interpreted with caution.

Table 9: Analysis of the normalised residuals using Scherbaum et al. (2004, 2009) methods for the data recorded in the Rhine Graben.

Model	Distance metric	Site classification	Mean normalised residuals	Median normalised residuals	Standard deviation normalised residuals	Median LH	Rank	LLH
Model for the Rhine Graben with <u>variable</u> stress parameter								
Stress par. 10 MPa	R_{rup}	EC8	0.856 (D)	0.919 (D)	1.104 (A)	0.320 (B)	D	2.733
		Flat response	---	---	---	---	---	---
		Reference stations	-0.215 (A)	-0.126 (A)	0.794 (A)	0.579 (A)	A	1.812
Stress par. 5 MPa	R_{rup}	EC8	0.937 (D)	0.982 (D)	1.124 (A)	0.283 (C)	D	2.870
		Flat response	---	---	---	---	---	---
	R_{JB}	Reference stations	-0.137 (A)	-0.044 (A)	0.823 (A)	0.589 (A)	A	1.826
Stress par. 2.5 MPa	R_{rup}	Reference stations	-0.106 (A)	-0.007 (A)	0.792 (A)	0.592 (A)	A	1.785
		---	---	---	---	---	---	---
Model for the Rhine Graben with <u>constant</u> stress parameter								
Stress par. 10 MPa	R_{rup}	EC8	0.614 (C)	0.686 (C)	1.103 (A)	0.367 (B)	C	2.474
		Flat response	---	---	---	---	---	---
		Reference stations	-0.478 (B)	-0.430 (B)	0.768 (A)	0.556 (A)	B	1.915

Figure 29 compares the data recorded in the Rhine Graben with the magnitude-dependent stress parameter model with a large magnitude stress parameter of 5 MPa. The scaling with both distance seem to reproduce the observations.

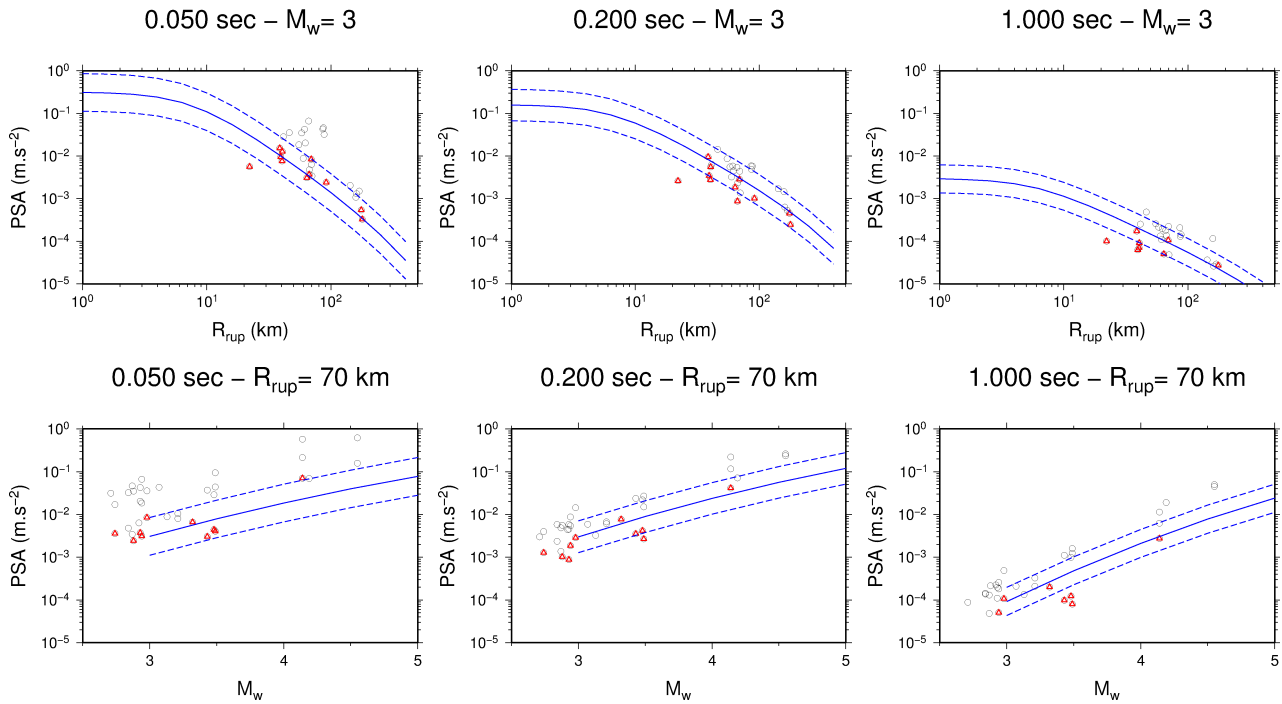


Figure 29: Spectral acceleration versus distance for $M_w=3$ (top) and magnitude for $R_{rup}=70$ km (bottom), for three periods 0.05 sec (left), 0.200 sec (middle), and 1.000 sec (right). RAP data recorded in the Rhine Graben (EC8 classification: empty circles; Flat response classification: black dot; Reference site classification: red triangles) are compared to the model for the Rhine Graben with a stress parameter of 5 MPa (blue curves).

7. Comparison of stochastic models for France, United Kingdom and Switzerland

Three different stochastic models have been developed for three regions in France: the Alps, the Pyrenees and the Rhine Graben. Differences in stress parameter and attenuation parameters have been observed for these three regions by Drouet et al. (2010). The Alps are characterized by small stress parameter and a stronger anelastic attenuation compared to the Pyrenees and the Rhine Graben. On the other hand, the Pyrenees are characterized by relatively high stress parameters and a stronger geometrical spreading. These comparisons rely on the assumption that the site reference used in the three regions are comparable. This assumption may be further investigated in the light of the SIGMA WP3 actions regarding site characterization.

Figure 30 compares the behaviour of the ground-motion amplitude predicted by the three models against distance for $M_w=3.0, 4.5$ and 6.0 and at two spectral periods (0.01 and 1.0 s). Differences in the rate of attenuation with distance are due to differences in attenuation parameters and differences in the rate of increases with magnitude to differences in the stress parameter models. The differences are more pronounced for small magnitudes and for low spectral period (0.01 s) than for longer periods (1.0 s). The main difference are the low amplitudes predicted by the model for the Alps for small magnitude events due to the low stress parameter values for this region. The rate of increase with magnitude is stronger than for the other two models, and all the models are equivalent for magnitude above 4.5. As shown in Figure 31, the difference for $M_w=3.0$ due to the low stress parameter for the Alps is visible up to 0.4 s, above which all the model are similar. For large magnitudes, the models are similar over the whole period range. Figure 32 shows that the standard deviations of the models are slightly different, with larger values for the Rhine Graben model, followed by the Alps and the Pyrenees. These differences have to be attributed to differences in the attenuation parameters uncertainties since all other components have the same uncertainty for the 3 models. As one can see in Table 1, the larger uncertainties on the attenuation parameters are obtained for the Rhine Graben followed by the Alps and the Pyrenees, which is consistent with the differences observed in the model standard deviations.

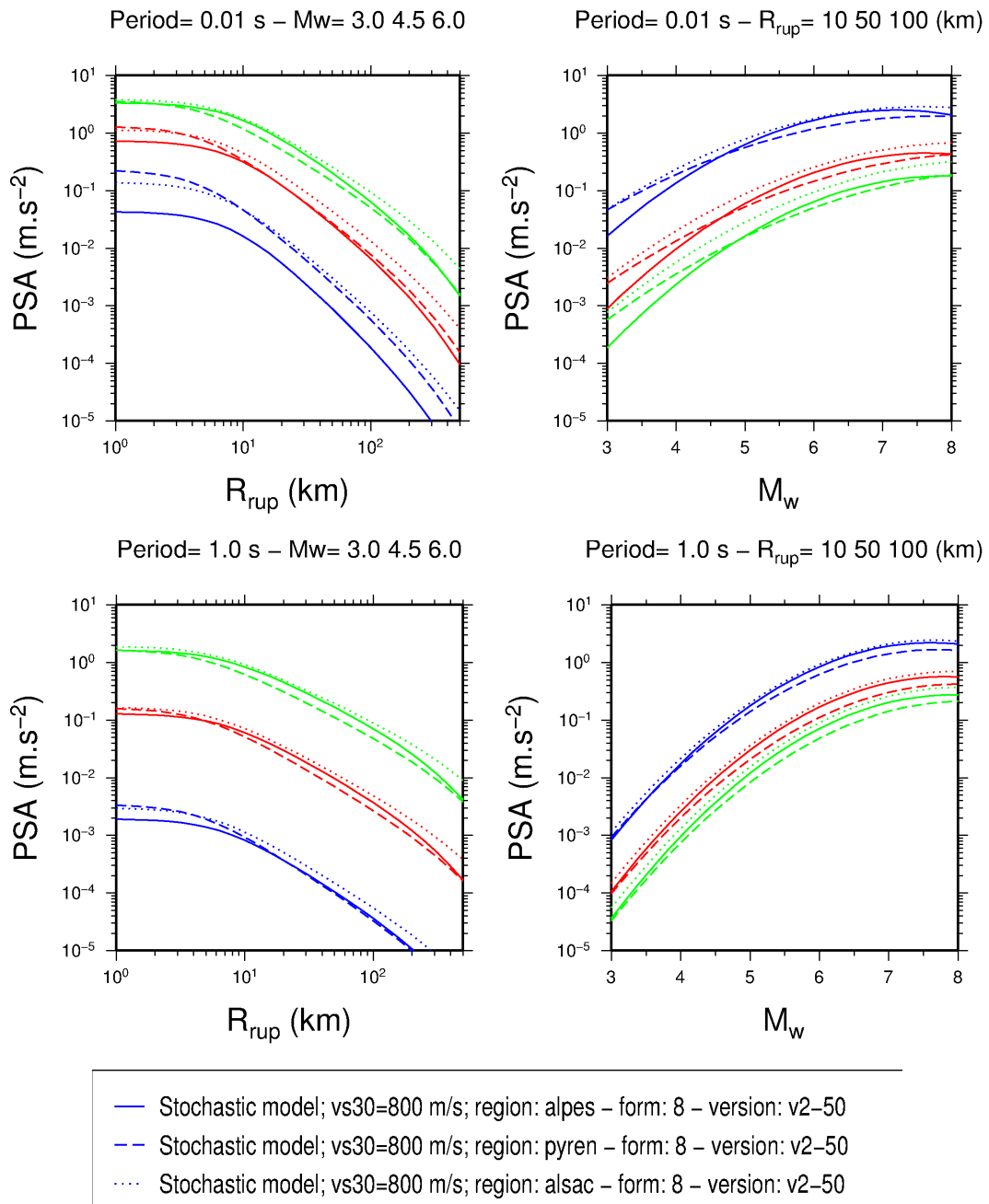


Figure 30: Amplitude against distance (left) and against M_w (right) at two different spectra periods 0.01 s (top) and 1.0 s (bottom) for the 3 regional stochastic GMPEs (Alps: solid lines; Pyrenees: dashed lines; Rhine Graben: dotted lines) using a large magnitude stress parameter of 5 MPa.

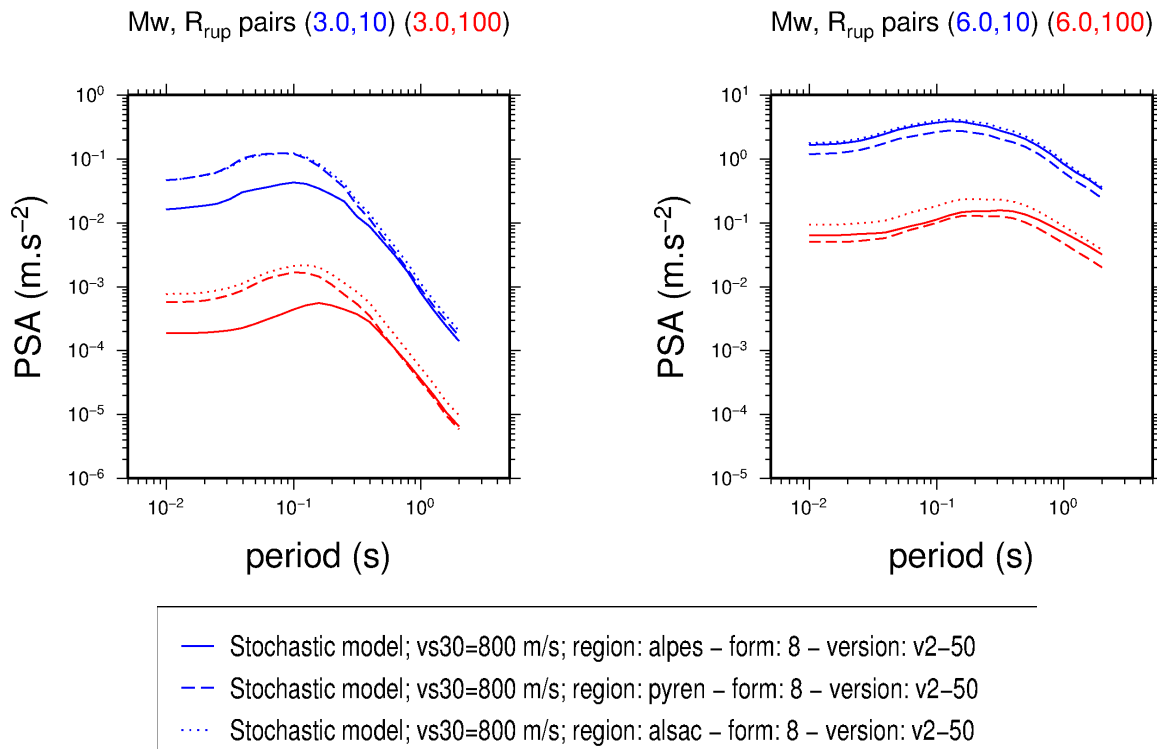


Figure 31: Amplitude against period for different magnitude-distance scenarii $M_w=3$ at $R_{rup}=10$ and 100 km (left) and $M_w=6$ at $R_{rup}=10$ and 100 km (right) for the 3 regional stochastic GMPEs (Alps: solid lines; Pyrenees: dashed lines; Rhine Graben: dotted lines) using a large magnitude stress parameter of 5 MPa.

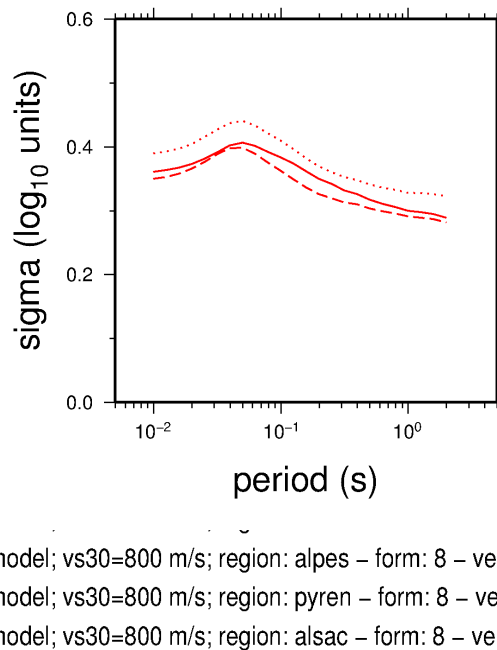


Figure 32: Standard deviation against period for the 3 regional stochastic GMPEs (Alps: solid lines; Pyrenees: dashed lines; Rhine Graben: dotted lines) using a large magnitude stress parameter of 5 MPa.

As explained in section 2.2.b two stochastic models have been recently developed for the United Kingdom (Rietbrock et al., 2013) and for Switzerland (Chiou 2011; Edwards & Fäh, 2013). The stress parameter models for these two GMPEs have been presented in section 2.2.b. Note that the uncertainty associated with the models is estimated in two different ways. Rietbrock et al. (2013) propagated the uncertainties on the input parameters for the simulations, while Edwards & Fäh (2013) used only median input parameters and subsequently determined the uncertainty by analysis of the residuals. In Chiou (2011) only modeling uncertainties are indicated, and in the present study we combined these with the uncertainty given in Edwards & Fäh (2013) in order to compute the total uncertainty of the Swiss model.

Note also that the site conditions are slightly different in the two models. Rietbrock et al. (2013) used a $v_{s30}=2300$ m/s, while Edwards & Fäh (2013) and Chiou (2011) used $v_{s30}=1105$ m/s. The two models also use two different distance metrics, R_{JB} for Rietbrock et al. (2013), and R_{eff} (see Boore, 2009) for Edwards & Fäh (2013) and Chiou (2011).

Figure 33 compares the distance scaling of the 3 versions of the stochastic model developed for the Alps (using a magnitude-dependent stress parameter for standard rock and hard rock site conditions, and a constant stress parameter for standard rock conditions) with the stochastic model for UK (using the two versions: constant vs. variable stress parameter), and with the Swiss stochastic model (using the two extreme versions of the stress parameter model). Figure 34 compares the magnitude scaling for different distances, and Figure 35 compares the spectral shapes and standard deviations. Regarding the large uncertainties in the estimation of input parameters from the analysis of the weak motion data, the different model assumptions and predictive variables (distance and site in the present case), there is a good agreement between the models characteristics. The spread in median predictions is similar to what is observed in comparisons of empirical GMPEs.

The stochastic model for the UK and the model for the Alps (present study) with magnitude-dependent stress parameter predict similar ground-motions especially at distances lower than about 70 km. For larger distances, since Rietbrock et al.'s (2013) model includes a segmented geometrical spreading, the two models behave differently. The scaling with magnitude is very similar between the two models for both the magnitude-dependent stress parameter version and the constant stress parameter version (Figure 34). Note that the constant stress parameter version of the UK model uses a low stress value (1.8 MPa), while the model for France uses a comparatively large value (5 MPa). Consequently, the absolute amplitudes predicted by the first model are lower than those predicted by the second. Finally, the shape of the spectra differ, not surprisingly, since very hard rock conditions are used for the UK model, while standard rock is used for the French model. The standard deviation of the French model lies in between the standard deviations predicted by both version of the UK model.

The model for Switzerland appears to be different mainly for small magnitudes. It is however difficult to appreciate how different it is since it uses the R_{eff} distance metric (see Boore, 2009), which may not be comparable to the Joyner-Boore distance used in Figure 33 to Figure 35. For magnitude greater than 4.5, the amplitude predicted by the Swiss model using the largest stress parameter (48 MPa) agrees roughly with the other two. Edwards & Fäh (2013) used a very strong geometric decay for distance smaller than 20 km ($1/R^{1.29}$) which is counter-balanced by a very high stress parameter. The versions of the model with a lower stress parameter will lead to smaller amplitudes compared to the other stochastic models for France and the UK.

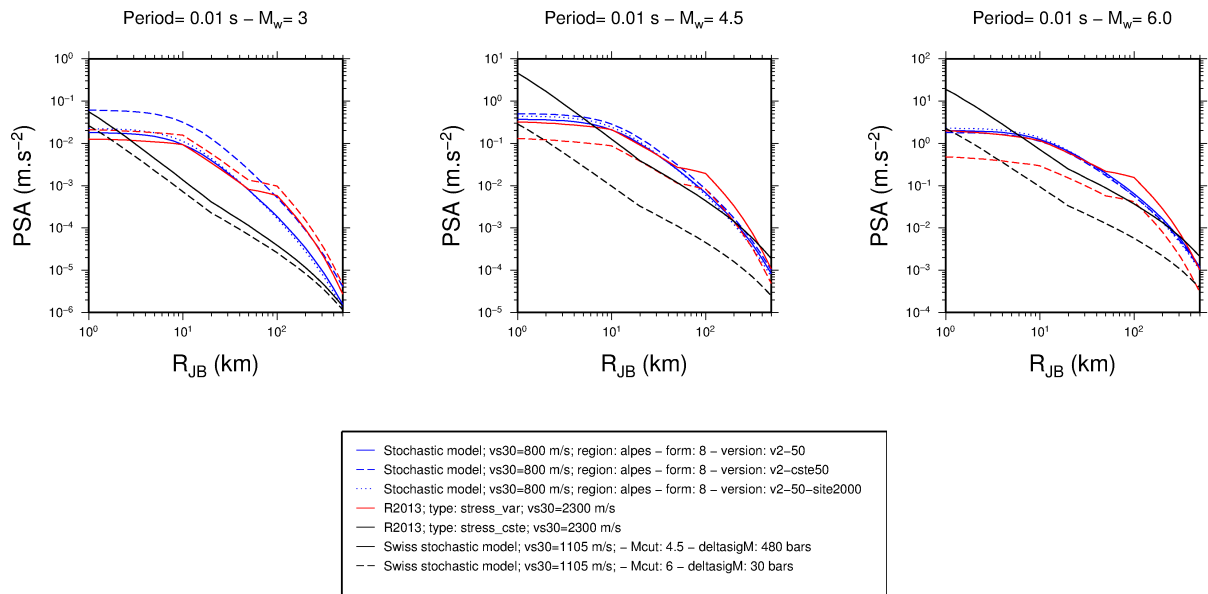


Figure 33: Amplitude versus distance at 0.01 s (PGA) for $M_w=3.0$ (left), 4.5 (middle) and 6.0 (right) for three European stochastic models.

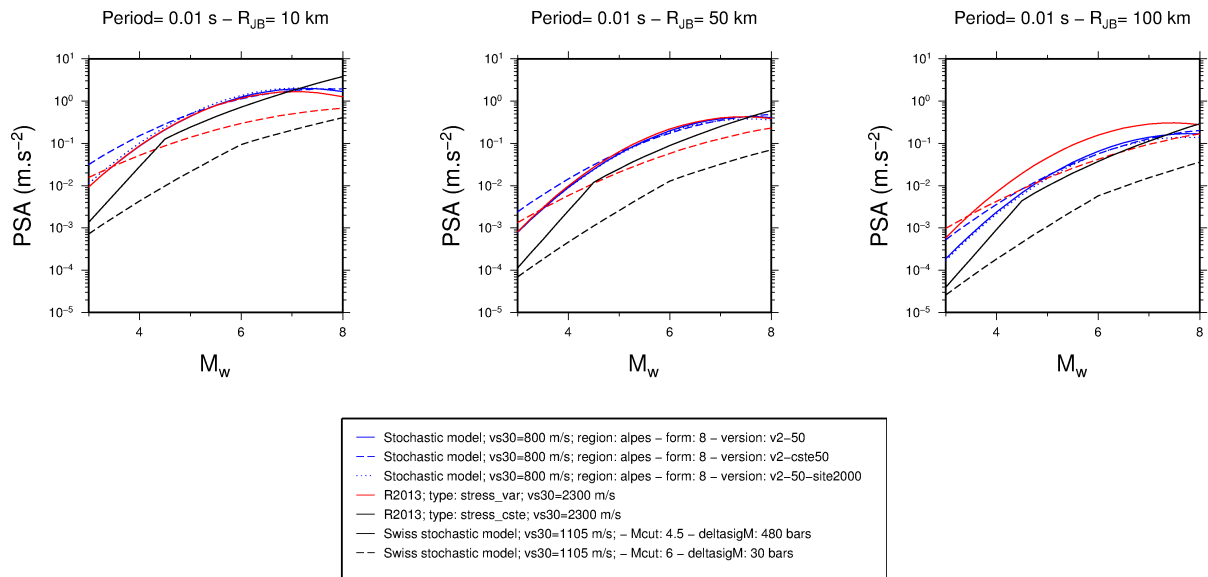


Figure 34: Amplitude versus magnitude at 0.01 s (PGA) for $R_{JB}=10$ km (left), 50 km (middle) and 100 km (right) for three European stochastic models.

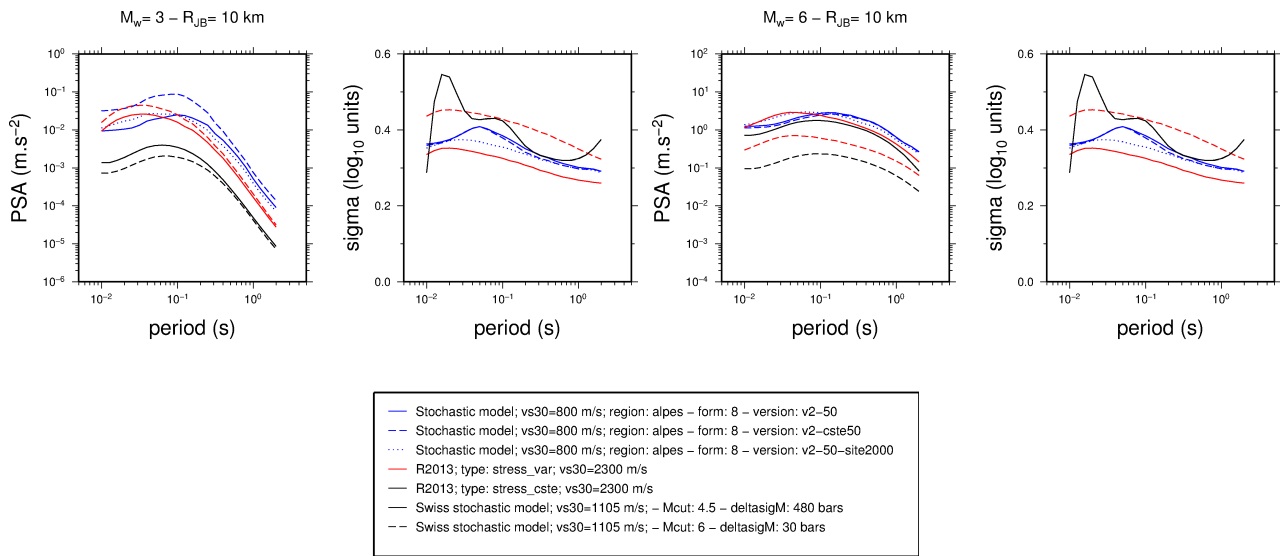


Figure 35: Amplitude and sigma versus period for $M_w=3.0$ and $R_{JB}=10$ km (left), and $M_w=6.0$ and $R_{JB}=10$ km (right) for three European stochastic models.

8. Rock and Hard Rock site conditions

As already mentioned earlier two types of site conditions were considered. One corresponding to “standard” rock conditions with $v_{S30}=800$ m/s and $\kappa=0.03$ s, and the other corresponding to hard rock site conditions with $v_{S30}=2000$ m/s and $\kappa=0.01$ s. Figure 36 compares the spectra predicted by these two models for $M_w=3$ and 6 at $R_{rup}=10$ and 100 km. For short periods (below 0.1 s), and at close distances, the hard rock model predicts higher amplitudes than the rock model, while at longer distances the two models are similar. For longer periods (above 0.1 s), the hard rock model predicts slightly lower amplitudes than the rock model whatever the magnitude and distance.

Van Houtte et al. (2011) developed an adjustment in order to convert ground-motion for hard rock site to rock site. This adjustment has been performed on the hard rock stochastic model and the resulting model is also shown on Figure 36. The adjustment performs well for long periods (above 0.1 s), and is also coherent with the stochastic rock model for short distances (especially for small magnitudes). However at large distances and short periods (below 0.1 s), the adjustment leads to low amplitudes compared to the hard rock model. There is apparently a distance dependence that has not properly been taken into account in Van Houtte et al. (2011). In general the adjustment always predicts smaller amplitudes than the hard rock model for short periods (below 0.1 s). This is probably the result of the low kappa's used for the hard rock site conditions in Van Houtte et al. (2011) (0.01, 0.008 and 0.005 s), while the hard rock stochastic model uses a log-normal distribution with mean 0.01 s, leading to larger kappa's on average. Figure 37 compares the standard deviations of the two stochastic models and the adjusted one. Due to error propagation, the standard deviation of the adjusted one is much higher than for the other models. It is interesting to note that for both the stochastic rock model and the adjusted one, there is a peak in the standard deviation of around 0.05 s.

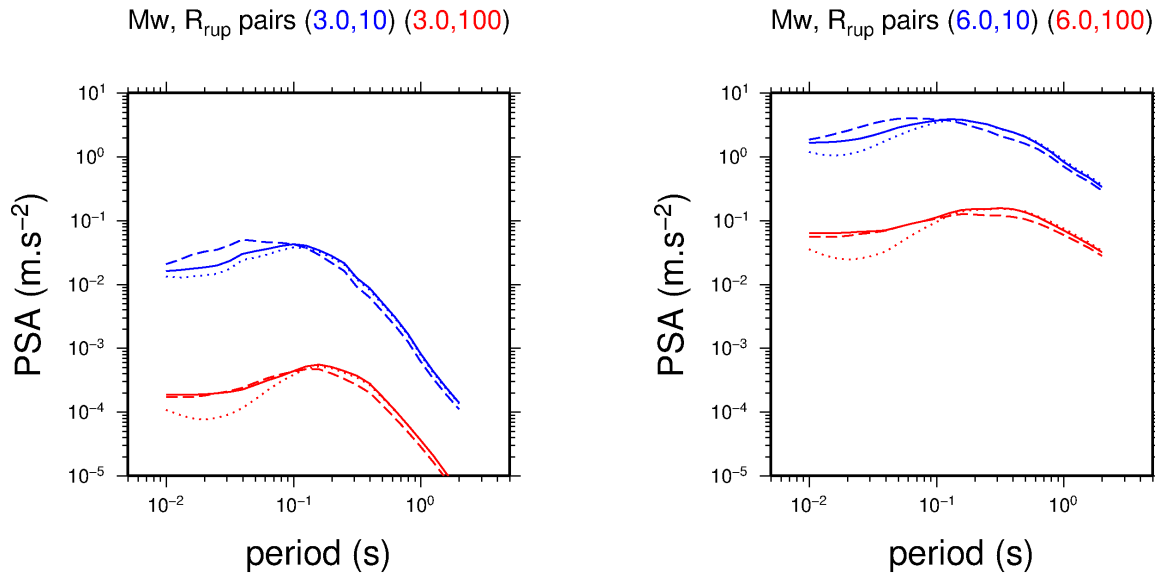


Figure 36: Comparison of the spectra for different magnitude-distance scenarii $M_w=3$ at $R_{rup}=10$ and 100 km (left) and $M_w=6$ at $R_{rup}=10$ and 100 km (right) for the stochastic model for the Alps using rock and hard rock site conditions (solid and dashed lines, respectively), and for the hard rock model adjusted to rock using Van Houtte et al. (2011) adjustment (dotted lines).

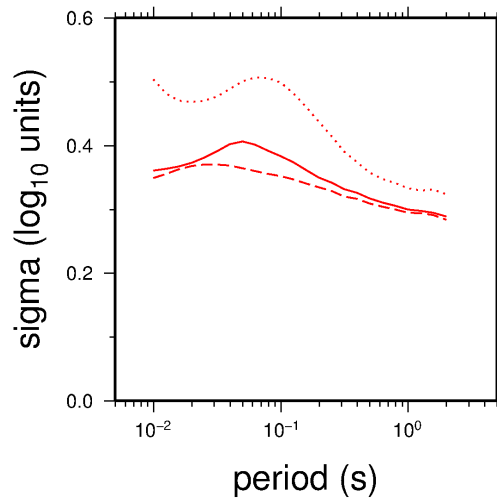


Figure 37: Comparison of the standard deviations for the stochastic model for the Alps using rock and hard rock site conditions (solid and dashed lines, respectively), and for the hard rock model adjusted to rock using Van Houtte et al. (2011) adjustment (dotted lines).

9. Conclusion

Three stochastic ground-motion prediction equations have been developed in this study for three regions in France: the Alps, the Pyrenees and the Rhine Graben. This work updates and improves a previous version of the stochastic models described in the deliverable SIGMA-2012-D2-33 (Drouet, 2012). The models are built in two steps. First, synthetic ground-motion data is computed using the Stochastic Model SIMulation SMSIM (Boore, 2003). Second the synthetic data are used to build a GMPE by regression analysis assuming a functional form.

SMSIM uses a point-source model but given some adjustments on the single distance used for the simulation, extended fault effects can be included in the simulations. We used two different types of adjustments and showed that the R_{eff} model (Boore, 2009) better takes into account the finite-fault. Consequently, all the simulations are done using this model. As in the previous version of the model, the time domain simulations are used, as opposed to the Random Vibration Theory (RVT) option also available in SMSIM (see Drouet, 2012). Simulations are carried out for $M_w=3$ to 8, epicentral distances from 1 to 250 km, and 20 spectral periods between 0.01 and 3 s, as well as for PGA and PGV. Two

site conditions are considered: “standard” rock site with $v_{S30}=800$ m/s and $\kappa=0.03$ s, and hard rock site with $v_{S30}=800$ m/s and $\kappa=0.03$ s.

For each simulated magnitude, 40 simulations are done varying the fault orientation, dimensions, and hypocenter location on the fault (note that this information is only used to compute the different distance metrics, the simulations are done using a point-source model: SMSIM), and the stress parameter. The stress parameter model is built considering observed stress parameters in the three regions from Fourier spectral analysis (Drouet et al., 2010), and extrapolating towards larger magnitude using information available in the literature. Different versions of the models are built regarding different hypotheses on stress parameter for large events. All the parameters used as input in the stochastic simulations are considered as random variables assuming normal or log-normal distributions. Consequently, uncertainty on the input parameters is propagated to the synthetic ground-motions.

GMPEs are built by regression of the synthetic data using two different methods: least-squares and random-effect. Tests have been made to assess the influence of the starting model on the regression and the influence of the functional form. GMPEs coefficients are determined for the 4 distance metrics considered: R_{epi} , R_{hypo} , R_{JB} , and R_{rup} . A sensitivity analysis is carried out to understand the influence of the uncertainty on each input parameter to the total GMPE uncertainty. The major contributors to the total uncertainty are the stress parameter model, the site model (both site amplification and κ). The uncertainties on the attenuation parameters have a second order influence, and those linked with duration, fault orientation and hypocenter location are negligible compared to the other. Stress parameter uncertainty directly maps into between-event variability, while the uncertainties on the other parameters mainly influence the within-event term. The total ground-motion variability obtained is comparable to that obtained in empirical GMPEs under the ergodic assumption (variability of ground-motion including various sites and various sources). The within- and between-event terms are also similar to that obtained in empirical GMPEs, especially those that include small magnitudes events. In order to perform site-specific PSHA, the model is flexible enough to refine the variability on v_{S30} and κ in order to produce a model using single-station variability.

The stochastic GMPEs are compared with data from large earthquakes included in the Resorce database (Akkar et al., 2011) including data from the Euro-Mediterranean region, and data from the NGA project including mainly data from California and Taiwan and some other active regions (Chiou et al., 2008). Statistical analysis of the residuals following the methods of Scherbaum et al. (2004, 2009) allowed us to compare the performance of the different versions of the stochastic models (variations in the stress parameter for large events). It appears that a stress parameter of 5 MPa is a good choice to achieve a good fit between the models and the real data especially for the European data.

The stochastic models are also compared to the small magnitude data recorded in the different regions. The main difficulty in this exercise is the poorly known site characteristics for the French stations. Different rock site classifications are consequently considered. A reasonable fit is obtained for the three regions. However, for the Pyrenees, small magnitude data are overestimated by the models which have a too weak magnitude scaling. This is probably due to the large stress parameter values obtained in this region which are of the same order as the stress parameter used for large events. However, the scaling with magnitude of the observed stress parameters appears to be strong. Moreover, the stochastic models for the three regions are also compared with each other. The main difference is seen between the model for the Alps with the stronger dependence of stress parameter on magnitude and the other two models. The differences between the three regions due to the attenuation parameters are rather low. A more detailed analysis of the Fourier spectra including more data (for example the RSSP data), and trying to use a reference site coherent with the other regions may help to better characterize stress parameters in this region.

Even if improvements are still possible for the stochastic models presented in this study, we feel that they can be used in PSHA analysis. Indeed, comparisons with data show a good fit throughout the magnitude range, and the analysis of the total variability obtained shows a good coherency with results from other studies. Moreover, these models can be used in site-specific analysis if a detailed knowledge of the site response is available.

10. References

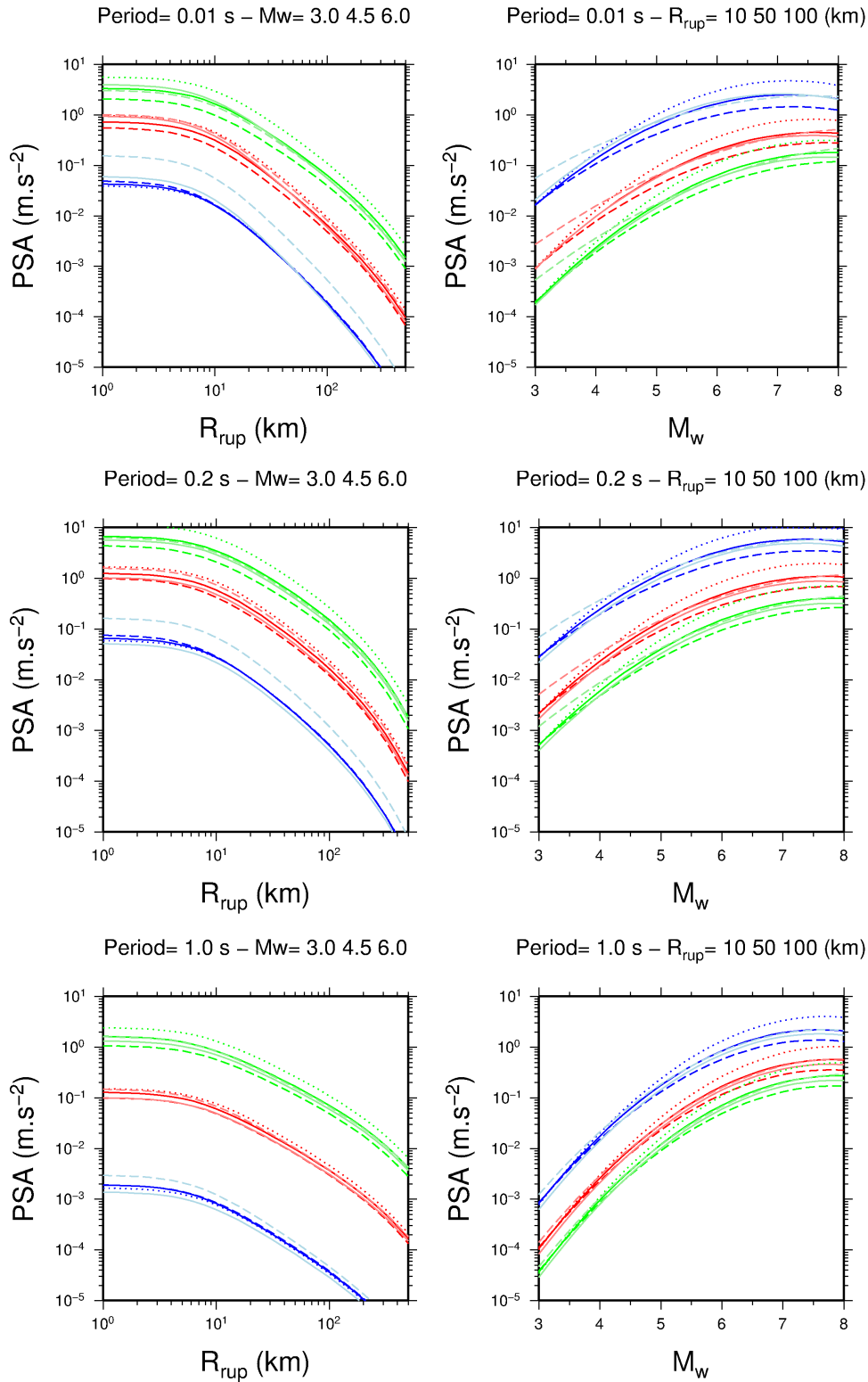
- Abrahamson N., and Silva W. (2008). Summary of the Abrahamson and Silva NGA ground-motion relations. *Earthquake Spectra* 24 (1), 67-97.(Correction, Abrahamson N., and Silva W. (2009). Erratum to “Summary of the Abrahamson and Silva NGA ground-motion relations”. Published on PEER NGA website. http://peer.berkeley.edu/products/abrahamson-silva_nga_report_files/AS08_NGA_errata.pdf).
- Akkar S., Bommer J.J. (2007). Prediction of elastic displacement response spectra in Europe and the Middle East. *Earthquake Engng Struct. Dyn.* 36, 1275–1301
- Akkar S., Frobert L., Godey S., Sandikkaya M. A., Senyurt M., and Traversa P. (2011). RESORCE seismic motion databank : 2011 version, including the improvement of meta-parameters. *Deliverable SIGMA-2011-D2-15*.

- Al-Atik L., Abrahamson N., Bommer J.J., Scherbaum F., Cotton F., Kuehn N. (2010). The Variability of Ground-Motion Prediction Models and Its Components. *Seismological Research Letters* 81 (5) , 794-801.
- Allmann and Shearer (2009). Global variations of stress drop for moderate to large earthquakes. *Journal of Geophysical Research* 104, doi:10.1029/2008JB005821.
- Anderson J. G. (2000). Expected shape of regressions for ground-motion parameters on rock. *Bulletin of the Seismological Society of America* 90 (6B), S43-S52.
- Atkinson G.M., Silva W. (2000). Stochastic Modeling of California Ground Motions. *Bulletin of the Seismological Society of America* 90 (2), 255–274.
- Atkinson G.M. (2004). Empirical Attenuation of Ground-Motion Spectral Amplitudes in Southeastern Canada and the Northeastern United States. *Bulletin of the Seismological Society of America* 94 (3), 1079–1095.
- Berge-Thierry C., Cotton F., Scotti O., Griot-Pommeret D.A. and Fukushima Y. (2003). New empirical response spectral attenuation laws for moderate European earthquakes. *Journal of Earthquake Engineering* 7 (2), 193-222.
- Beauval C., Tazan H., Laurendeau A., Delavaud E., Cotton F., Guéguen P., and Kuehn N. (2012). On the testing of ground-motion prediction equations against small magnitude data. *Bulletin of the Seismological Society of America* 102 (5), 1994-2007.
- Boore, D. M., and Joyner W. B. (1997). Site Amplifications for Generic Rock Sites. *Bulletin of the Seismological Society of America* 87 (2), 327-341.
- Boore, D. M. (2003). Simulation of ground motion using the stochastic method. *Pure Appl. Geophys.* 160, 635–676.
- Boore, D. M. (2009). Comparing stochastic point-source and finite-source ground-motion simulations: SMSIM and EXSIM. *Bull. Seismol. Soc. Am.* 99, 3202–3216.
- Brune, J. N. (1970). Tectonic stress and the spectra of shear waves from earthquakes. *J. Geophys. Res.* 75, 4997-5009. (Correction, *Ibid*, 1971, *J. Geophys. Res.* 76, 5002.)
- Caputo R., Mucciarelli M., and Pavlides S. (2008). Magnitude distribution of linear morphogenic earthquakes in the Mediterranean region: insights from palaeoseismological and historical data. *Geophys. J. Int.* 174 (3), 930-940.
- Chiou B., Darragh R., Gregor N., and Silva W. (2008). NGA Project Strong-Motion Database. *Earthquake Spectra* 24(1), 23-44.
- Chiou B. S.J. (2011). Parameterization of the Simulated Data from Swiss Stochastic Ground Motion Model. *PEGASOS Refinement Project, Technical Report No EXT-TB-1066*.
- Cotton F., Scherbaum F., Bommer J. J., and Bungum H. (2006). Criteria for selecting and adjusting ground-motion models for specific target regions: Application to Central Europe and rock sites. *Journal of Seismology* 10, 137-156.
- Cotton F., Pousse G., Bonilla F., and Scherbaum F. (2008). On the Discrepancy of Recent European Ground-Motion Observations and Predictions from Empirical Models: Analysis of KiK-net Accelerometric Data and Point-Sources Stochastic Simulations. *Bulletin of the Seismological Society of America* 98 (5), 2244–2261.
- Cotton F., Archuleta R., and Causse M. (2013). What is sigma of the stress drop? *Submitted to ???*.
- Douglas J, and Jousset P. (2011). Modeling the Difference in Ground-Motion Magnitude-Scaling in Small and Large Earthquakes. *Seismological Research Letters* 82 (4), 504-508.
- Drouet S., Souriau A., and Cotton F. (2005). Attenuation, seismic moment and site effects for weak motion events. Application to the Pyrenees. *Bull. Seism. Soc. Am.* 95, 1731-1748.
- Drouet S. (2006). Analyse des données accélérométriques pour la caractérisation de l'aléa sismique en France métropolitaine. *Thèse de Doctorat, Spécialité : Géophysique, Université Toulouse III*, 212 p.
- Drouet S., Cotton, F., and Guéguen P. (2010). V_{S30} , kappa, regional attenuation and M_w from accelerograms: application to magnitude 3–5 French earthquakes. *Geophysical Journal International* 182(2), 880–898.
- Drouet S., Bouin M.-P., and Cotton F. (2011). New moment magnitude scale, evidence of stress drop magnitude scaling and stochastic ground motion model for the French West Indies. *Geophysical Journal International*. 187 (3), 1625–1644.
- Drouet S. (2012). Development of regional Ground-Motion Prediction Equations covering a wide magnitude range

- based on stochastic simulations: Application to the Alps, Pyrenees and Rhine Graben regions in France. *Deliverable SIGMA-2012-D2-33*.
- Dujardin A. (2013). Site specific ground motion simulations. Investigation of the magnitude dependence of peak ground motion decay with distance. *Deliverable SIGMA-2013-D2-73*.
- Edwards B., and Fäh D. (2013). A Stochastic Ground-Motion Model for Switzerland. *Bulletin of the Seismological Society of America* 103 (1), 78-98.
- Fukushima Y. (1996). Scaling relations for strong ground motion prediction models with M^2 term. *Bulletin of the Seismological Society of America* 86 (2), 329-336.
- Joyner W. D., and Boore D. M. (1993). Methods for regression analysis of strong-motion data. *Bulletin of the Seismological Society of America* 83 (2), 469-487.
- Mc Guire, R. K. and T. C. Hanks (1980). RMS accelerations and spectral amplitudes of strong motion during the San Fernando earthquake. *Bull. Seismol. Soc. Am.* 70, 1907-1920.
- Pavlidis S., and Caputo R. (2004). Magnitude versus faults' surface parameters: quantitative relationships from the Aegean Region. *Tectonophysics* 380, 159-188.
- Régnier J., Laurendeau A., Duval A.-M., and Guéguen P. (2010). From heterogeneous set of soil data to VS profile: Application on the French permanent accelerometric network (RAP) sites. *Proc. 14 EECE*, Ohrid, 30 August-03 September 2010.
- Rietbrock A., Strasser F., and Edwards B. (2013). A Stochastic Earthquake Ground-Motion Prediction Model for the United Kingdom. *Bulletin of the Seismological Society of America* 103, 57-77.
- Scherbaum F., Cotton F., and Smit P. (2004). On the use of response spectral-reference data for the selection and ranking of ground-motion models for seismic-hazard analysis in regions of moderate seismicity: The case of rock motion. *Bulletin of the Seismological Society of America* 94 (6), 2164-2185.
- Scherbaum F., Delavaud E., and Riggelsen C. (2009). Model selection in seismic hazard analysis: An information-theoretic perspective. *Bulletin of the Seismological Society of America* 99 (6), 3234-3247.
- Van Houtte C., Drouet S., and Cotton F. (2011). Analysis of the Origins of κ (Kappa) to Compute Hard Rock to Rock Adjustment Factors for GMPEs. *Bulletin of the Seismological Society of America* 101, 2926-2941.
- Wells D. L., and Coppersmith K. J. (1994). New empirical relationships among magnitude, rupture length, rupture width, rupture area, and surface displacement. *Bulletin of the Seismological Society of America* 84 (4), 974-1002.

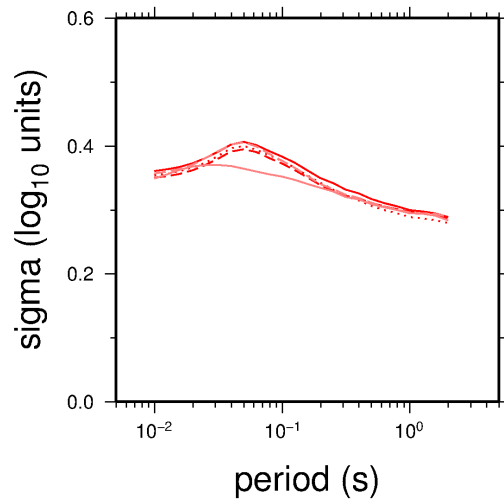
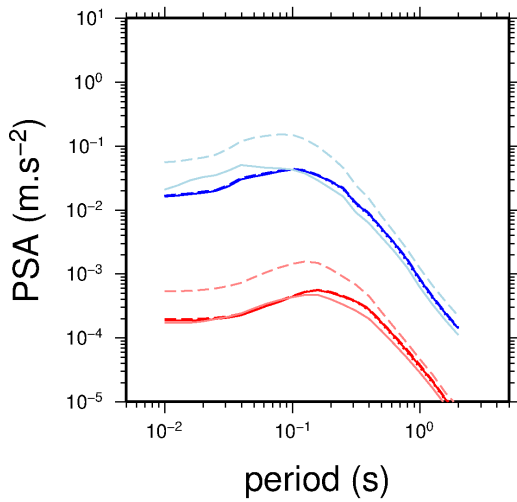
11. Annex

11.1. Comparison plots of the different model versions for the Alps

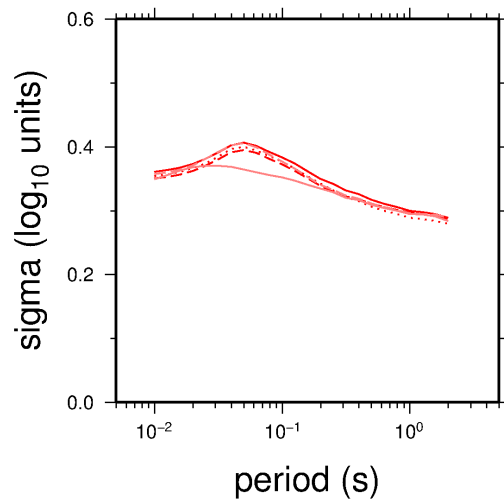
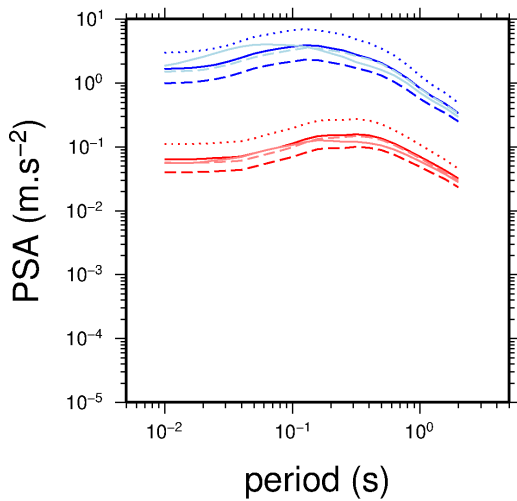


- Stochastic model; vs30=800 m/s; region: alpes – form: 8 – version: v2-50
- - Stochastic model; vs30=800 m/s; region: alpes – form: 8 – version: v2-25
- ⋯ Stochastic model; vs30=800 m/s; region: alpes – form: 8 – version: v2-100
- Stochastic model; vs30=800 m/s; region: alpes – form: 8 – version: v2-50-site2000
- - Stochastic model; vs30=800 m/s; region: alpes – form: 8 – version: v2-cste50

Mw, R_{rup} pairs (3.0,10) (3.0,100)

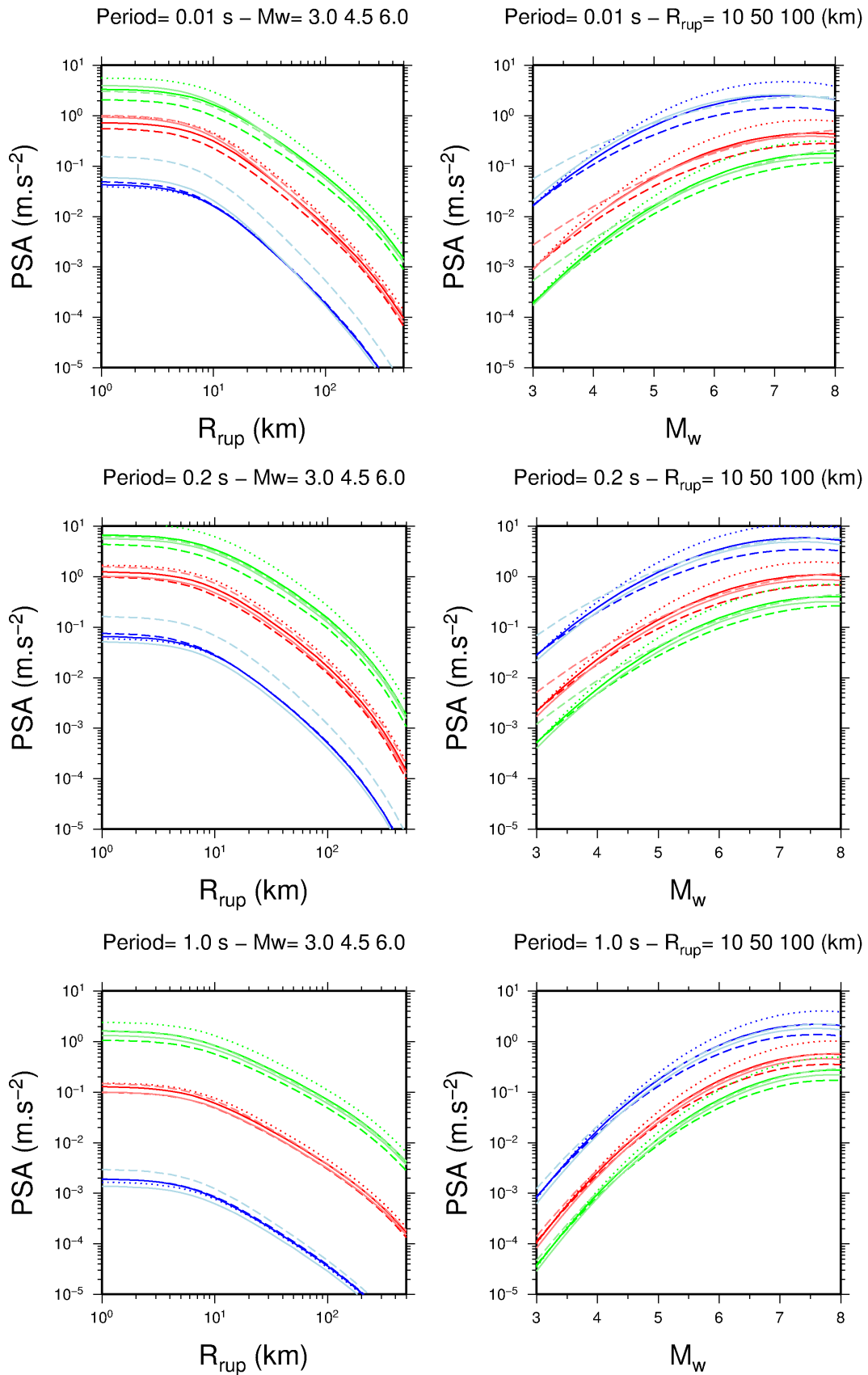


Mw, R_{rup} pairs (6.0,10) (6.0,100)



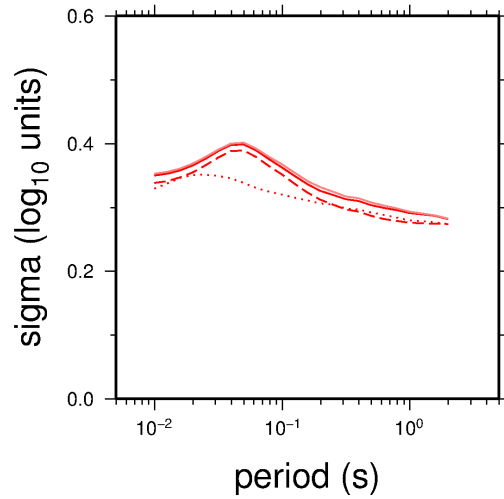
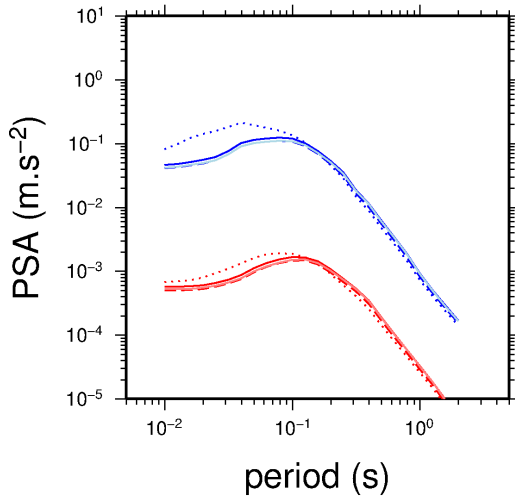
- Stochastic model; vs30=800 m/s; region: alpes – form: 8 – version: v2-50
- - Stochastic model; vs30=800 m/s; region: alpes – form: 8 – version: v2-25
- ⋯ Stochastic model; vs30=800 m/s; region: alpes – form: 8 – version: v2-100
- Stochastic model; vs30=800 m/s; region: alpes – form: 8 – version: v2-50-site2000
- - Stochastic model; vs30=800 m/s; region: alpes – form: 8 – version: v2-cste50

11.2. Comparison plots of the different model versions for the Pyrenees

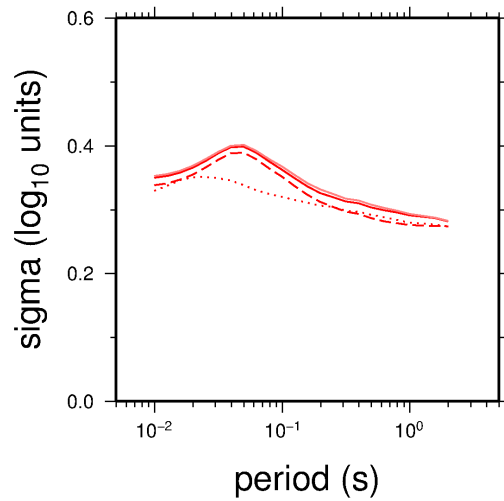
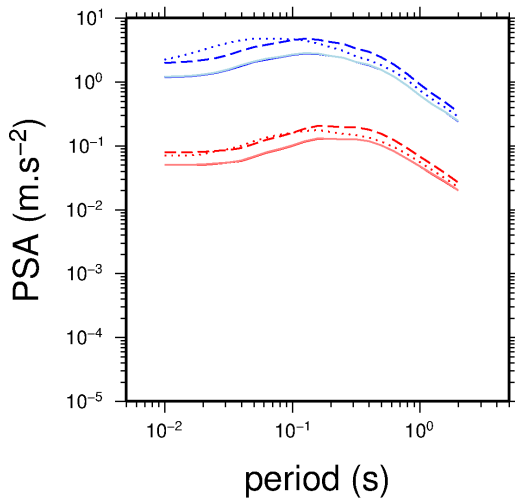


- Stochastic model; vs30=800 m/s; region: alpes – form: 8 – version: v2-50
- - Stochastic model; vs30=800 m/s; region: alpes – form: 8 – version: v2-25
- ... Stochastic model; vs30=800 m/s; region: alpes – form: 8 – version: v2-100
- Stochastic model; vs30=800 m/s; region: alpes – form: 8 – version: v2-50-site2000
- - Stochastic model; vs30=800 m/s; region: alpes – form: 8 – version: v2-cste50

Mw, R_{rup} pairs (3.0,10) (3.0,100)

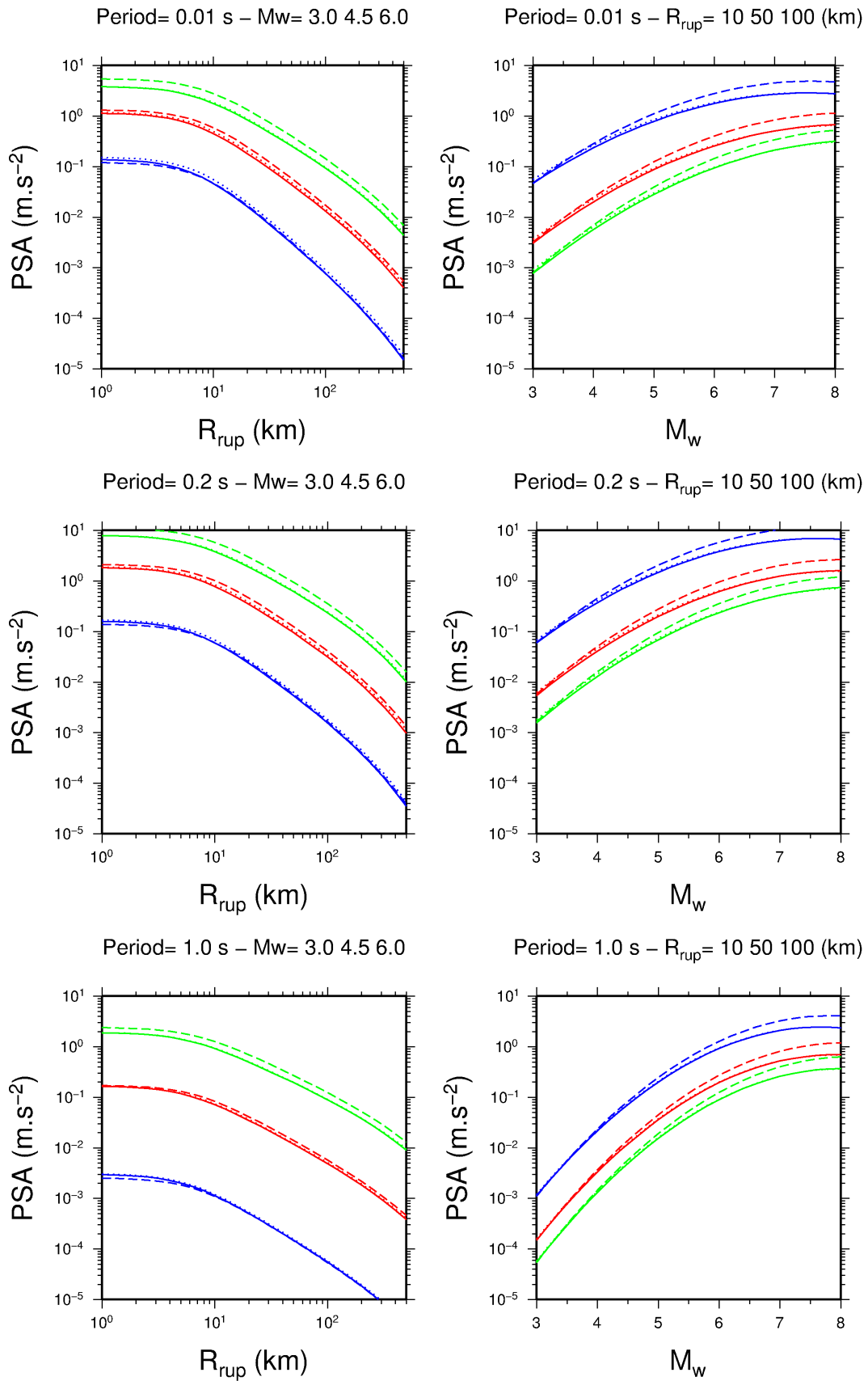


Mw, R_{rup} pairs (6.0,10) (6.0,100)



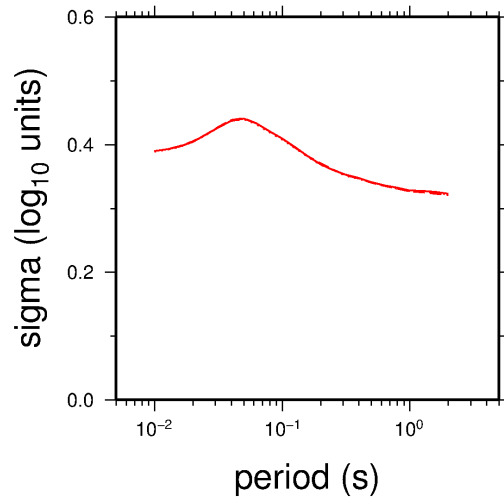
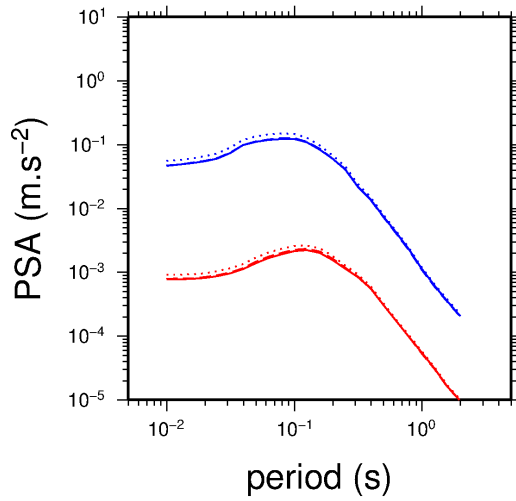
- Stochastic model; vs30=800 m/s; region: alpes – form: 8 – version: v2-50
- - Stochastic model; vs30=800 m/s; region: alpes – form: 8 – version: v2-25
- ... Stochastic model; vs30=800 m/s; region: alpes – form: 8 – version: v2-100
- Stochastic model; vs30=800 m/s; region: alpes – form: 8 – version: v2-50-site2000
- - Stochastic model; vs30=800 m/s; region: alpes – form: 8 – version: v2-cste50

11.3. Comparison plots of the different model versions for the Rhine Graben

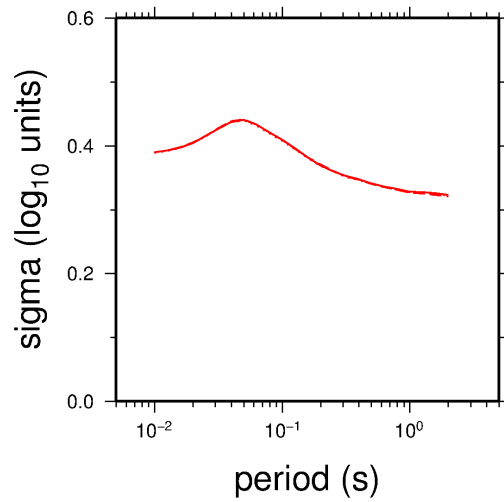
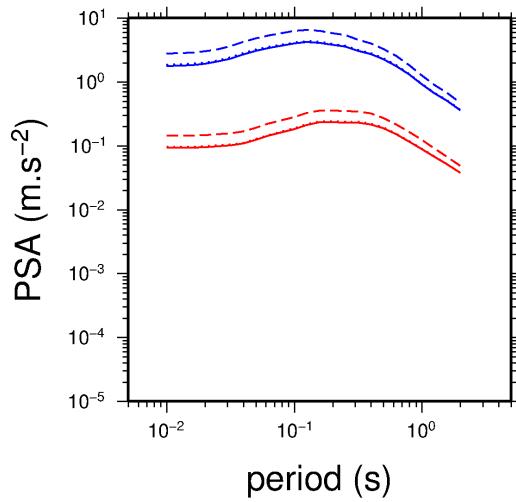


- Stochastic model; vs30=800 m/s; region: alsac – form: 8 – version: v2-50
- - Stochastic model; vs30=800 m/s; region: alsac – form: 8 – version: v2-100
- ⋯ Stochastic model; vs30=800 m/s; region: alsac – form: 8 – version: v2-cste50

Mw, R_{rup} pairs (3.0,10) (3.0,100)



Mw, R_{rup} pairs (6.0,10) (6.0,100)



- Stochastic model; vs30=800 m/s; region: alsac – form: 8 – version: v2-50
- - Stochastic model; vs30=800 m/s; region: alsac – form: 8 – version: v2-100
- ⋯ Stochastic model; vs30=800 m/s; region: alsac – form: 8 – version: v2-cste50

11.4. Divers

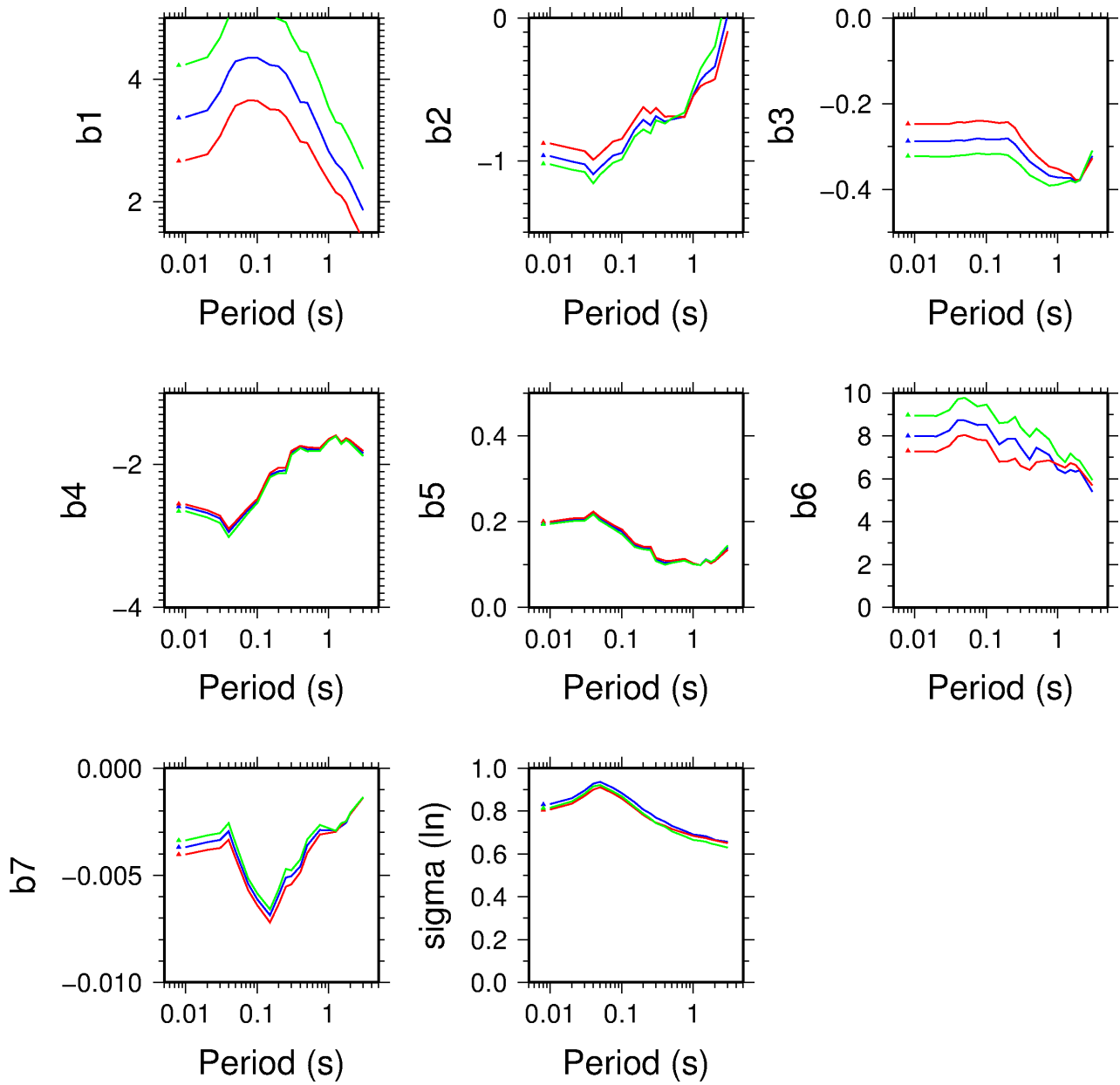


Figure 38: Comparison of the coefficients determined using least-squares regression with starting model 1 from Table 1 (blue), and for the three different stress drop models: 2.5 MPa (red); 5 MPa (blue); 10 MPa (green).

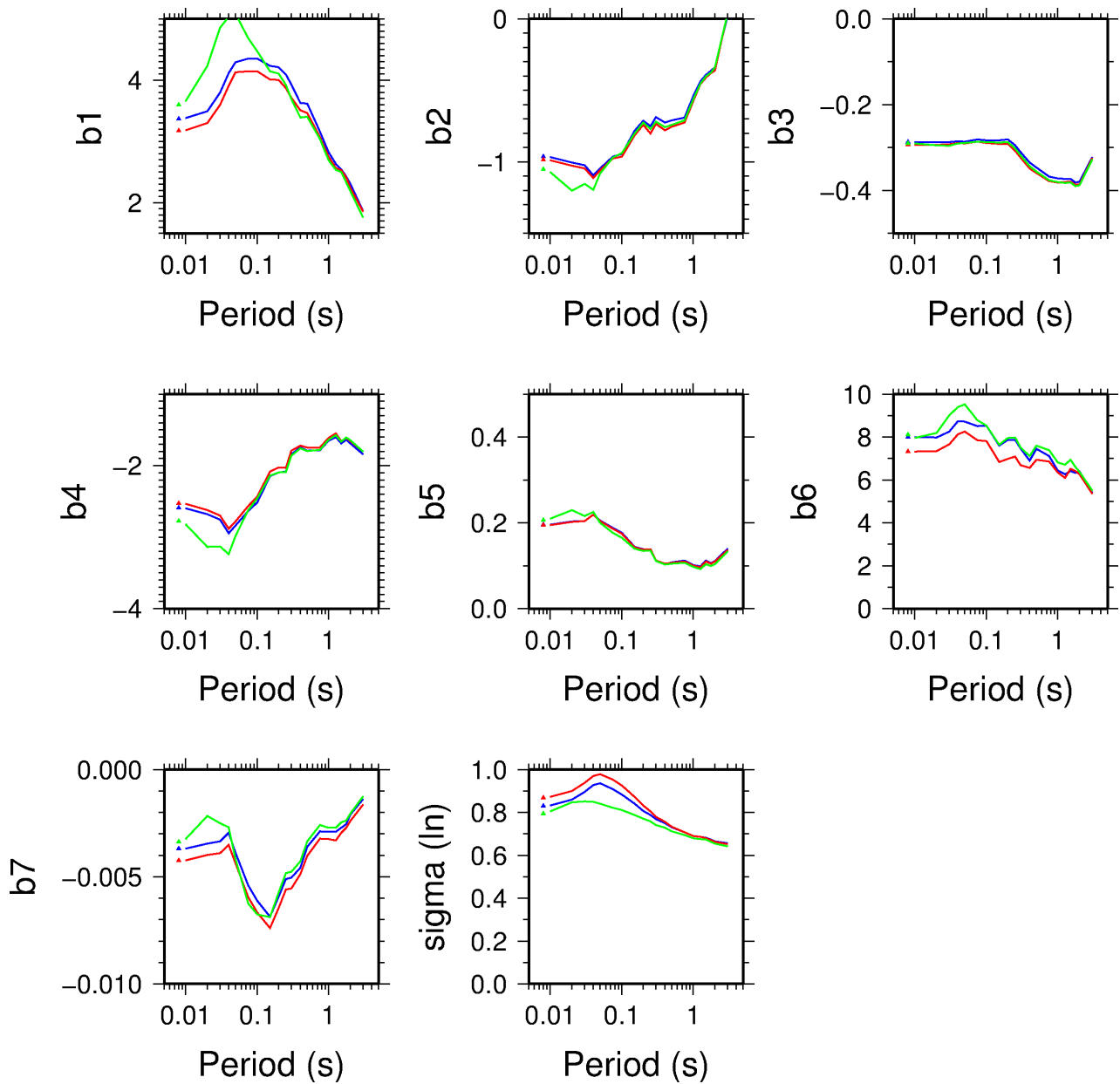


Figure 39: Comparison of the coefficients determined using least-squares regression with starting model 1 from Table 1 and for the model using 5 MPa (blue), the same model with increased variability for the stress drop of small events (red), and the same model for site conditions (amplification and κ) relative to $v_{S30}=2000$ m/s (green).

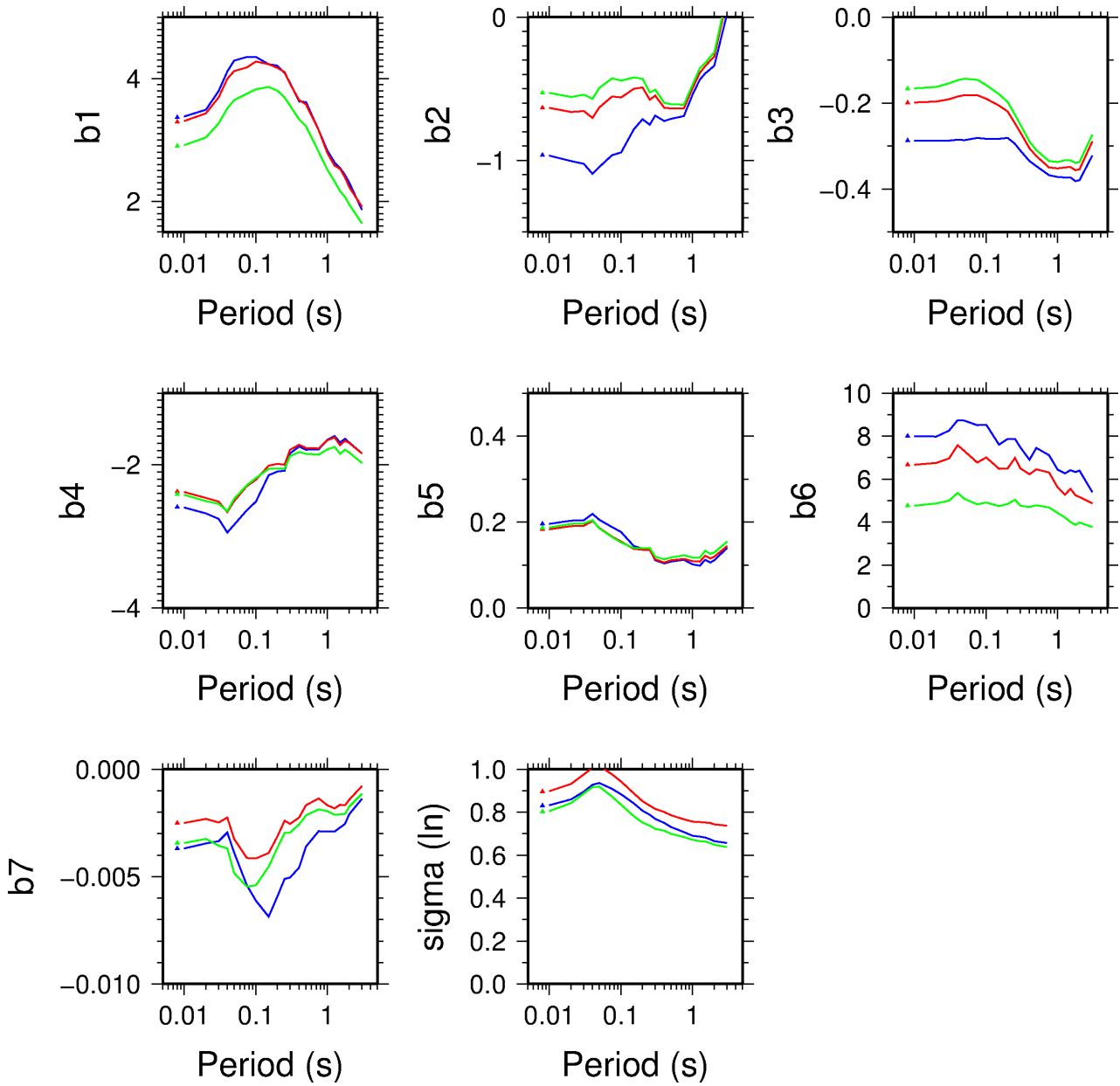


Figure 40: Comparison of the coefficients determined using least-squares regression with starting model 1 from Table 1 and for the model using 5 MPa for the Alps (blue), the Rhine Graben (red), and the Pyrenees (green).

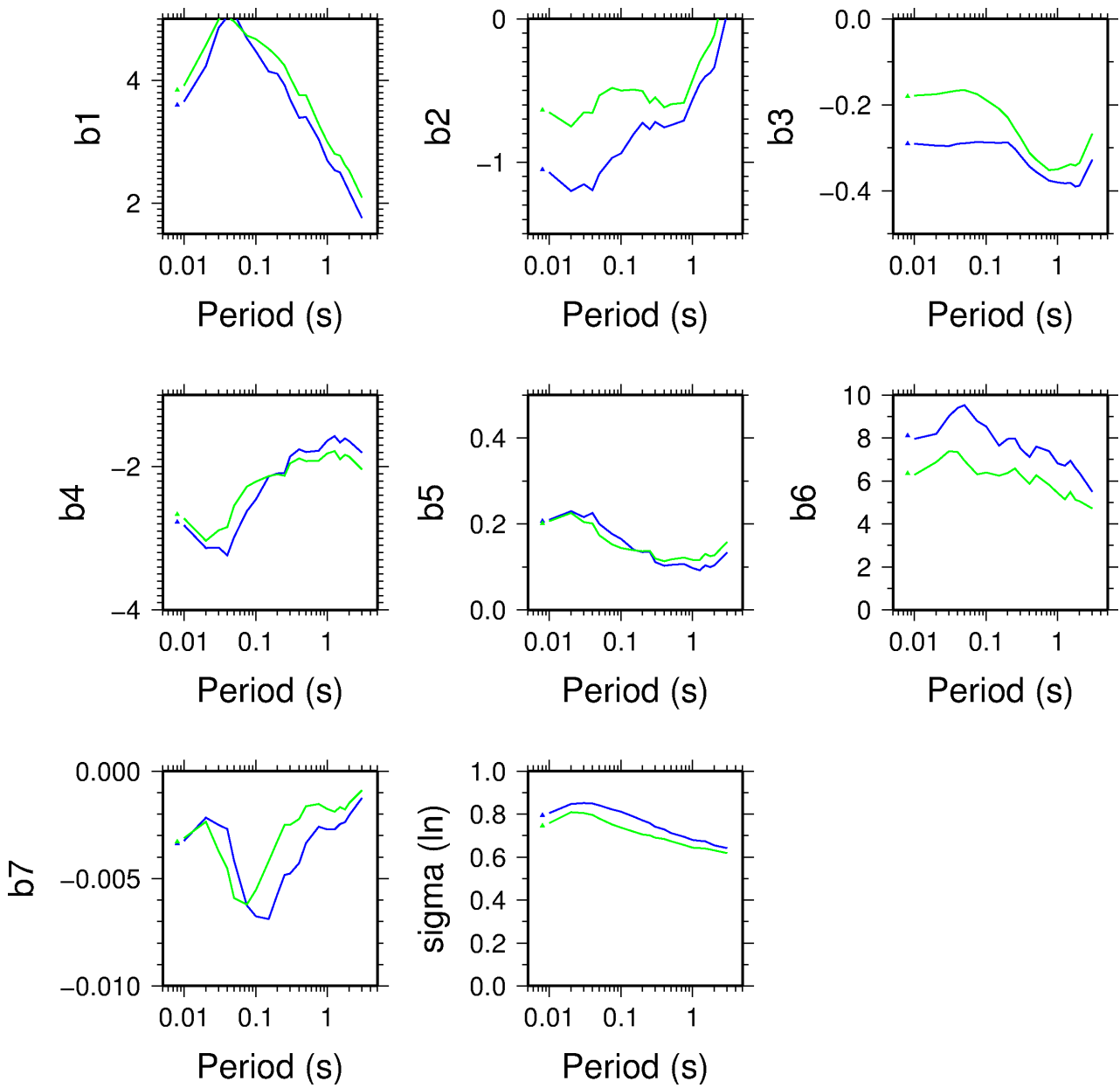


Figure 41: Comparison of the coefficients determined using least-squares regression with starting model 1 from Table 1 and for the model using 5 MPa and site conditions (amplification and κ) relative to $v_{s30}=2000$ m/s for the Alps (blue), and the Pyrenees (green).

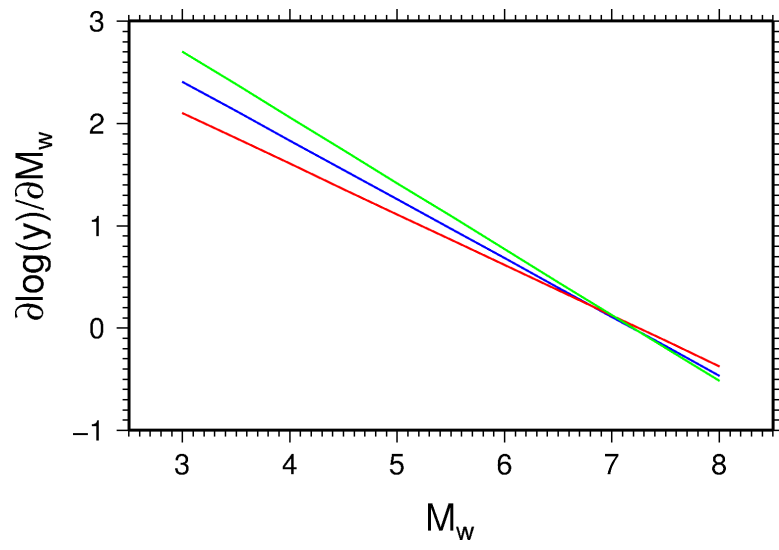


Figure 42: Magnitude-scaling in the stochastic model using stress drop values of 2.5 MPa (red), 5 MPa (blue) and 10 MPa (green), for the large events.

Project SIGMA

Review of:

STOCHASTIC GMPEs FOR FRANCE.

(Ref : SIGMA-2012-D2-71)

Jean B. Savy
May 29, 2013

1. Scope of the work reviewed

This is a review of the research work documented in EDF Ref: SIGMA-2012- D2-71 by Stéphane Drouet. This work is to be presented at the CS5 of June 5-7th, 2012, in Paris.

The reviewed study is a continuation of a previous SIGMA development work that I reviewed and that was presented at the CS3 meeting in May 2012 in Rome. The 2012 study set the methodological bases for the use of stochastic models for estimating ground-motion in France using the stochastic model simulation programs SMSIM (Boore, 2003).

The general conclusion of the work was that the methodologies and data available as well as the computational tools are now sufficiently mature to permit use of stochastic models to generate artificial data for determination of classical GMPEs, but the simulation model could be improved in the light of recent work. One of the concluding remark of my review was:

“...we can now generate cheaply and as accurately as, or better than, using attenuation equations, credible estimates of ground motion within a PSHA calculation...”

One important needed improvement to the model was to have a better characterization of the uncertainties in the input parameters to the model.

Furthermore, as more recent developments in SIGMA are focusing on identifying the parameters in the entire PSHA analysis that dominate the uncertainty estimates of ground-motion, the present study is very important, not only as its goal is to improve prediction of ground-motion, as a matter of scientific interest, but also as it will give important insights to be used by WP4 in the sorting out of uncertainty-dominant parameters.

The areas of investigations in the presently reviewed study were split into three groups:

1. Improve the stochastic model, and generate catalogs of ground-motion for the three regions of concern: the Pyrénées, the Alps, and the Rhine Graben.
2. Implement methodology to determine a best fit GMPE
3. Perform sensitivity analyses on the stochastic model parameters

2. General review conclusions

This document describes a considerable amount of work. The development and analysis part of the study are well constructed with a systematic exploration of the sensitivity to the independent parameters of the stochastic GMPEs. The methods used are appropriate and state-of-the-art.

What I consider as the main flaw is in its contextualization with respect to the other studies being conducted in SIGMA. We, in SIGMA, now emphasize the relationships between the different WPs, and the document reviewed here does not attempt to situate its effort vis-à-vis the rest of SIGMA.

On the form, I found the writing style rather casual, often imprecise and lacking clarity and I recommend some editing for the final version.

- *Improvement of the Stochastic model:*

The two main improvements include the development of an empirical relationship between magnitude M_w and stress parameter, and the use of the effective distance R_{eff} to better account for the fault dimension, as recommended by Boore (Boore, 2009). The appropriate data are used and segregated into the three different regions of interest. The correlations are not very good (see fig. 6) but the uncertainty is taken into account in the simulations, with a net improvement over the previous study (see fig. 5).

As I understand it, there is no correlation between all the parameters simulated for each simulation with SMSIM, but the author mentions (on page 5) that sets of values have been used for the simulation. “*In order to overcome this problem, we decided to use 40 different mechanism/stress parameter values for each magnitude.*” (Page 5 above fig 5). I interpret this sentence as meaning that discrete sets of values were used, thus creating a de-facto correlation between the parameters, but there is no explanation how the sets of values were chosen, and this point must be clarified.

- *Methodology to determine best fit GMPEs:*

Good choice of functional form, flexible enough to fit the data, as simple as is possible and consistent with modern works on the subject. Well documented.

The two-stage regression method developed by Brillinger/Joyner-Boore (Brillinger and Preisler 1984, 1985, and Joyner and Boore, 1993) is fully appropriate and gives reasonable results. However, here again there is no attempt to determine the correlation structure of the coefficients set, although it is noted on page 16 that “*It shows that the between-event term is almost entirely driven by the uncertainty on the stress parameter which has a negligible impact on the within-event term*”, implying some sort of correlation. At this point in SIGMA, having an estimate of this correlation would not be important since it will not be used, but it would be a valuable contribution that could be used by practitioners that want to use the GMPEs in simulations of ground motion.

- *Sensitivity analysis:*

Very thorough analysis. The study sheds some light on which parameters are important and which general direction our understanding of the uncertainty is going, but it would be erroneous to take those results as physical reality as too many input parameters to the study are still rather arbitrary.

The bottom line is that this is a well executed task. The document reads generally well, although clarifications or supplemental information are needed at times.

One important flaw in this study is that the author did not try to make the bridge with how the results would be used in a PSHA of France. Specifically, a lot of effort went in a better characterization of the models for large earthquakes and for large distance, but we know that the seismic hazard will be mostly coming from small to medium events at distances between 25 to 50 km. Thus more effort should have been directed towards those ranges of magnitude and distance.

Other flaws that I see are mainly from a desire to extend the limits of what is already achieved. For example, it appears to me that the stochastic model as it is implemented here is in fact no more than another GMPE. The difference with the classical GMPEs being that it provides a full realistic spectral estimate as opposed to independent frequencies spectral estimates. As such, it would be interesting to consider using similar regression techniques as those used in this study to determine its parameters.

3. Detailed comments

Executive Summary

Overall the executive summary covers well the extent of the work, but it needs general editing and clarification. For example on page 2, line 3 of paragraph 1, it is mentioned that the GMPEs are developed for a "broad magnitude range" without actually mentioning the actual usable range.

- I found that the label of "Stochastic ground-motion equation prediction equations" of the GMPEs derived from stochastic model data leads to confusion between the stochastic model and the stochastically generated data GMPEs. Could a different label be used?
- The two rock conditions considered, namely "standard rock" and "hard rock" are described by the same characteristics of " $V_{s30}=800$ m/s and $\kappa=0.002$ s", and this is repeated later in the conclusion.
- "Stress parameter uncertainty directly maps into between-event variability, while the uncertainties on the other parameters mainly influence the within-event term. The total ground-motion variability obtained is comparable to that obtained in empirical GMPEs under the ergodic assumption (variability of ground-motion including various sites and various sources). The within- and between-event terms are also similar to that obtained in empirical GMPEs, especially those that include small magnitudes events."

The result described by this sentence is very important, albeit not surprising, if not even expected, but the final conclusion is not necessarily true. Since apparently no correlation was introduced between the simulated parameters, at least in a formal fashion, then most of them are actually statistically independent, and the uncertainty is likely to be much larger than empirical. If correlation were to be introduced, the total uncertainty in the ground-motion prediction would likely be reduced. Consequently the fact that predicted uncertainty matches that of observed uncertainty could very well be just a coincidence. If however it can be demonstrated that all the parameters are really independent, then the statement would be true, but this has not been done in this study.

- A strong conclusion in sentence "It appears that a stress parameter of 5 MPa is a good choice to achieve a good fit between the models and the real data" is misleading since the value of 5MPa was not demonstrated to be convincingly superior to 10Mpa, or possibly other values. The sentence should be modified.
- In sentence "Even if improvements are still possible for the stochastic models presented in this study, we feel that they can be used in PSHA analysis." , It is not clear whether the statement is meant for the stochastic model, or whether it is mean for the stochastically derived data GMPE. In any case, it is a moot statement since PSHA results were never compared in this study, and it should be removed or qualified for what it is, an arbitrary statement (which we are all tempted to do too often).
- The use of "coherent" and coherence" in the document should be replaced by "consistent" and "consistence", in the entire document, except where it is appropriate, namely when it is used with the statistical meaning of statistical relationships between bodies of data.

Other detailed comments

- Page 2:§2.1
To facilitate the comprehension of the text, all the definitions of distance should be repeated, including R_{rup} and R_{epi} , R_{hypo} etc.

- Page 2, §2.1 equation defining $G(R_{\text{eff}})$:
Define $G(\)$. Need to give some basic information on the equation, what it means and how Boore (2009) solved for R_{eff} .
- Page 3: Fig 2.
The choice of showing ratios of distances to R_{rup} does not help much in comparing directly the effect of R_{mod} and R_{eff} . The present figures can be kept but additional figures should show the ratios of R_{mod} to R_{eff}
- In figure 3, for $R_{\text{rup}}=10\text{km}$
it seems that the two spectra are different by a constant multiplicative factor.
- Page 5, top of the page
“Finally, for each scenario (magnitude, mechanism/stress parameter, distance, azimuth), 10 different simulations were used varying the attenuation parameters (γ, Q_0, α)”
We have no clear idea of what was done here. The exact scheme, including type of distributions should be described.
- Page 5
“In order to overcome this problem, we decided to use 40 different mechanism/stress parameter values for each magnitude. In this case (Figure 5 right-hand side) the distributions are closer to Gaussian distributions and mean values match with input mean values of the model”
Clarify. Does this sentence mean that 40 sets of mechanisms/stress parameters/etc were used? Were the sets physically consistent?
If so, then this scheme would implicitly include some sort of correlation between the parameters, and then we need to know how they were selected.
Also, why do we want the distribution to be Gaussian? Why not uniform? For as much as I know it seems that at best we have an idea of range for most of the parameters, which would favor a uniform distribution.
- Page 8, coefficients of the equations of $\ln(\Delta\sigma)$
Please limit the number of decimal points. After 1 or maybe 2 they do not make any sense.
- Site model
No comments. Eventually this part will have to be updated with results from WP3.
- Page 11, Attenuation model
“In order to increase the variability, the uncertainties on the attenuation parameters were arbitrarily increased to 0.1, 0.2 and 0.05 for γ , Q_0 , and α , respectively.”
It is true that the modification was done in an arbitrary fashion, but there was a rationale for doing so and it should be clearly mentioned here, with some basic explanations, to avoid giving the impression of a completely arbitrary choice.
- Pages 12 and after, section 3.
The choice of comparing only the coefficients of the prediction equation for the different cases does not give the kind of information needed. The parameter of interest is the ground-motion, not the coefficients of the equation, and I would like to see, maybe in addition to the existing plots, some comparisons of the ground-motion predictions and for distances and magnitudes relevant to the PSHA studies for France (relevant ranges of distance and magnitudes that dominate the seismic hazard surface).
- Page 15 and after, Section 4
All parameter values seem to lead to reasonable results, but more details on their selection are needed.
- Page 19, Section 5.
Parameters μ and σ need to be better defined.
They are both representing the predicted mean and standard deviation of the logarithm of the ground-motion whose distribution is assumed to be a lognormal distribution. Therefore, from the relationship between Normal and Lognormal variates (see Ang and Tang 1975), μ is the log of the median of the actual variate, the ground-motion value, and σ is the standard variation of this same variable.

- Page 20, top of page.
Replace “*coherent*” by “consistent”
- Page 20, top of page
“*In turn, it shows that the uncertainties on the input parameters are well defined.*”
Please clarify the meaning of “well defined”
- Page 22, results in Figure 23.
Why does J-B distance metric lead to a higher LLH? (With the Resorce data base it lowered it), and since increasing the stress parameter seems to lead to a better fit, why not try an even higher value such as 15 MPa, or even more to explore the limits of the upper bound of an acceptable range?
- Page 24 Table 7.
I did not understand this table. It needs more explanations.
- Page 25, bottom first §
Replace “*coherent*” by “consistent”
- Page 28, Table 9
The LLH results look good, but isn’t it, in part, because there are so few data points?
- Page 30, Figure 30.
The choice of 1s and 0.01s periods are almost entirely irrelevant to the intended applications. A better choice would be in the range of 2 to 5 Hz, and a maximum of about 25 to 50 Hz.
- Page 31, figure 31.
Why are the high frequencies not more attenuated? This needs to have a comparison with actual data.

4. References

Ang Alfredo and Wilson Tang, “Probability Concepts in Engineering Planning and Design, Volume I, Basic Principles”, John Willey and Sons, Inc., 1975

Brillinger David and Haiganoush Preisler. “An Exploratory Analysis of the Joyner-Boore Attenuation Data” BSSA, Vol.74, No.4, pp1441-1450, 1984

Brillinger David and Haiganoush Preisler. “Further Analysis of the Joyner-Boore Attenuation Data” BSSA, Vol.75, No.2, pp. 611-614, 1985

Joyner William and David Boore. “Methods for Regression Analysis of Strong-Motion Data”., BSSA, Vol. 83, No. 2, pp. 469-487, 1993

Respectfully submitted, May 29, 2013.

Jean Savy

Comments on deliverable D2-71

Stochastic GMPEs for France

Ref SIGMA-2013-D2-71 Version 01

Frank Scherbaum
University of Potsdam
Potsdam, May 28, 2013

General Comments

The report SIGMA-2013-D2-71, Version 01, documents a follow-up study to the first generation of regional GMPEs for France based on stochastic simulation as documented in the report SIGMA-2012-D2-33. It addresses and/or improves on several aspects of the model, such as the incorporation of effects of the finiteness of the sources, the underlying stress drop model and the regression method. The study also includes a comparison with other stochastic models which have been developed for European regions, a comparison with empirical data from the RESORCE and the NGA database, as well as a comparison with small magnitude data from France. In addition, in order to understand the influence of the uncertainty on particular input parameters of the model, a sensitivity study was conducted. Particularly interesting for the purpose of using the stochastic model for PSHA are the consequences of this sensitivity study for the aleatory part of the model, a component which in the context of developing stochastic models is rarely covered with the attention it deserves.

The report documents an enormous amount of work and contains a number of interesting findings. It is well written and easy to read but I obtained the impression that it has been generated in a hurry, since it still contains a considerable number of typos and layout problems (such as orphan lines, or uncorrected automatic capitalizations after referencing figures, etc).

Below, I am commenting on those aspects of the study where I believe further clarification might be helpful. Most of the comments concern minor details. None of them questions the study but rather criticizes the lack of in-depth interpretation of some of the results. For easier reference, I am numbering them consecutively independent on the section they appear in.

Individual comments

1) On page 2, the site conditions for rock and hard rock are wrongly stated as being identical (citations are given in Times New Roman13 font):

„with $v_{S30}=800$ m/s and $=0.03$ s, and hard rock site with $v_{S30}=800$ m/s and $=0.03$ s.“

- 2) The section on the near-source saturation effects nicely illustrates the direction dependence of spectral amplitude when using Reff . What does not become clear how this would be used in the context of PSHA?
- 3) Page 5, Figure caption 5 reads: „Black arrows indicate mean stress drop value from the input stress drop model.“ Are these really mean values of the stress parameter or are these mean values of the log of the stress parameter?
- 4) Are the terms stress parameter and stress drop used interchangeably or are they supposed to correspond to different quantities?
- 5) In the context of trying to adequately capture epistemic uncertainties, it seems to me that the stress drop model should have a larger spread where the „knowledge“ decreases. However, Fig. 8 on page 9 would suggest to me that we know less about the small magnitude earthquakes than the large ones, since the model spread is largest for the small magnitude events.
- 6) The upper left panel in Fig. 10 shows site amplification function for stations in the Alps, Pyrenees, and Rhine Graben. Most of the red and green curves seem to indicate a break at high frequencies. Couldn't you get estimates of κ from these „corner frequencies“?
- 7) A more in-depth discussion of the pros and cons for the individual regression technique would have been nice.
- 8) What are the three lines in the sigma panel in the bottom row of Figure 13.? Are the lower two ones within-event and between-event standard deviation?
- 9) What I find of particular relevance for using the stochastic model in the context of PSHA is the sensitivity study in chapter 4 which shows some very interesting results. The discussion of these findings, however, is too brief for my taste. For example the sigma panel in the bottom row of Fig. 16 shows a very interesting effect of the uncertainty on κ , which is completely ignored in the discussion. This uncertainty seems to control the decay of overall sigma with period which is different in shape from the shape of sigma in empirical models of Boore and Atkinson (2008) and Akkar and Bommer (2010). What does this tell us?
- 10) What are the dashed lines in Fig. 21 and 23 on pages 21 and 23, respectively?
- 11) On page 23, it is stated „Based on observations from weak-motion data there may be a need of a magnitude-dependent stress parameter in order to produce stochastic models (Edwards & Fäh, 2013; Rietbrock et al. 2013)“. While the statement is carefully uses the vague term „ may “, it would have been nice to see a more in-depth discussion of this observation. It has been discussed at least since the early 80-ies of the last century (e. g. Hanks, 1982), that a frequency band limitation would cause an apparent decrease of stress drop with decreasing magnitude. The question which occurs to me in this context is if in the inversion source parameters, the effect of κ is corrected before the stress parameter is determined?
- 12) Figure 31 is puzzling in that the change in the shape of the response spectra for the different regions is not only a change in amplitude but also in peak frequency, which at

least for the larger magnitudes is controlled by kappa rather than by stress drop. However, the interpretation in the report on page 29 only refers to differences in stress drop. I cite „As shown in Figure 31, the difference for $M_w=3.0$ due to the low stress parameter for the Alps is visible up to 0.4 s, above which all the model are similar.“ What are the differences in average kappa between the different regions?

13) On page 34 it is stated „It is interesting to note that for both the stochastic rock model and the adjusted one, there is a peak in the standard deviation of around 0.05 s.“. Do you have any explanation?

Concluding remarks

Overall, I find this a very valuable follow-up study to the work documented in the report SIGMA-2012-D2-33 which contains a wealth of information. In a way, this is also the source of my main (slight) criticism. Probably because of the many results, some of them are presented in a - sloppily speaking - „this is what I have done, here are the figures“ way, where more discussion would have been quite helpful.

References

Hanks, T. C. (1982), f_{max} , Bulletin of the Seismological Society of America December 72(6A), 1867-1879